UNCLASSIFIED

SECURITY CLASSIFICATION OF THIS PAGE

DTIC ELECTE SEP 28 1989 S D B

REPORT DOCUMENTATION PAGE

(2)

AD-A212 916

1a. REPORT SECURITY CLASSIFICATION: UNCLASSIFIED	1b. RESTRICTIVE MARKINGS
2a. SECURITY CLASSIFICATION AUTHORITY	3. DISTRIBUTION/AVAILABILITY OF REPORT: Approved for public release; distribution is unlimited.
2b. DECLASSIFICATION / DOWNGRADING SCHEDULE	
4. PERFORMING ORGANIZATION REPORT NUMBER(S)	5. MONITORING ORGANIZATION REPORT NUMBER(S): AFOSR-TR- 89-1231
6a. NAME OF PERFORMING ORGANIZATION: Univ of Alaska; 6b. OFFICE SYMBOL (If applicable):	7a. NAME OF MONITORING ORGANIZATION: AFOSR/NP
6c. ADDRESS (City, State, and ZIP Code): 903 Koyukuk Avenue, North Fairbanks, AK 99775-0800	7b. ADDRESS (City, State, and ZIP Code): Building 410, Bolling AFB DC 20332-6448
8a. NAME OF FUNDING / SPONSORING ORGANIZATION: AFOSR; 8b. OFFICE SYMBOL (If applicable): NP	9. PROCUREMENT INSTRUMENT IDENTIFICATION NUMBER: AFOSR-85-0266
8c. ADDRESS (City, State, and ZIP Code): Building 410, Bolling AFB DC 20332-6448	10. SOURCE OF FUNDING NUMBERS: PROGRAM ELEMENT NO. 61102F; PROJECT NO. 2309; TASK NO. A2; WORK UNIT ACCESSION NO.

11. TITLE (Include Security Classification)

(U) CRUSTAL STRUCTURE STUDIES UTILIZING EARTHQUAKE SEQUENCES

12. PERSONAL AUTHOR(S)

Larry D. Gedney, David B. Stone, and John N. Davies

13a. TYPE OF REPORT	13b. TIME COVERED	14. DATE OF REPORT (Year, Month, Day)	15. PAGE COUNT
Final	FROM 9/1/85 TO 8/31/88	August 1989	104

16. SUPPLEMENTARY NOTATION

17. COSATI CODES			18. SUBJECT TERMS (Continue on reverse if necessary and identify by block number)
FIELD	GROUP	SUB-GROUP	Earthquakes; Crustal Structure; Ykon Flats; Barter Island; Fairbanks refraction
	08.11		

19. ABSTRACT (Continue on reverse if necessary and identify by block number)

The original goal was to use the Dall City earthquake sequence of Feb-Mar'85 to investigate the crustal structure of north-central Alaska. The scope was later modified to include studies of some earthquakes just north of the Alaska Range, the Gold King earthquakes, and later still to include data gathered from chemical explosions detonated by USGS as part of their Trans-Alaska Crustal Transect (TACT) program. The work divided roughly into Dall City events, Gold King events, Yukon Flats Experiment, permanent network/explosion data, and Barter Island - Fairbanks refraction. The models used in this study were applied to most of Alaska, and thus large differences were expected. In general the models for the areas north of Fairbanks are reasonably similar which is consistent with the fact that relocations of events using these different models don't produce any clear preference; and south is expectedly much more complex, given young accreted terranes with an underthrusting Pacific plate.

20. DISTRIBUTION / AVAILABILITY OF ABSTRACT	21. ABSTRACT SECURITY CLASSIFICATION
X ☐ UNCLASSIFIED/UNLIMITED X ☐ SAME AS RPT. ☐ DTIC USERS	UNCLASSIFIED

22a. NAME OF RESPONSIBLE INDIVIDUAL	22b. TELEPHONE (Include Area Code)	22c. OFFICE SYMBOL
Major John F. PRINCE	(202) 767-4908	AFOSR/NP

DD FORM 1473, 84 MAR 83 APR edition may be used until exhausted. All other editions are obsolete.

SECURITY CLASSIFICATION OF THIS PAGE

UNCLASSIFIED

89 9 27 030

FINAL TECHNICAL REPORT

AFOSR-TR- 89-1231

TO

AIR FORCE OFFICE OF SCIENTIFIC RESEARCH

CRUSTAL STRUCTURE STUDIES UTILIZING EARTHQUAKE SEQUENCES

GRANT AFOSR-85-0266

Principal Investigators:
Larry D. Gedney
David B. Stone
John N. Davies

August 1989

INTRODUCTION

This project was initiated by Larry Gedney of the Geophysical Institute of the University of Alaska. About halfway through the study Larry Gedney retired, and David Stone and John Davies became the principal investigators.

The original goal of the proposal was to use the Dall City earthquake sequence of February and March, 1985 (fig.1) to investigate the crustal structure of north-central Alaska. The scope of the proposal was later modified to include studies of a group of earthquakes just north of the Alaska Range, the Gold King earthquakes (fig.1) and later still to include data gathered from chemical explosions detonated by the U.S.Geological Survey as part of their Trans-Alaska Crustal Transect (TACT) program (fig.3). When we embarked on the study of the Yukon Flats area using the TACT explosions, there were insufficient funds left in the AFOSR-85-0266 contract, so we supplemented these funds through a proposal to the National Science Foundation (NSF) and through the use of student interns, also funded by the NSF.

As with any project of this size and scope, it overlapped with other ongoing studies of the crustal structure of Alaska, most notably a study of a Fairbanks - Fort Yukon - Barter Island line, and a study of Interior Alaska between Fairbanks and the Alaska Range. The basic funding for these latter two studies came from a combination of State of Alaska funds, the U.S.Geological Survey, and the Rice-University of Alaska Industrial Associates Program, with considerable indirect support from this contract (AFOSR 85-0266) in terms of such things as the analysis of common data sets.

RESEARCH

Although all the work completed has the same common goal of investigating the crustal structure of Alaska, it divides into roughly five parts.

Dall City Events.

The occurrence of the Dall City sequences of events, which started in February of 1985 (Estabrook et al, 1985; Dixon, 1989) and ended (?) with a magnitude 5.5 event and aftershocks in July of 1987, allowed the crustal models being used for earthquake locations to be tested and refined. A description of these events and the focal mechanism studies can be found in Appendix I, ("seismicity and focal mechanism studies of the 1985 Dall City earthquakes, north-central Alaska" by Estabrook et al.) The initial crustal models deduced from these events

are described by Gedney in his annual technical report for this contract (Appendix II, Crustal structure studies utilizing earthquake sequences, L.Gedney) and a more detailed comparison made with other crustal models in Estabrook, 1985 (abstract given as Appendix III), and Estabrook et al. 1988, (Appendix IV).

Gold King events.

The Gold King events, so-called because of their proximity to the Gold King airstrip and seismometer station (fig. 1) have considerable importance to our understanding of the crustal structure of Alaska. Their importance lies in the fact that they apparently mark the northeasternmost seismic activity directly associated with the downgoing Pacific plate (Gedney and Davies, 1986, Appendix V). The group of events in question lie at depths between 100 and 140 km, and by combining them with the hypocenter contours for events to the west and south, the location of that portion of the underthrusting Pacific plate can be determined. To the east of the Gold King events, it appears that the Pacific plate is absent. There are some hypocenters about 300 km south, south of the Wrangell Mountains, that are consistent with the Pacific plate reaching 100km depths beneath the active volcanic center of Mt. Wrangell itself, thus requiring a break or a sharp bend in the Pacific plate (Stephens et al. 1984; Perez and Jacob, 1980). If it is assumed that the boundary between the Pacific plate near Gold King and where it is observed to be dipping beneath the Wrangell Mtns further to the south is a transform boundary, then this boundary can be depicted by a small circle about the Pacific - North American relative motion pole, as shown in figure 2. The shaded area shown in figure 2 is thus the area where the surface geology of Alaska is underlain by oceanic crust. The interaction, or coupling between Alaska and the underthrust Pacific plate may be generating the stresses causing the intraplate seismicity of Interior and Arctic Alaska as well as producing complex crustal velocities in southern Alaska.

Yukon Flats Experiment

The Yukon Flats experiment was designed to exploit the fact that the U.S.Geological Survey TACT program detonated a number of large (up to 6000 lb) chemical explosions. The basic aim of our experiment was to determine the crustal structure beneath the Flats (Technical report by Stone and Davies, 1987, Appendix VI).

The geologic and tectonic history of the Yukon Flats is very poorly understood. It is located at a junction of several terranes and major fault systems including the Tintina and Kaltag faults and the Porcupine lineament (figures 1,3,4). Because there are few constraints on its history, it has been postulated to be underlain by ocean crust as a result of either entrapment or extension, and has also been postulated to be

QUALITY INSPECTED 4

Codes
Dist | Avail and/or Special
A-1

down-dropped continental crust. The basin itself is known to be deep, with oil industry estimates of 15 to 20 thousand feet of sediment on top of local basement. In 1987 the TACT program detonated all the large shots shown in figure 5, plus a number of smaller ones. The TACT group has plans for the early 1990s to continue the shots to the north along the Trans-Alaska pipline route as well as running an east-west line between Manley and Circle hot springs (figure 1). With the future shots, we hope to be able to add a shot off the east end of the Yukon river stations shown, and thus more-or-less reverse the profile. At the present time we only have data from the 1987 shots, which thus gives us an unreversed profile along the Yukon river, but also gives us a fan-like distribution of paths across the Yukon Flats for a more general analysis of velocity versus depth (figure 5).

For the 1987 investigation of the Yukon Flats area, all of the stations were temporary with the exception of Fort Yukon, which is part of the University of Alaska permanent network. Out of the 13 temporary stations, all but 2 recorded at least some of the shots. The best records were those that were recorded on either the borrowed USGS 5-day recorders, or those that transmitted directly to Fairbanks via telephone.

Figure 5 shows the travel-time plots for the Yukon Flats fan shooting experiment. The interpretation of these data was greatly aided by a serendipidous earthquake at Dall City. The magnitude 5.5 event was large enough for us to identify the Pn arrivals with ease, and thus to "calibrate" ourselves to recognize Pn in the much less energetic explosion data. From the travel times we deduce that the crustal structure beneath the Yukon Flats and adjacent Yukon-Tanana uplands consists of an 8.7 km thick layer with a velocity of 5.4 km/s, a 22.6 km layer with a velocity of 6.0 km/s, and a Moho velocity of 8.45 km/s. This gives a total crustal thickness of 33.3 km, which is in accord with the models derived by Estabrook (1985) and Estabrook et al., (1988).

Permanent network/Explosion data.

The same TACT explosions were recorded on the permanent network operated by the Geophysical Institute of the University of Alaska (figures 1 and 7). To investigate the crustal structure, a composite travel-time curve has been assembled. The curve includes data along a line from near to the Canadian border on the Alcan highway to the Koyukuk river on the Trans-Alaska pipline route. The travel-time curve is shown in figure 8. Although all of the composite line is in what is loosely termed Interior Alaska, and most of it traverses the Yukon-Tanana composite terrane, it is probable that it samples several different crustal configurations. Taking the travel-time curve at its face value, it gives a crustal structure consisting of a 2.3 km thick layer with a velocity of 5.2 km/s, a 21.7 km layer with a velocity of 5.9 km/s and a Moho velocity of 7.8 km/s. This gives a total crustal thickness of 24 km,

considerably thinner than that predicted by most models (Estabrook et al., 1988; Stone et al., 1987).

Another approach to modeling the TACT explosion data was taken by Johnson, 1989, (abstract given as Appendix VII), who treated the explosions as earthquakes, and located them using the standard HYPOELIPSE reduction program, but with various crustal models. The general conclusions from her study are that for the Fairbanks area, on which she concentrated, the location parameters were not consistently better for any one model over any other.

In our annual report dated September 1987 (Appendix VII) Stone and Davies described a series of explosions proposed for the Fort Greely area that we hoped to use for further crustal structure experiments. These explosions were designed to create tank traps, and the combination of poor coupling (they were designed to blow dirt out rather than put energy into the ground) and bad weather conditions has prohibited us from getting useable data so far.

Barter Island - Fairbanks refraction

Another approach to large scale crustal modeling is that of Estabrook (1985) and Estabrook et al., (1989). In this case well located earthquakes near Barter Island, Fort Yukon and Fairbanks were used as energy sources, and arrival times at the seismometer arrays at Barter Island, Fort Yukon and Fairbanks used to construct travel-time curves. As can be seen from figures 2 and 3 and Table 1. from Appendix IV, the depth to basement varies from about 33km in the Fairbanks area through 35 km near Dall City to about 40 km beneath the Brooks Range, with Moho velocities between 7.88 and 7.94 km/s.

CONCLUSIONS

Figure 9 shows a composite of crustal models for Alaska. It must be recognized that these models cover most of Alaska, and thus large differences are expected. In general it can be seen that the models for the areas north of Fairbanks are reasonably similar which is consistent with the fact that relocations of events using these different models do not produce any clear preference. South of Fairbanks the situation appears to be much more complex, as might be expected with the greater complexity of young accreted terranes combined with a currently underthrusting Pacific plate.

REFERENCES

Churkin M., Foster H.L., Chapman R.M., Weber F.R., Terranes and suture zones in east central Alaska, Jour. Geophys. Res., V.87.,p3718-3730, 1982.

Dixon J.P., The seismicity of the 1985 Dall City earthquake sequence; Univ. of Alaska MS thesis, in preparation, 1989.

Estabrook C.H., Seismotectonics of northern Alaska; Univ of Alaska MS thesis, 139pp, 1985.

Estabrook C.H., Stone D.B., Davies J.N., Seismotectonics of northern Alaska; Jour. Geophys. Res., V.93, p12026-12040, 1988.

Gedney L., Davies J.N., Additional evidence for down-dip tension in the Pacific plate beneath central Alaska; Bull. Seism. Soc. Amer., V.76, p1207-1214, 1896.

Hanson K., Berg E., Gedney L., A seismic refraction profile and crustal structure in central Interior Alaska, Bull. Seis. Soc. Amer., V.58., p1657-1665, 1968.1968.

Howell, D.G., editor, Tectonostratigraphic Terranes of the Circum-Pacific Region. Circum-Pacific Council for Energy and Mineral Resources, Earth Science Series No.1, Houston, Texas, 581p, 1985.

Jin D.J., Herrin E., Surface wave studies of the Bering Sea and Alaska area, Bull. Seis. Soc. Amer., V.70., p2117-2144, 1980.1980.

Johnson J.M., Accuracy of earthquake location determinations in the Fairbanks, Alaska area based on artificial explosion experiments; Univ. of Alaska MS thesis, 69pp, 1989.

Jones, D.L., Silberling, N.J., Berg, H.C., Plafker, G., Map showing tectonostratigraphic terranes of Alaska, columnar sections, and summary descriptions of terranes. U.S.Geol. Surv. Open-file Report 81-792, 20 p, 1981.

Minster J.B., Jordan T.H., Molnar P., Haines E., Numerical modelling of instantaneous plate tectonics, Geophys. Jour. Roy. Astr. Soc.. V.36., p541-576, 1974.

Perez O.J., Jacob K.H., Tectonic model and seismic potential of the eastern Gulf of Alaska and Yakataga seismic gap, Jour. Geophys. Res., V.85., p7132-7150, 1980.

Stephens C.D., Fogelman K.A., Lahr J.C., Page R.A., Wrangell Benioff zone, southern Alaska, Geology, V.12., p373-376, 1984.

Stone D.B., Present day plate boundaries in Alaska and the Arctic, Jour. Alaska Geol Soc. V.3., p1-14, 1983.

Stone D.B., Davies J.N., Stihler S., Estabrook C.H., Basement (Pn) velocities in Interior Alaska and the Yukon Flats; EOS, V.66, p1459, 1987.

FIGURES

Figure 1.
This figure shows the setting of the Yukon Flats (northerly shaded area) and the rest of Interior Alaska (loosely defined as including the Tanana valley (shaded) northward to the Brooks Range on the north boundary of the map). The small 3-letter codes represent the tectono-stratigraphic terranes of Jones et al., (1981); Howell, (1985); and Churkin et al., (1982). Also shown are the larger of the TACT shot points (*) with the shot point number and explosive charge in 1000s of pounds. The seismic stations used are shown as triangles, solid for permanent and open for temporary. The road system is shown with a dot and dash symbol. The square labelled GKC in the Tanana valley is the Gold King site used to locate the northern edge of the Pacific plate. The M in the west central part of the map represents Manley Hot springs, and the temporary station CS Circle. These two locations approximate the ends of the proposed 1990 or 1991 TACT lines.

Figure 2.
The Pacific-Alaska plate interaction in the southern Alaska, redrawn from Stone, (1983). Hypocenter depth contours (in kilometers) and the shading pattern represent the extent to which the Pacific plate has been underthust beneath Alaska. Stars represent recent volcanoes, and the thin lines the major fault systems. The RM1 lines are the hypothetical tracks of the Pacific plate about the Euler poles of relative motion determined by Minster et al., (1974).

Figure 3.
The route of the TACT transect is shown by the heavy dashed line. The major faults are shown as solid lines, but it should also be noted that all the terranes are fault bounded. The Yukon Flats can be seen to lie in the complex area between the Tintina and Kaltag faults, the Porcupine lineament, and the composite terranes of the Brooks Range.

Figure 4.
This figure shows the relationship between the Yukon Flats and the various geologic provinces of Alaska. The part of Interior Alaska investigated by the studies reported here include parts of the Ruby Schist belt, the Yukon Flats, the Yukon-Tanana crystaline province and part of a complex of Paleozoic through Cenozoic carbonates and clastic rocks.

Figure 5.

An outline of the Yukon Flats area (shaded) with representative paths from the shot points to seismometer stations (triangles) shown. The shot points are labelled with their number and the size of the shot in 1000s of lbs. The location of the fortuitous 1987 Dall city event is also shown.

Figure 6.
Travel-time plots for all the explosion data recorded by the stations in the Yukon Flats area together with the arrivals from the Dall City event. Because of the shot point-station distribution, these data represent a fan-shooting experiment.

Figure 7.
The distribution of all the TACT shot points (triangles) many of which were used for several seperate explosions. All the stations used in the various studies are represented by stars. The solid lines represent the vertical plane onto which all the adjacent shot points and receivers were projected to produce the travel-time curve shown in figure 8.

Figure 8.
A travel-time curve constructed using all the data along the solid line shown in figure 7. The best estimates of the velocities are also shown. Since this is a composite of shot points and stations distributed along the whole length of the line, it is effectively a reversed profile.

Figure 9.
A composite of the various crustal velocity models for Alaska. The two new models associated with this study are shown by the heavy lines labelled "TACT 1987".

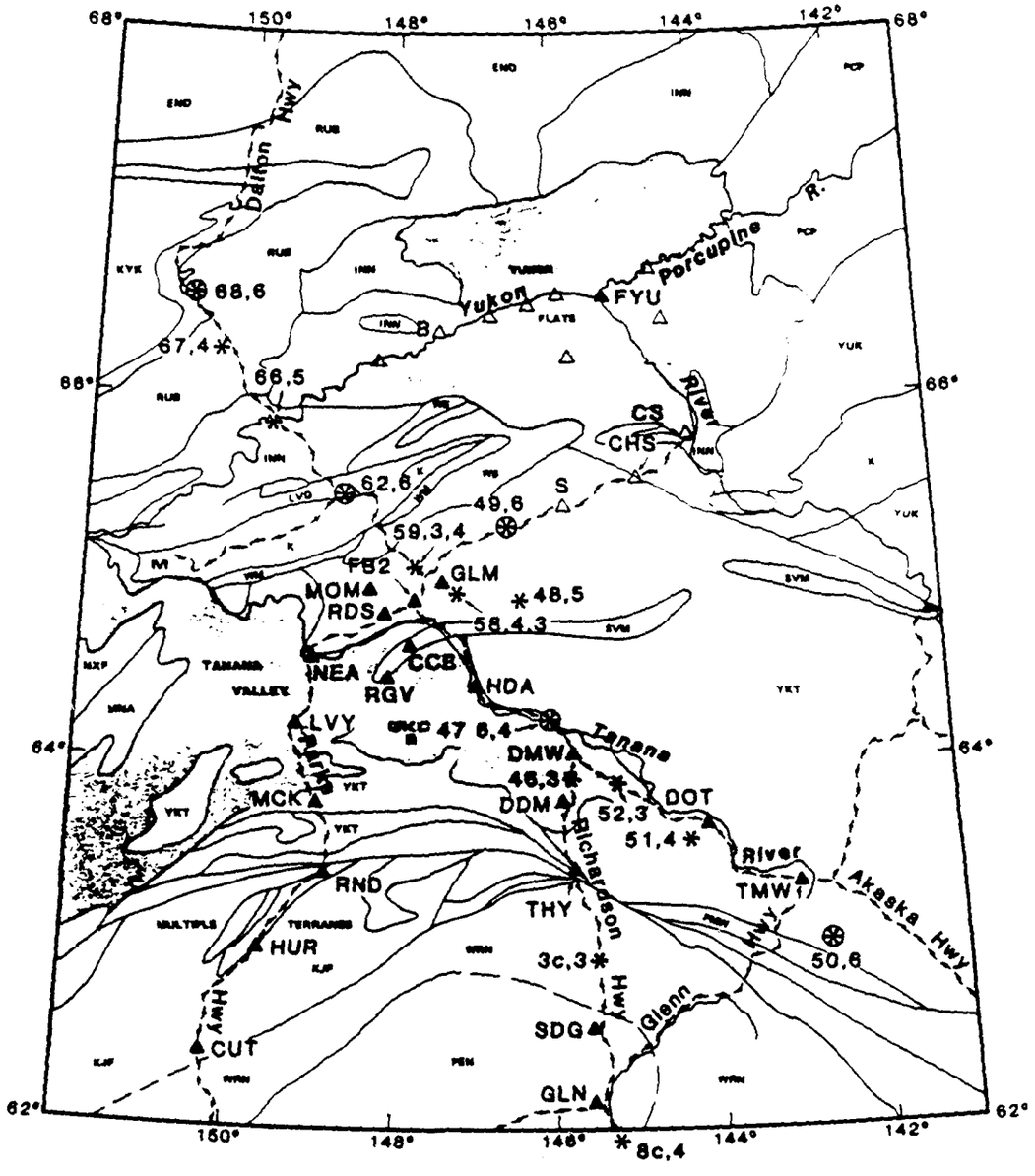

Figure 1.
This figure shows the setting of the Yukon Flats (northerly shaded area) and the rest of Interior Alaska (loosely defined as including the Tanana valley (shaded) northward to the Brooks Range on the north boundary of the map). The small 3-letter codes represent the tectono-stratigraphic terranes of Jones et al., (1981); Howell, (1985); and Churkin et al., (1982). Also shown are the larger of the TACT shot points (*) with the shot point number and explosive charge in 1000s of pounds. The seismic stations used are shown as triangles, solid for permanent and open for temporary. The road system is shown with a dot and dash symbol. The square labelled GKC in the Tanana valley is the Gold King site used to locate the northern edge of the Pacific plate. The M in the west central part of the map represents Manley Hot springs, and the temporary station CS Circle. These two locations approximate the ends of the proposed 1990 or 1991 TACT lines.

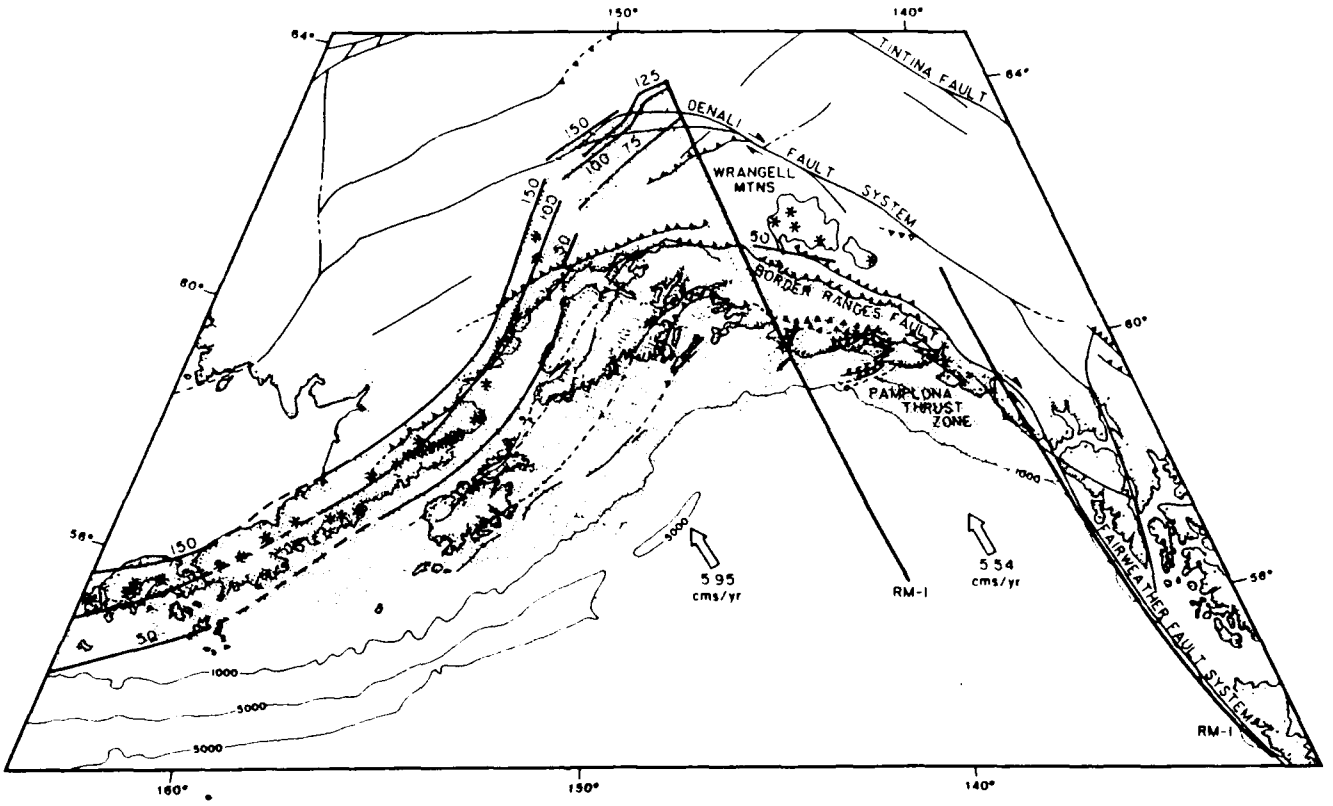

Figure 2.
The Pacific-Alaska plate interaction in the southern Alaska, redrawn from Stone, (1983). Hypocenter depth contours (in kilometers) and the shading pattern represent the extent to which the Pacific plate has been underthust beneath Alaska. Stars represent recent volcanoes and the thin lines the major fault systems. The RM1 lines are the hypothetical tracks of the Pacific plate about the Euler poles of relative motion determined by Minster et al., (1974).

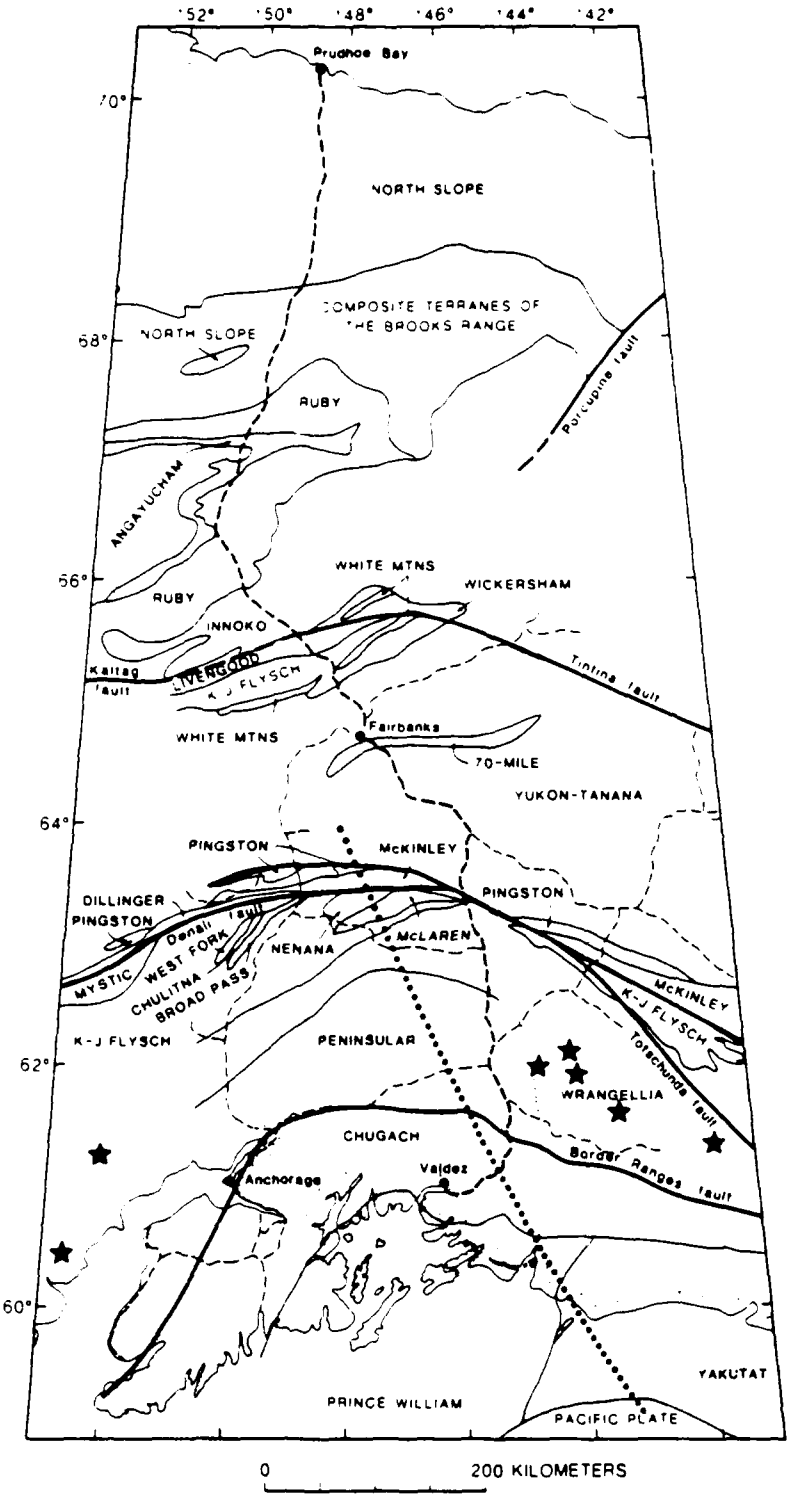

Figure 3.
The route of the [illegible] transect is shown by the heavy dashed line. The major faults are shown as solid lines, but it should also be noted that all the terranes are fault bounded. The Yukon flats can be seen to lie in the complex area between the Tintina and Kaltag faults, the Porcupine lineament, and the composite terranes of the Brooks Range.

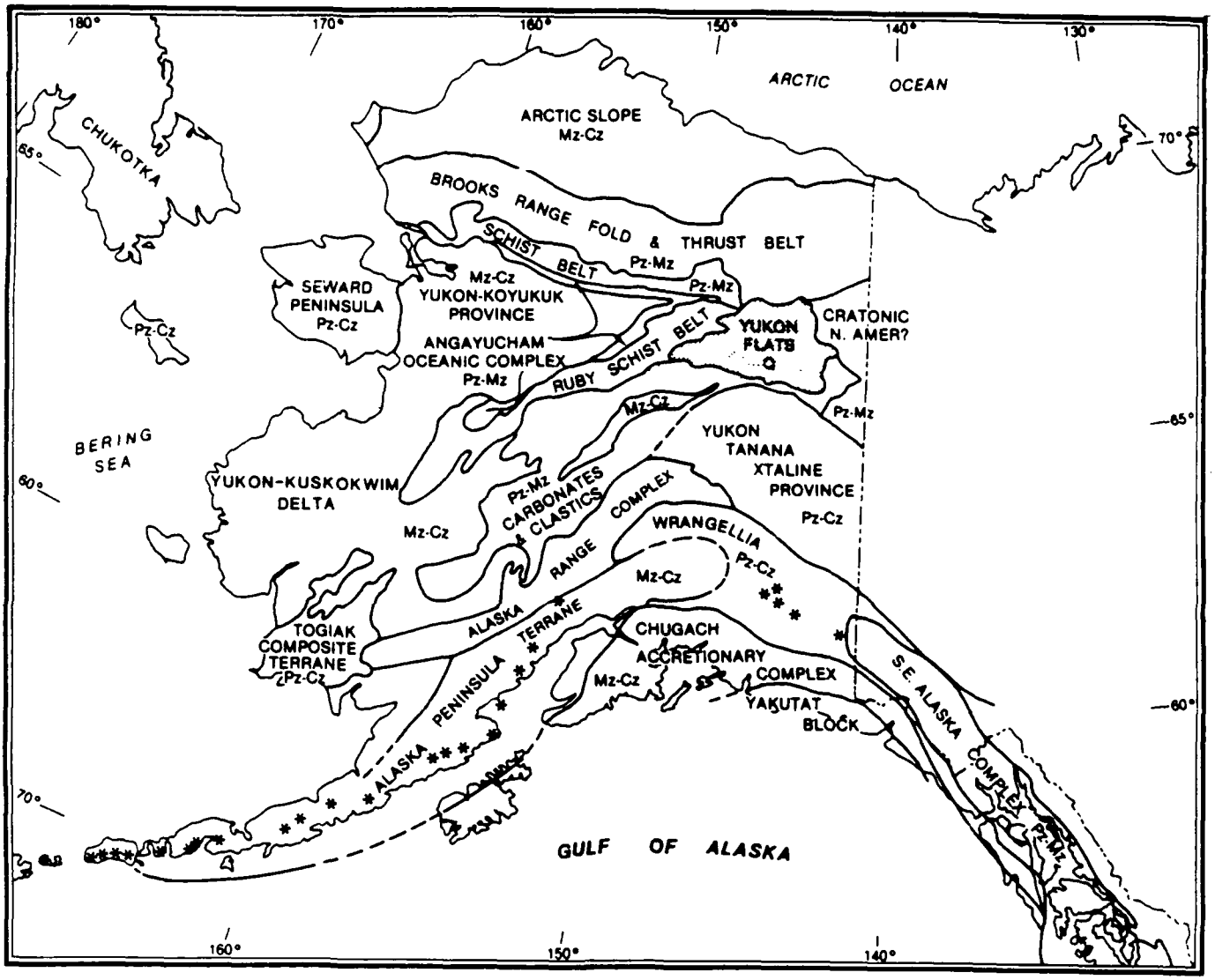

Figure 4.
This figure shows the relationship between the Yukon Flats and the various geologic provinces of Alaska. The part of Interior Alaska investigated by the studies reported here include parts of the Ruby Schist belt, the Yukon Flats, the Yukon-Tanana crystaline province and part of a complex of Paleozoic through Cenozoic carbonates and clastic rocks.

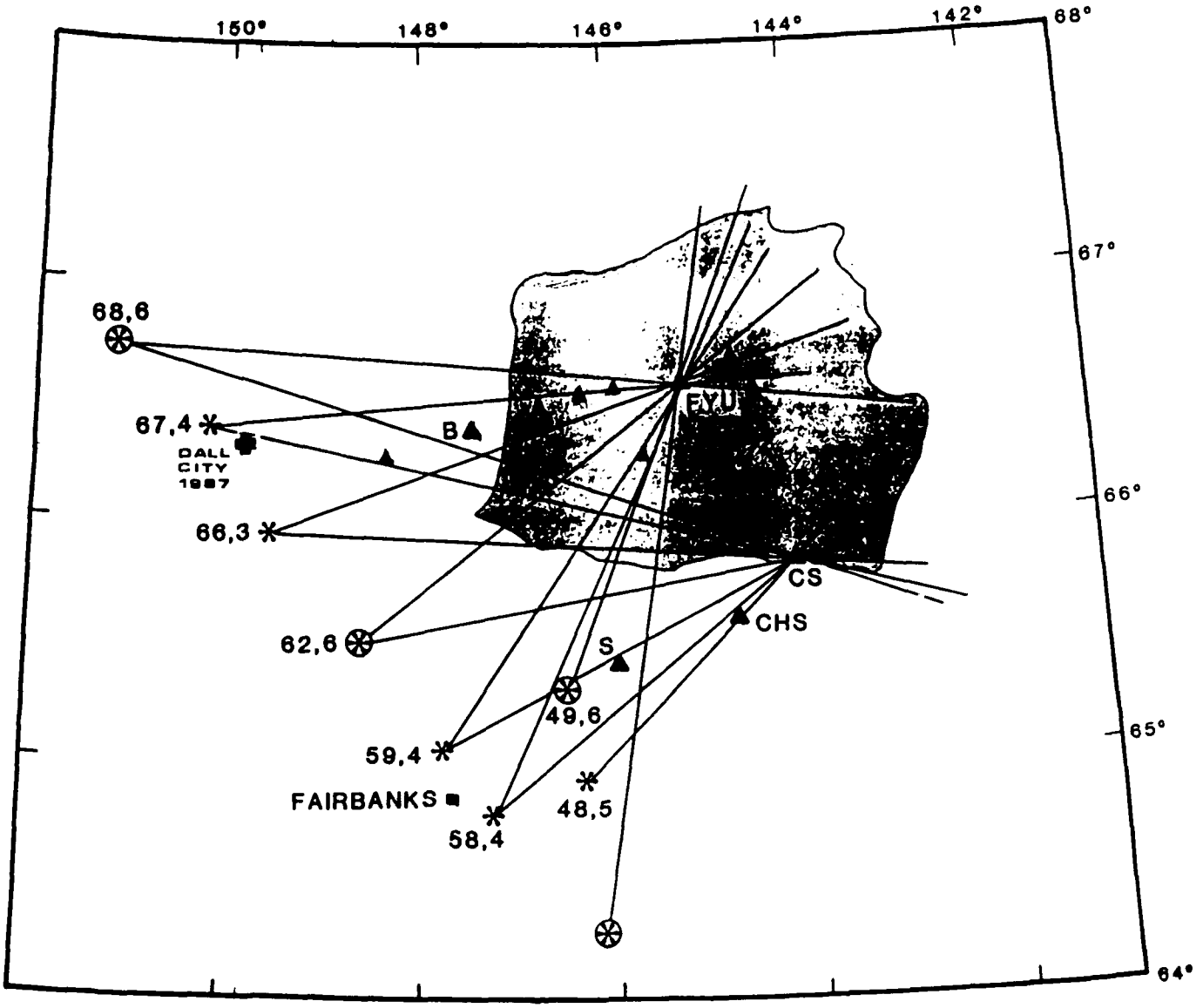

Figure 5.
An outline of the Yukon Flats area (shaded) with representative paths from the shot points to seismometer stations (triangles) shown. The shot points are labelled with their number and the size of the shot in 1000s of lbs. The location of the fortuitous 1987 Dall city event is also shown.

Table 1: Station Configuration

Time Period	Stations Used
1 17 February	Regional Network
17 February 15 March	BEH and Regional
15 March 14 April	BEH, RGV, FISH and Regional
10 April 14 June	BEH, NNC, SNO, FISH and Regional
14 June Present	Regional Network

Table 2: Focal Mechanism Parameters for Dall City Earthquakes

Time					Pole to Plane 1			Pole to Plane 2						
YRMODY	HRMN	Lat.	Long.	Mag.	extreme (tr pl)	prefer* (tr pl)	extreme (tr pl)	extreme (tr pl)	prefer* (tr pl)	extreme (tr pl)	P Axis* tr pl	T Axis* tr pl	B Axis* tr pl
750309	1419	65.9	149.7	4.6ML	(282,28)	(278,26)	(276,25)	(017,08)	(012,08)	(010,08)	328,25	232,12	116,62
850214	0504	66.3	149.8	5.4mb	(096,20)	(303,00)	(316,10)	(004,10)	(034,00)	(224,17)	168,00	258,00	vert.
850309	1408	66.3	149.8	6.0mb	(286,12)	(287,16)	(293,22)	(198,10)	(198,00)	(200,12)	334,12	241,10	108,74

tr-trend pl-plunge *-preferred solution

Table 3: Location parameters of the largest events at Dall City during February to April of 1985

DATE	ORIGIN	LAT N	LONG W	DEPTH	MB	MS	ML GIA	ML PMR	NP	NS	GAP	DMIN	D3	RMS	ERH	ERZ
850214	5 4 0.78	66N15.77	149W46.04	10.00	5.0	5.0		5.4	9	0	81	176.8	177.7	0.26	1.9	99.0
850214	17 7 10.30	66N16.12	149W51.32	10.00				4.1	8	0	154	173.9	179.8	0.18	1.5	99.0
850214	1740 38.96	66N12.85	150W 6.28	8.70*				4.4	6	0	153	162.2	181.3	0.36	12.3	25.5
850214	23 6 58.40	66N22.83	149W36.16	10.00				4.3	9	0	159	185.7	186.7	0.16	1.8	99.0
850309	1357 57.26	66N15.93	149W47.61	13.97	4.6		5.0	4.8	10	0	83	27.9	177.6	0.16	1.9	3.0
850309	14 8 3.20	66N15.88	149W49.51	14.26	5.9	6.0		6.0	8	0	86	27.8	178.7	0.15	2.1	2.9
850309	1546 55.74	66N15.53	149W51.02	9.22	4.4		4.7		10	0	88	27.2	178.1	0.12	1.9	3.4
850309	1621 23.32	66N16.43	149W48.52	18.30	4.4	4.8	5.1	4.4	10	0	84	28.9	178.7	0.17	1.9	2.7
850309	1649 7.16	66N17.82	149W50.02	15.75			4.7	4.3	10	0	85	31.5	181.6	0.16	1.9	3.0
850310	358 20.97	66N14.22	149W53.35	12.87			4.5	4.4	9	0	153	25.0	176.7	0.14	1.9	3.0
850310	1210 49.97	66N14.64	149W51.30	20.03			4.3	4.3	10	0	90	25.6	176.7	0.20	1.8	2.5
850310	1330 28.67	66N13.67	149W52.97	14.08	5.2	4.9		5.6	10	0	94	24.0	175.7	0.13	1.8	2.8
850310	1916 39.00	66N14.46	149W52.55	14.95			4.2	4.2	10	0	92	25.4	176.8	0.15	1.8	2.8
850310	23 5 23.14	66N15.23	149W55.19	11.14				4.4	10	0	95	27.1	180.0	0.13	2.2	3.2
850318	1333 11.13	66N15.38	149W51.72	14.08	4.3		4.6	5.0	3	3	214	21.2	39.2	0.01	4.9	8.1
850321	346 6.96	66N12.67	149W55.13	12.26	4.3		4.6	4.5	10	0	96	19.5	41.8	0.26	1.6	1.5
850322	055 42.53	66N16.15	149W48.33	13.58			4.2		9	0	122	23.7	39.8	0.27	1.4	1.7
850326	1932 46.55	66N14.69	149W52.27	14.32			4.2	4.3	10	0	96	20.8	40.0	0.42	1.3	1.5
850327	320 9.90	66N12.91	149W56.99	13.35			4.1		10	0	96	18.1	40.7	0.31	1.3	1.5
850328	1540 0.49	66N15.19	149W51.25	10.49			4.3	4.3	10	0	98	21.5	39.7	0.17	1.3	1.7
850401	214 32.29	66N15.41	149W49.97	16.56	4.6		4.5	4.7	10	0	99	22.5	40.0	0.21	1.3	1.5
850404	225 10.69	66N21.45	149W46.15	20.45			4.5	4.0	10	0	117	27.3	38.2	0.16	1.4	1.5

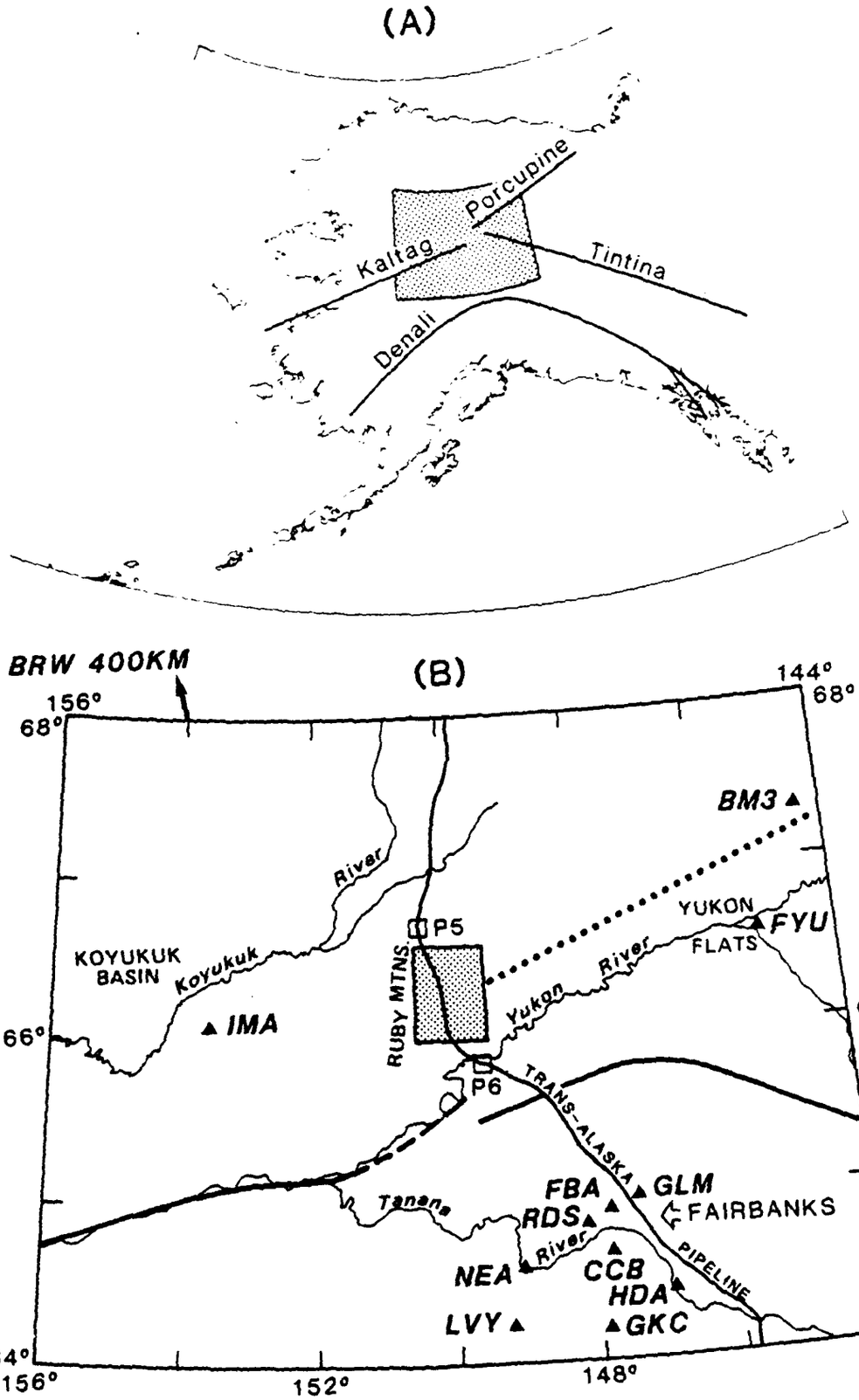
(A)
Porcupine
Kaltag
Tintina
Denali
BRW 400KM
(B)
156°
68°
144°
68°
BM3
River
YUKON
FYU
FLATS
P5
KOYUKUK
BASIN
Koyukuk
RUBY MTNS
Yukon River
IMA
66°
66°
P6
TRANS-ALASKA
FBA
GLM
FAIRBANKS
Tanana
RDS
River
PIPELINE
NEA
CCB
HDA
LVY
GKC
64°
64°
156°
152°
148°
144°

fig. 1

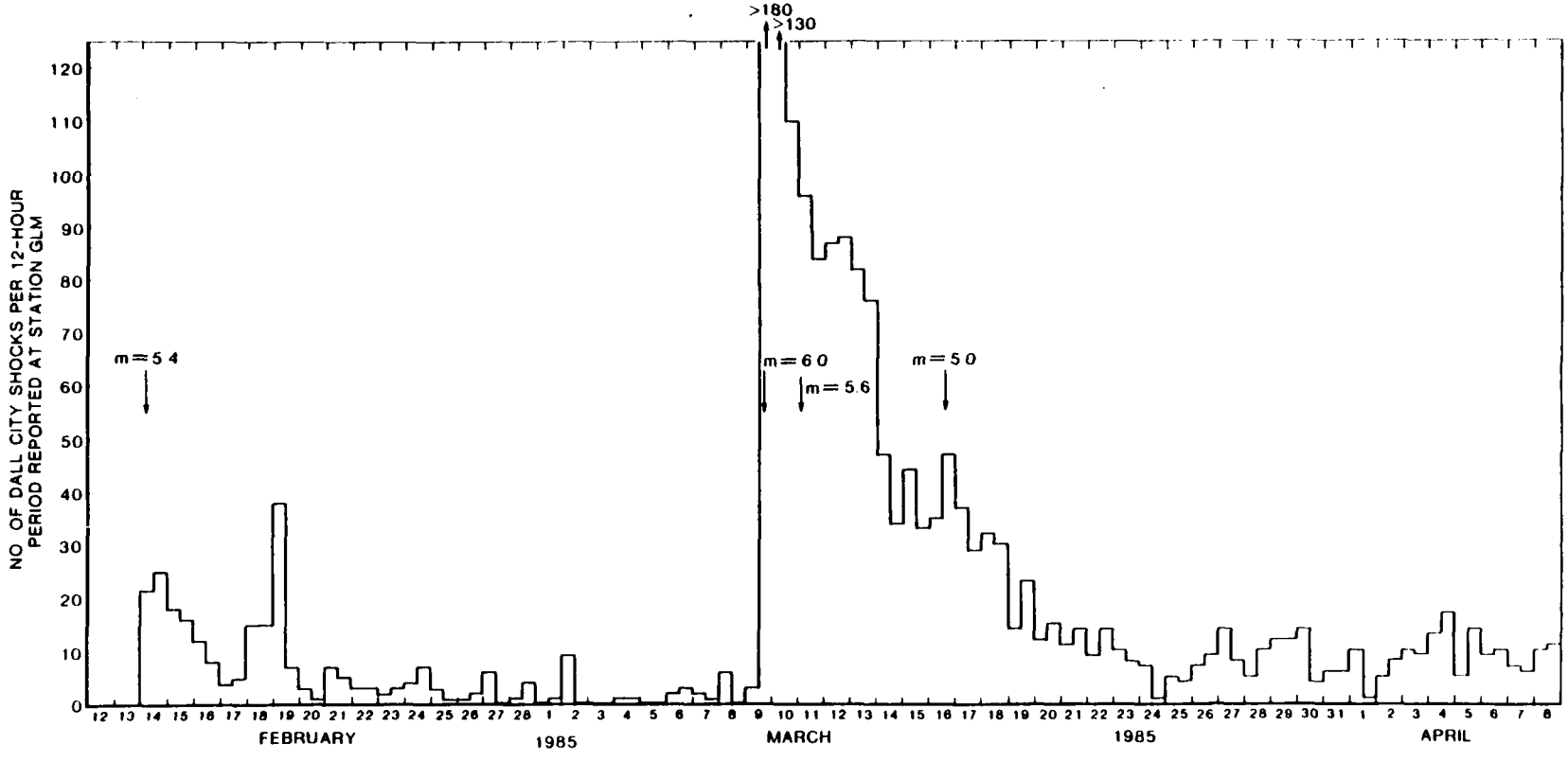
>180
>130
NO. OF DALL CITY SHOCKS PER 12-HOUR PERIOD REPORTED AT STATION GLM
120
110
100
90
80
70
60
50
40
30
20
10
0
m=5.4
m=6.0
m=5.6
m=5.0
12 13 14 15 16 17 18 19 20 21 22 23 24 25 26 27 28 1 2 3 4 5 6 7 8 9 10 11 12 13 14 15 16 17 18 19 20 21 22 23 24 25 26 27 28 29 30 31 1 2 3 4 5 6 7 8
FEBRUARY
1985
MARCH
1985
APRIL

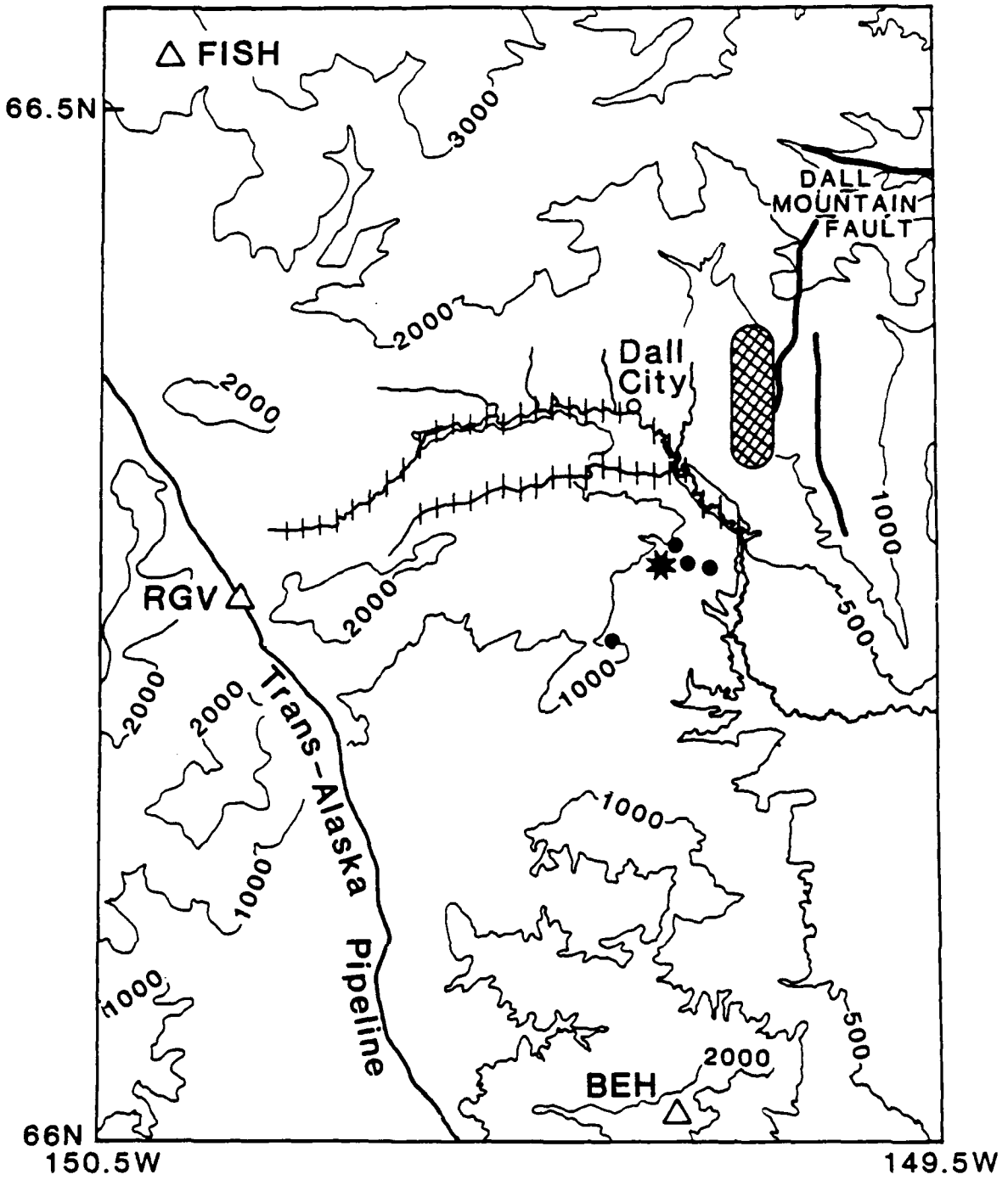
△ FISH
66.5N
3000
DALL
MOUNTAIN
FAULT
2000
Dall
City
2000
1000
RGV △
2000
500
1000
2000
2000
Trans-Alaska Pipeline
1000
1000
1000
500
2000
BEH △
66N
150.5W
149.5W

f.a.3

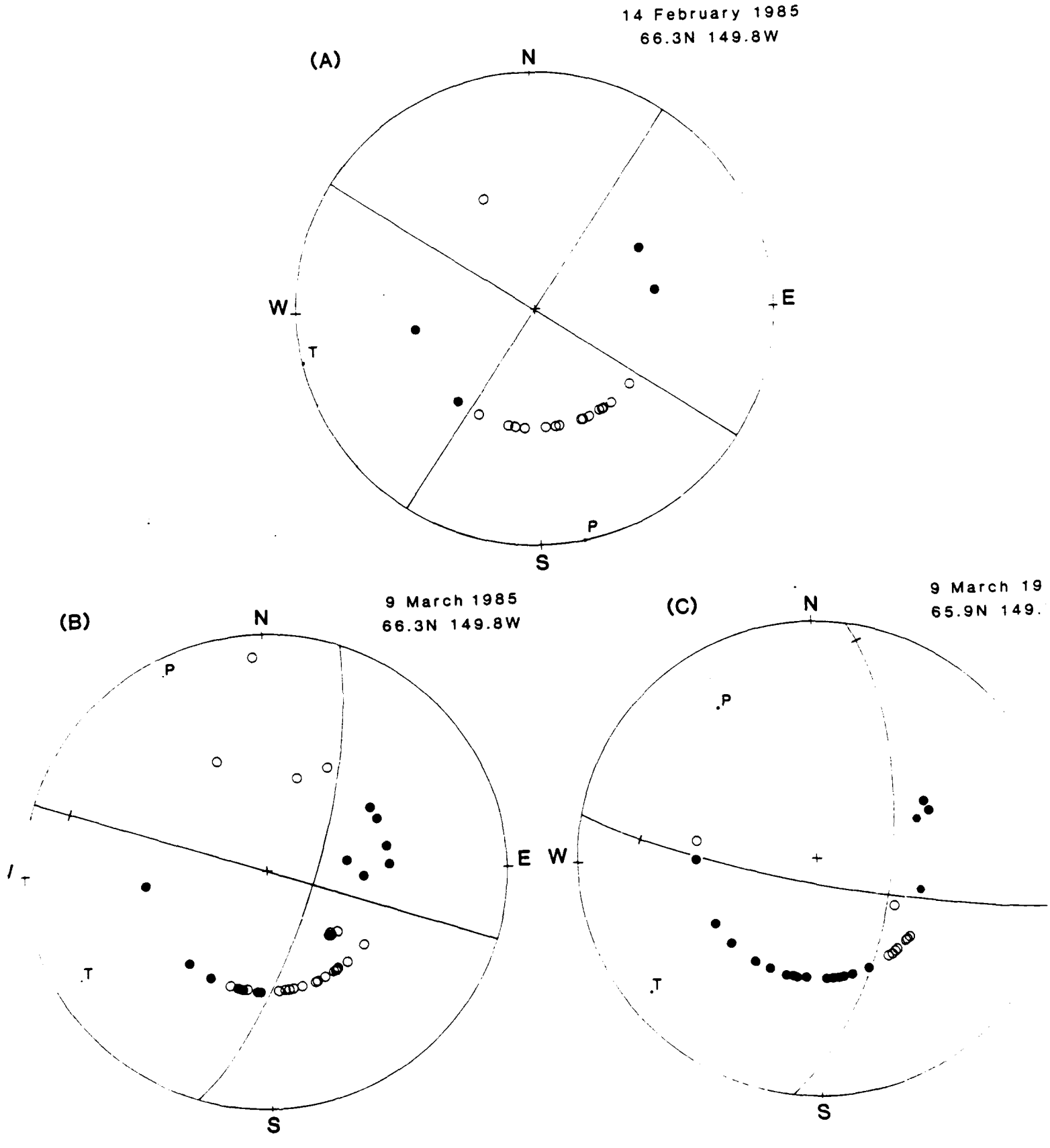
14 February 1985
66.3N 149.8W
(A)
N
W
E
S
T
P
(B)
9 March 1985
66.3N 149.8W
N
E
S
P
T
(C)
9 March 19
65.9N 149.
N
W
S
P
T

fig 4

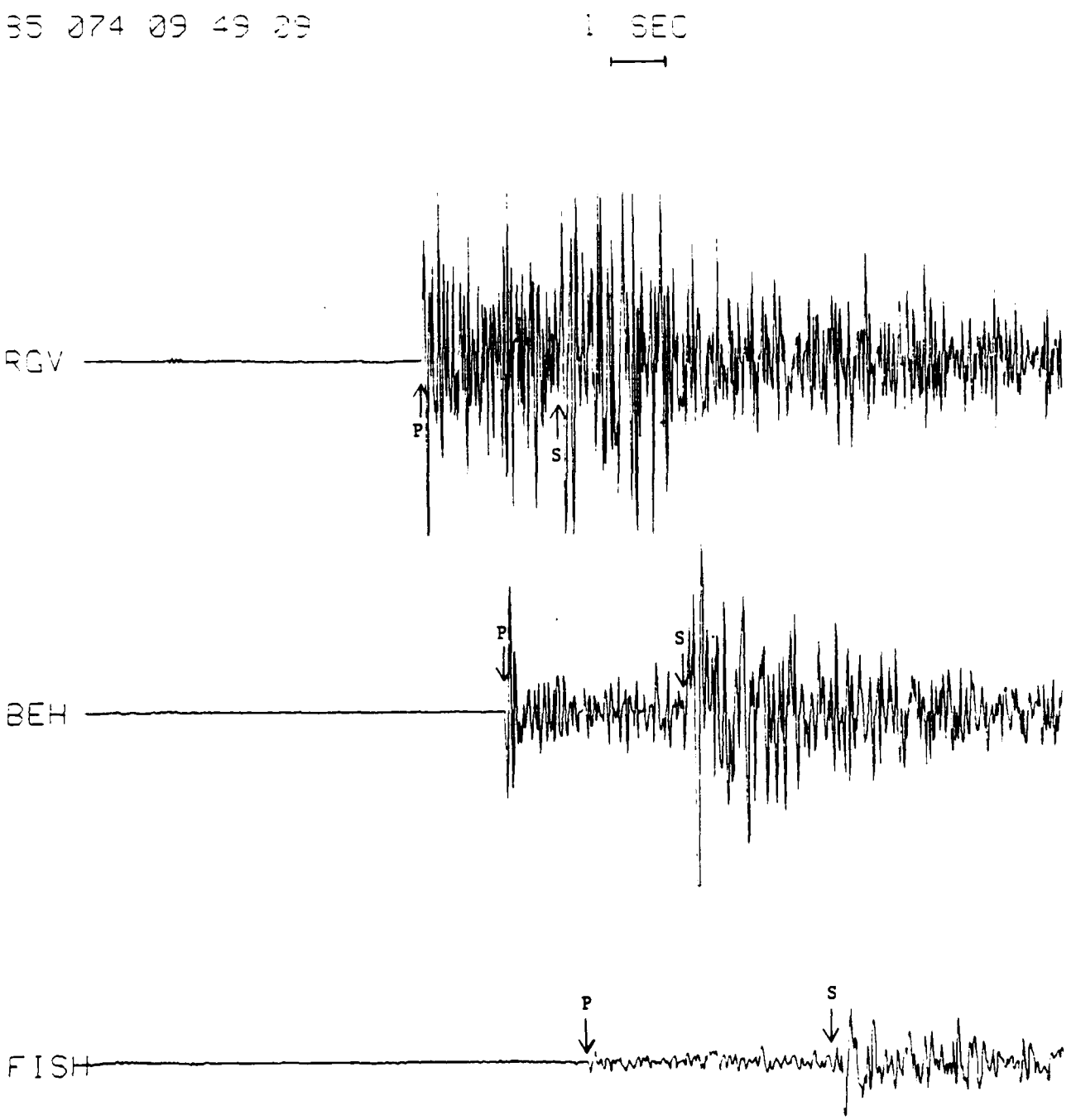

fig. 5

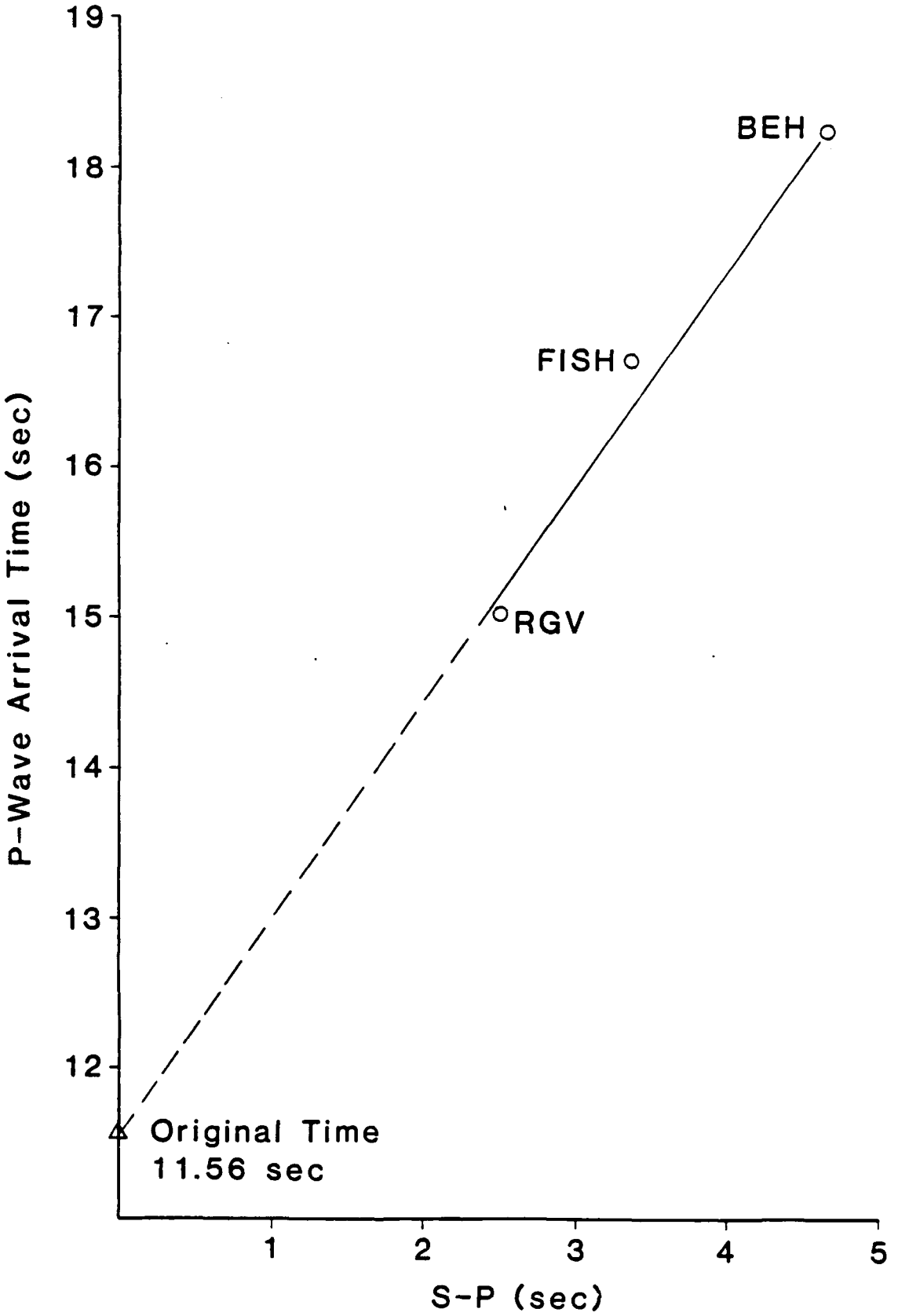
19
18
17
16
15
14
13
12
P-Wave Arrival Time (sec)
BEH
FISH
RGV
Original Time
11.56 sec
1
2
3
4
5
S-P (sec)

Fig. 6

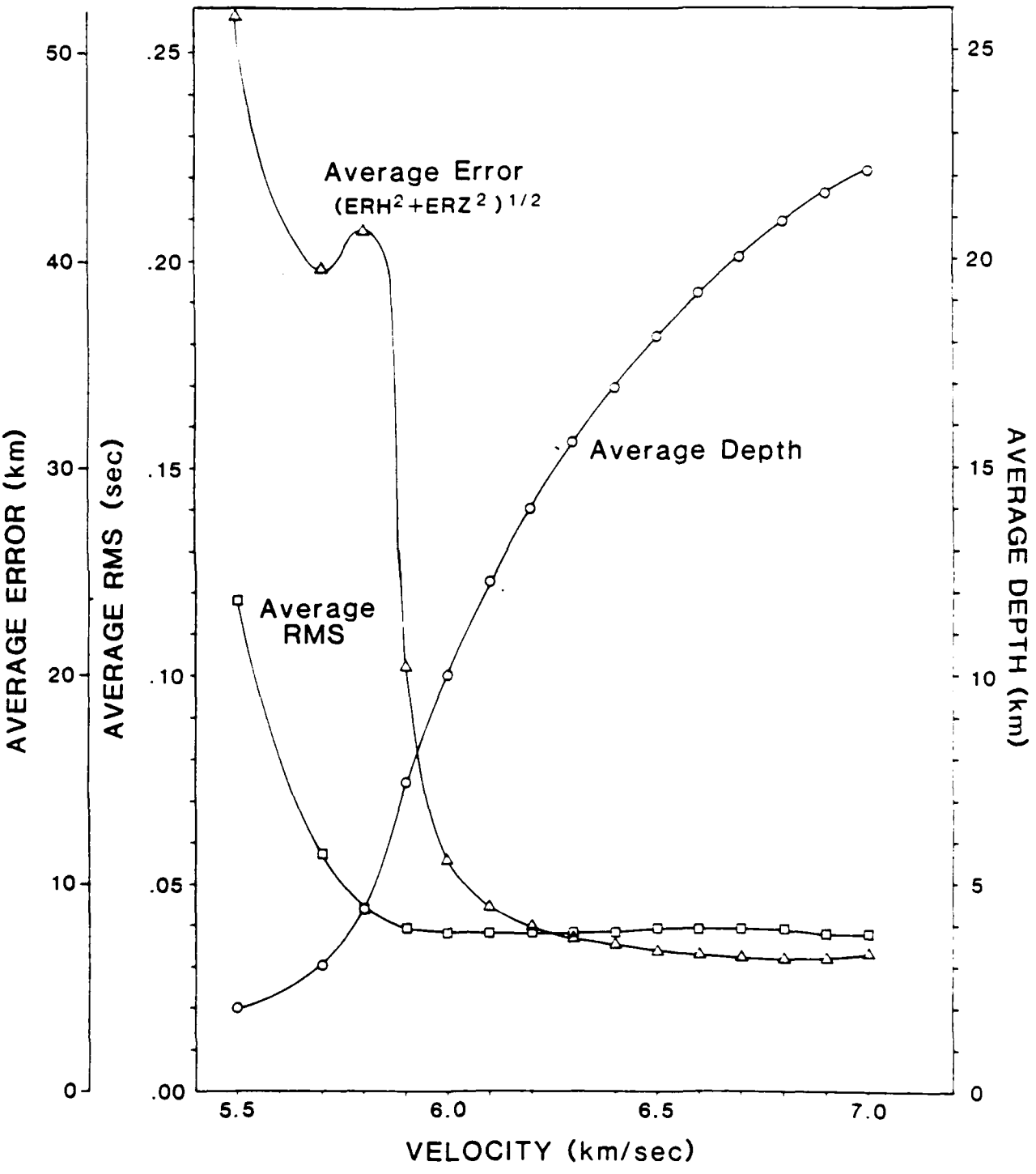
Average Error
(ERH² + ERZ²)^1/2
Average Depth
Average RMS
AVERAGE ERROR (km)
AVERAGE RMS (sec)
AVERAGE DEPTH (km)
VELOCITY (km/sec)
50
40
30
20
10
0
.25
.20
.15
.10
.05
.00
25
20
15
10
5
0
5.5
6.0
6.5
7.0

Fig. 4

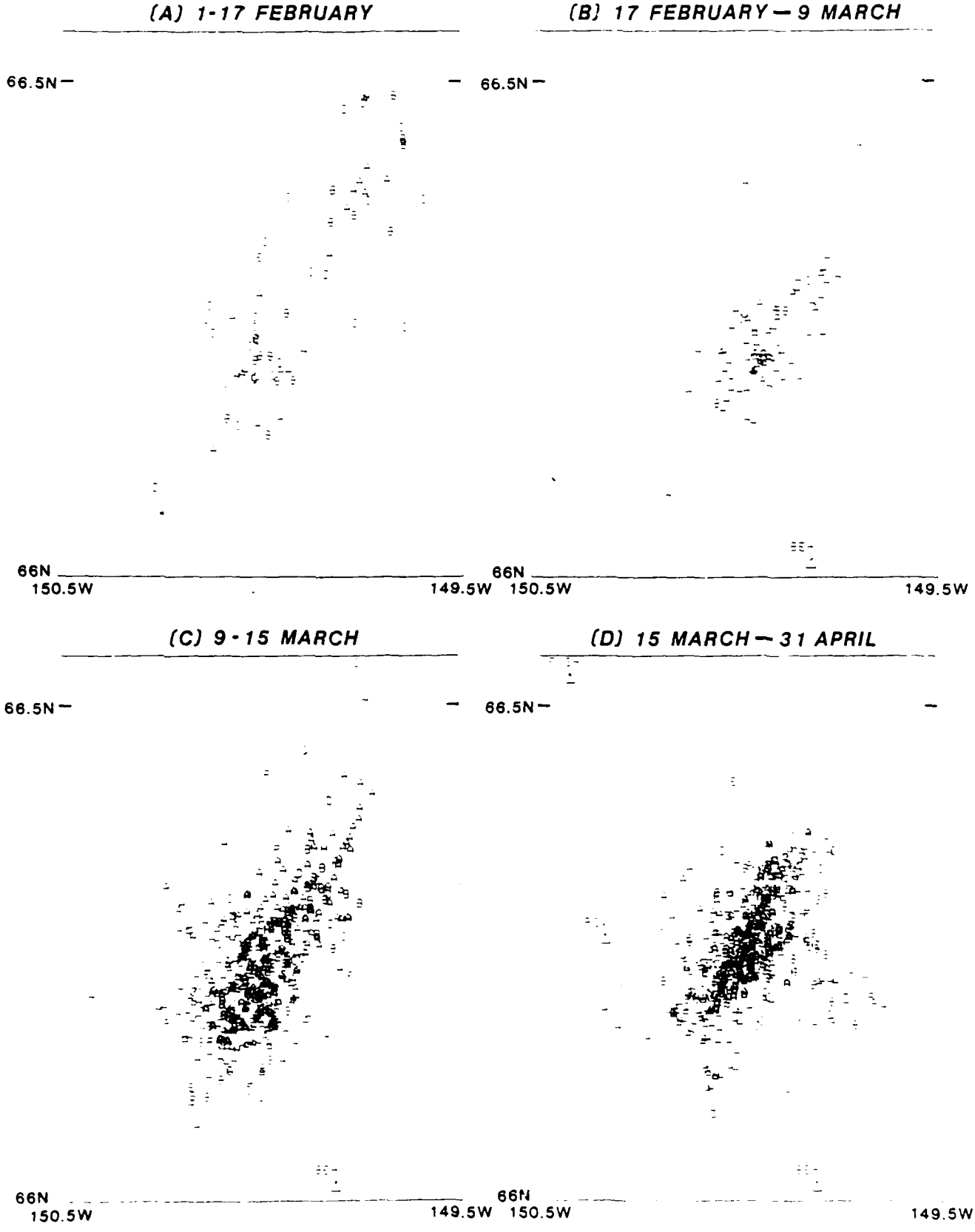
(A) 1-17 FEBRUARY
(B) 17 FEBRUARY — 9 MARCH
(C) 9 - 15 MARCH
(D) 15 MARCH — 31 APRIL
66.5N
66N
150.5W
149.5W

Fig. 8

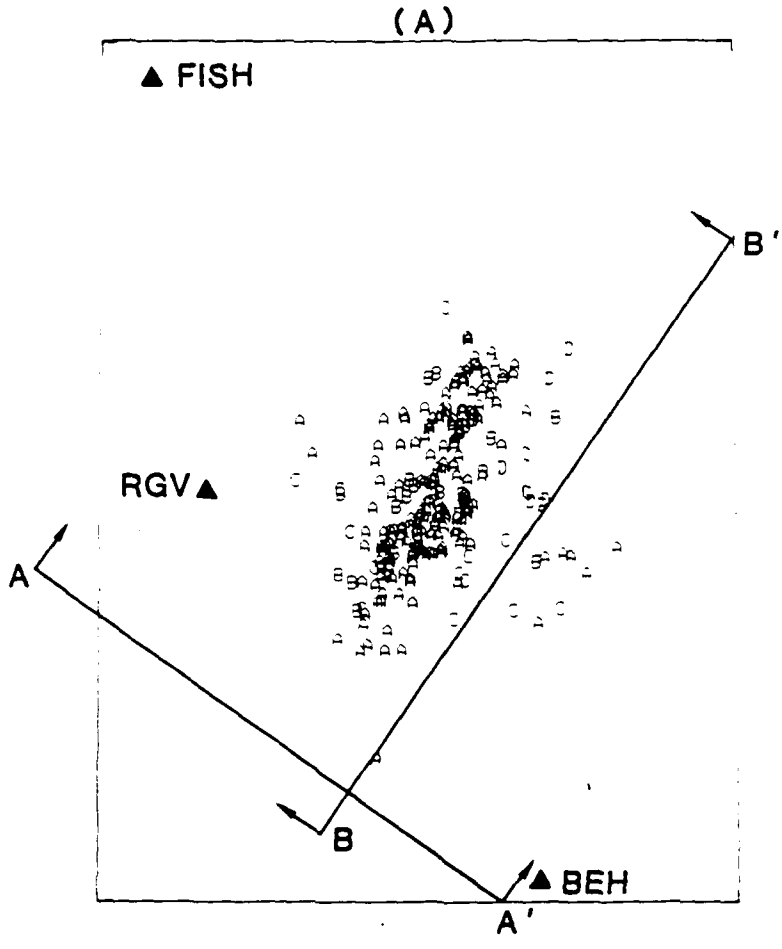

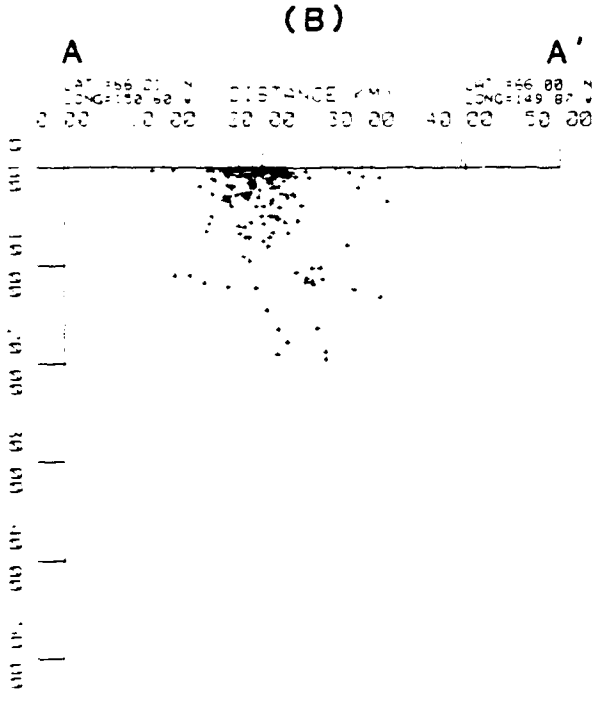

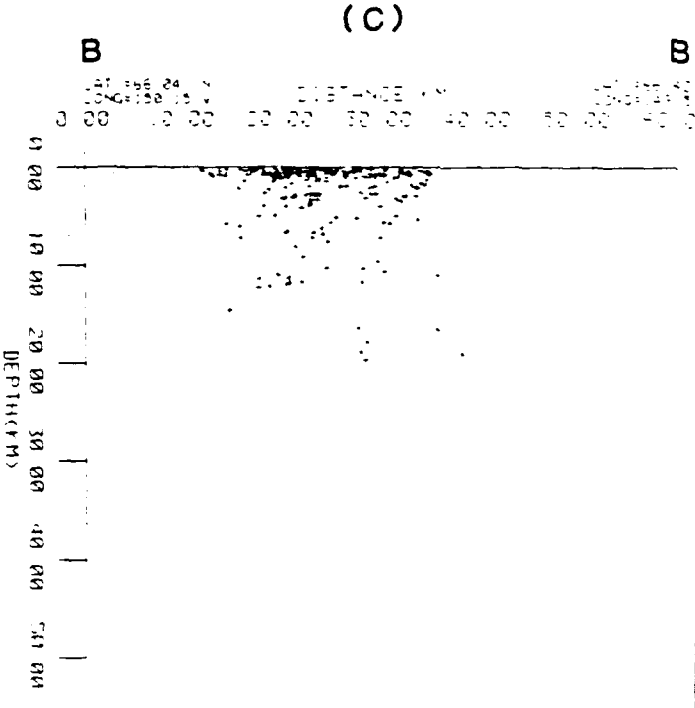

fig. 9

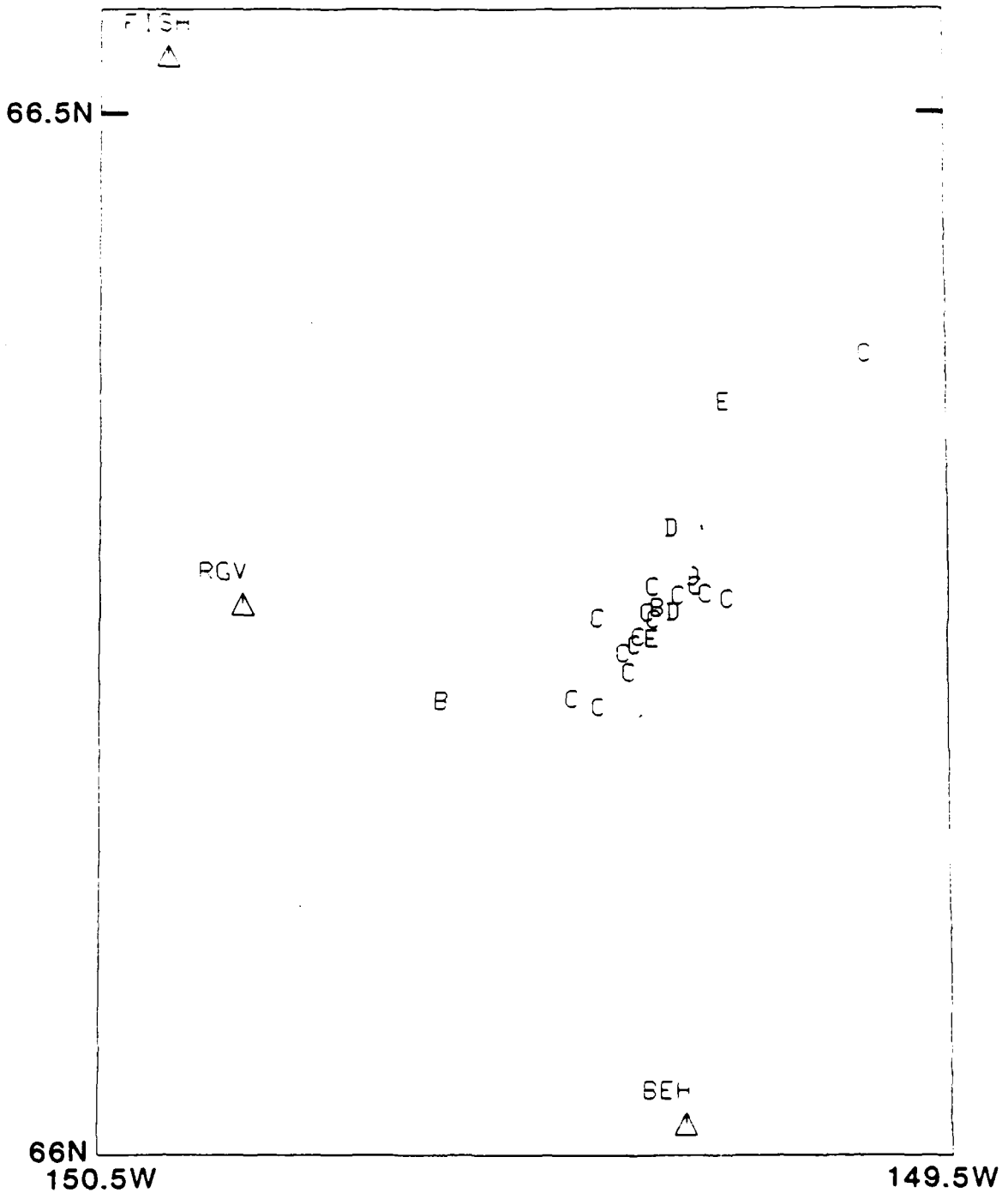

fig. 10

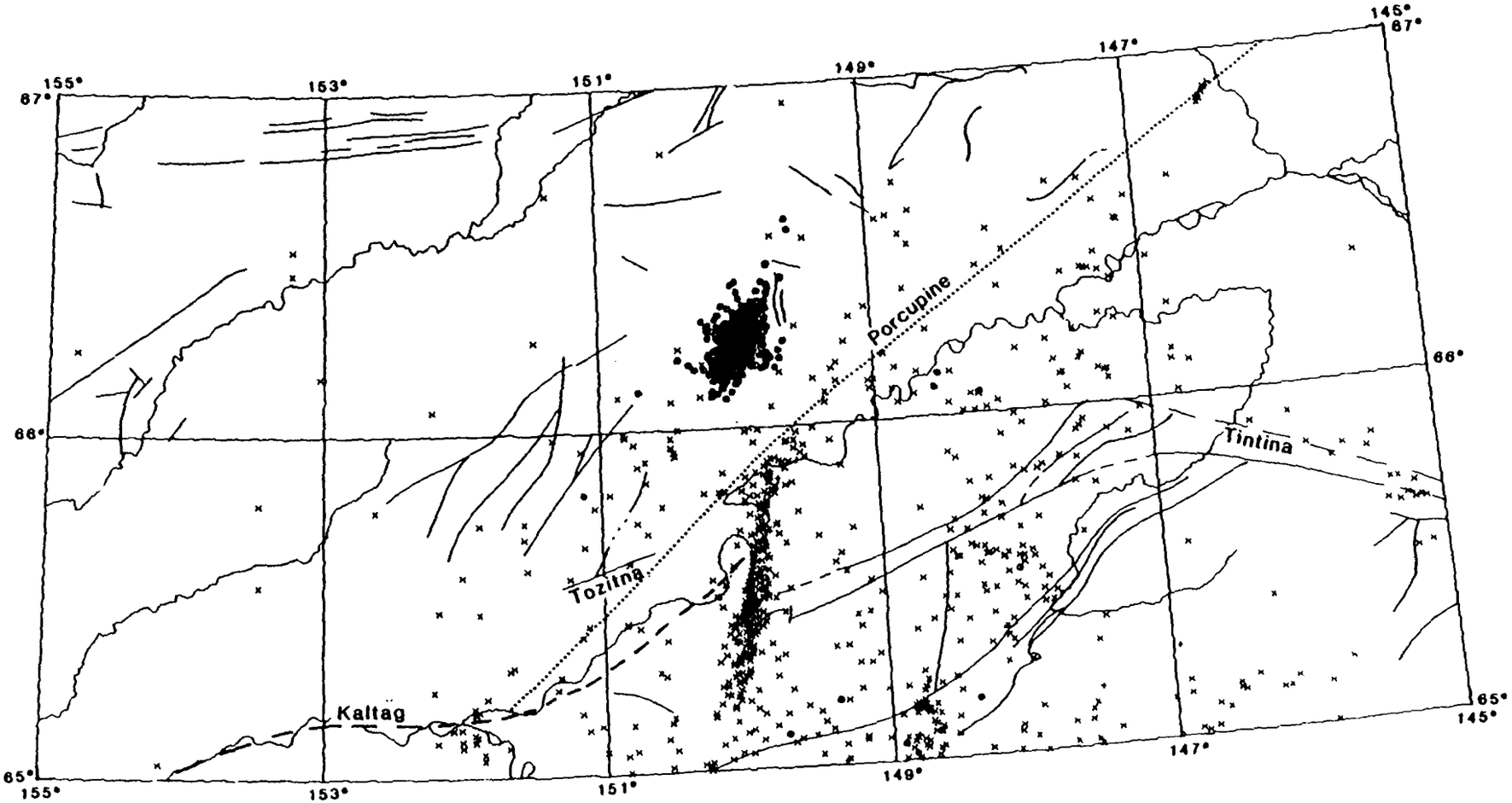
155°
153°
151°
149°
147°
145°
67°
66°
65°
Porcupine
Tintina
Tozitna
Kaltag

APPENDIX I

Seismicity and Focal Mechanism Studies of the 1985 Dall City Earthquakes, North-central Alaska

By Charles H. Estabrook, John N. Davies, Larry Gedney, Steven A. Estes and James P. Dixon

Abstract

In February and March of 1985, several moderate earthquakes occurred in central Alaska, 42 km north of the Yukon River crossing of the Trans-Alaska Pipeline. The largest of these, on 9 March (M_L 6.0) was felt widely in Interior Alaska; 38 events had magnitudes greater than 4.0. Several short period vertical seismometers were installed in the epicentral region by personnel from the Geophysical Institute of the University of Alaska. A P- and S-wave seismic velocity model determined using several well-recorded aftershocks indicates that granite is the major component of the upper crust in the epicentral area. This velocity model was used to locate the aftershocks. The aftershocks fall into two intersecting trends. The main trend (strike 28°) is 25 km long and dips 75-80° E, with depths ranging from the surface to 20 km. The secondary trend strikes 43°. These aftershocks are north of, but spatially separated from, the aftershock zone of the 1968, M_S 6.5 Rampart earthquake. They spread to the north and south along assumed fault planes related to the largest events and along a possible intersecting fault, with the largest earthquakes in the sequence occurring near the intersection of the two trends. Focal mechanism solutions of two of the largest events show left-lateral strike-slip faulting on NNE trending planes.

Introduction

In February and March of 1985, a sequence of five moderate earthquakes (magnitude 5 to 6) occurred in central Interior Alaska, approximately 40 km north of the Yukon River crossing of the Trans-Alaska Pipeline (Fig. 1). On 14 February (0504 UT), an event of magnitude 5.4 (M_L) occurred which was followed by a normal aftershock sequence. Figure 2 shows that activity had nearly ceased by the beginning of March. A remote seismic station (BEH, Fig. 3), installed on 17 February, was to be removed at about the time a second mainshock-aftershock sequence began. Early in the morning of 9 March (4:58 am AST; 1358 UT) an event of magnitude 5.0 (M_L) awoke a few people in the Fairbanks area. This was followed at 1408 UT by a magnitude 6.0 (M_L) shock, the largest earthquake to occur in Interior Alaska since the 1968 Rampart earthquake (Gedney *et al.*, 1969b; Huang and Biswas, 1983).

The 1408 event was felt widely in Interior Alaska -- as far away as Delta Junction, 300 km southeast, and Coldfoot, 200 km north in the Brooks Range. In Fairbanks, 180 km southeast of the epicenter, the Intensity of the earthquake (Modified Mercalli Scale) was IV; in Manley Hot Springs, 90 km from the epicenter, where grandfather clocks stopped, the Intensity was V; and at the Yukon River Crossing, where an Alaska Department of Transportation Trailer was shaken off its supports, the Intensity was probably VI.

In the epicentral area, where there are no manmade structures, the effects of the quakes included numerous stream overflows and spring rejuvenation. However, there was no observed ground breakage. Muddy water appeared to have overflowed on the West Fork of the Dall River approximately 10 km due north of the epicentral area (Fig. 3). Recent stream icings (spring rejuvenation following the largest events) were seen along the north-south portion of the Dall River (F. Weber, pers. comm.) and along the east-west portion, west of Dall City (the site of a prospectors' camp abandoned in 1901). These effects were observed during several flights over the epicentral area by helicopter and fixed-wing aircraft from February through April.

Geologic Setting

The Dall City earthquakes occurred in a region of low hills between the Ruby Mountains and the Yukon Flats in north-central Alaska (Fig. 1). Pelitic schists and granites of Paleozoic and Mesozoic age characterize the geology of the epicentral area (Brosgé *et al.*, 1973). Though structural features are often obscured by the extreme weathering of the schists and granites, several faults have been mapped in the epicentral area. The Dall Mountain fault (Brosgé *et al.*, 1973; Brogan *et al.*, 1975; and Plafker, unpubl. data) trends north-south approximately 10 km east of the epicenters. Several

northeast trending faults have been mapped in the area to the west of the epicenters (Dover and Miyaoka, 1985). The Tintina and Kaltag fault systems are found to the southeast and southwest of the epicenters respectively. These faults exhibit recent movement (Brogan *et al.*, 1975; Estabrook *et al.*, 1985). An aeromagnetic lineation, the Porcupine lineament (Brosgé *et al.*, 1970), crosses the area from the northeast. To the east of the epicenters is the Yukon Flats, a Quaternary basin which may have developed as an extentional graben from strike-slip movement along the Tintina fault (Kirschner *et al.*, 1985).

Data Sources

The seismic data for the Dall City events recorded by the Geophysical Institute can be divided into five sets (Table 1) based on differing combinations of local recording stations used to supplement the existing regional network (Fig. 1). Prior to the installation of a short-period vertical seismometer at the ALASCOM Microwave Repeater Site, Bench (BEH), on February 17, the closest station was at Indian Mountain (IMA), about 170 km west in the Koyukuk Basin. Hence the first data set was recorded with no local stations. BEH was the only local station operating until two additional stations began operating on March 15. Data recorded with the single local station, BEH and the regional network constitutes the second data set. Attempts were made to install a station

at Fish Microwave Repeater Site (FISH, Fig. 3) in February but the effort was abandoned due to extreme winter weather conditions (extremes greater than -41°C and 75 km/hr winds were recorded at BEH the same day) and a decrease in aftershock activity (Fig. 2). By 15 March attempts to install this station were successful and data were being collected from BEH, FISH and a third local station emplaced at a remote gate valve on the Trans-Alaska Pipeline (RGV, Fig. 3). Data from those stations in combination with that from the regional network comprise the third data set. The local network was modified slightly in April (fourth set) and entirely removed in June 1985 (fifth set).

Data from all of the Interior Alaska stations used by the Geophysical Institute are recorded in analog form on a Teledyne Geotech Develocorder. In addition, an event detection system, developed by Steven Estes, records signals from the same stations in digital form (8 bits/sample at 50 samples/s). An earthquake is recorded when the ratio of a short term average of the signal to the long term average exceeds 3.5 at three stations during a thirty second period. Both analog and digital data were used in this study.

Focal Mechanisms

Fault plane solutions were determined for the two largest earthquakes (14 February 0504 and 9 March 1408) in the

sequence. In addition, a solution was obtained for an earlier earthquake in the same area which occurred nearly ten years to the minute before the largest one in 1985 (1419, 9 March, 1975). The mechanisms were determined using a linearly increasing velocity model with the hypocentral depths fixed at 10 km. The parameters of these focal mechanisms are given in Table 2. All three events are strike-slip solutions with very similar nodal plane orientations (Fig. 4). The 14 February mechanism, which utilized only regional Alaska stations, is very dependent upon an emergent P-wave arrival at Barrow (BRW, the dilatation in the northwest quadrant). The 9 March solution utilizes first motion readings from the Canadian Seismograph Network, the U. S. Geological Survey's Central California Network and the Lamont-Doherty Geological Observatory station at Palisades, NY. This mechanism is much more tightly constrained. Note that a high-angle NNW trending nodal plane is common to both solutions. The 9 March, 1975 event occurred 25 km to the south of the other two and was smaller in magnitude (M_L 4.6) (Estabrook, 1985).

Crustal Velocity Determination

The local P- and S-wave velocity structure in the Dall City area was studied utilizing the availability of digital data and the close station spacing. The approach taken was to determine a V_p/V_s ratio for the Dall City area and then use

this ratio in the HYPOELLIPSE earthquake location program (Lahr, 1982) to find a minimum in the location and travel-time error estimates as a function of the model velocity.

Figure 5 shows an example of a Dall City event, with well recorded P- and S-waves, which was used in the velocity studies. Wadati diagrams were used to determine the V_p/V_s ratio (Fig. 6). The resultant V_p/V_s ratio of 1.68 ± 0.03 (for nine earthquakes) is very close to 1.69 that was determined by Gedney *et al.* (1969a) from aftershocks of the 1967 Fairbanks earthquakes.

Studies of seismic velocities in granitic and metamorphic rocks in the Ukrainian Shield (Lebedev and Korchin, 1979) show that V_p/V_s is higher for mafic rocks (1.77 ± 0.06) than for silicic rocks (1.68 ± 0.09). Pelitic schists have values comparable to silica-rich igneous rocks (Press, 1966). The presence of silica-rich metamorphics and granites at the surface in the Dall City area (Brosgé *et al.*, 1973), combined with a V_p/V_s ratio of 1.68, indicates that quartz-rich rocks (granites or schists) occur at depth in the region.

In an attempt to determine the P-wave velocity for the Dall City region, the crustal P-wave velocity in our model (Table 3) was increased at 0.1 km increments from 5.5 to 7.0 km/s. These velocities were used in the HYPOELLIPSE program to locate 10 earthquakes for which very good P- and S-wave arrivals were recorded at the local stations BEH, RGV and FISH.

The results of this study (Fig. 7) show that as we increase the crustal velocity in our model, the location errors ($(ERH^2 + ERZ^2)^{1/2}$) and root-mean-square (RMS) of the travel-time residuals decrease. It was hoped that a minimum in location error and RMS could be found. However, because the local station distribution is nearly linear, there is a trade-off between epicentral location and depth as the velocity increases. A crustal velocity of 6.0 km/s corresponds to the point at which RMS and location errors asymptotically approach a lower limit. Though velocities higher than this also have very small location errors and RMS, velocities greater than 6.3 km/s yield depths that are unreasonable for Interior Alaska (Fairbanks area: Gedney *et al.*, 1980) and south-central Alaska (Castle Mountain fault: J. Lahr, pers. comm., 1984).

Taking into consideration the factors of surface geology, a minimum value for the upper crustal velocity and the V_p/V_s ratio, we can constrain the geology and velocity at depth by making the assumption that if earthquakes in the Dall City area have depths similar to those of other earthquake sequences in continental Alaska, then the velocity of the upper crust must lie between 6.0 and 6.3 km/s. Since the stations used in the local velocity study vary from 15 to 40 km from the epicenters, the rays leaving an earthquake at 10-15 km depth will generally travel upward to the stations. Thus the local velocity corresponds to that of an upper crust having a thickness of at

least the depths of the earthquakes. This value of the upper crustal velocity agrees with the 6.04 km/s velocity determined from a regional earthquake in the eastern Brooks Range (Estabrook *et al.*, 1985).

Press (1966) reports that for depths to 15 km (5 kbars), granites have P-wave velocities of about 6.3 km/s while schists have velocities that vary from 6.5 to 6.9 km/s. Since the upper crustal velocity is 6.0-6.3 km/s, the rock type of the material at depth (about 10 km) must then be mainly granitic with possibly some schist, although some sedimentary rock types (graywacke and some limestones) also fit the P-wave velocity criteria of 6.0-6.3 km/s. More mafic rocks (gabbro, dunite and ophiolitic rocks) are ruled out as major components of the upper crust because their P-wave velocities are too high.

Seismicity

Because four distinct station distributions were used during the two month period to record the Dall City earthquakes, a uniform interpretation of the sequence is difficult. The first data set (Fig. 8a) contains earthquakes located only with stations at Pn distances. During this time, the depths of the events are not well constrained. Since BRW was the only station located to the north of the epicenters (further than 600 km), the epicenters will more likely be mislocated in the north-south direction. Lee and Stewart

(1981) showed that when there is a large gap in station distribution, the epicenter will be mislocated away from its real location toward that gap. The second data set (Fig. 8b) contains earthquakes located with the regional stations (as in set 1) and a single local station to the south of the Dall City area (BEH). In this set, errors in depth are reduced because the ratio of depth of the event to the distance to the local station is about 1:2. Epicentral errors are still likely because of the gap problem, though the errors should be smaller than without the local station. Earthquakes in the third set (Fig. 8c) are located with the regional network (same as the first two) and three local stations. With the linear local station distribution, computed hypocenters will move toward the largest gap, which is away from the axis of the local stations. This effect is minimized with accurate S-wave readings for the smaller events and the inclusion of regional stations FYU and BM3 (Fig. 3) to the east of the epicenters in the hypocentral location process.

Figure 8 contains maps of all the solutions obtained with data to the end of April 1985. Notice that scatter is reduced when local stations are used in the solutions. The trend of epicenters from the data sets delineates a N28°E trend. Figure 8d, in addition, shows a N43°E trend that intersects the main trend in the vicinity of the largest events.

To delineate the fine structure of the aftershock trend, the earthquakes located with three local stations plus the regional network were graded on the basis of quality. It is assumed that mislocated earthquakes will have large location and travel-time errors. From Figure 9a, which shows the best solutions of this period (ERH and ERZ $\leq$ 10 km, RMS $\leq$ 0.5 s), a very clear NNE-SSW lineation along with a possible ENE-WSW lineation emerges. Cross-sections of this data set are shown in Figures 9b and 9c. Figure 9b shows that the trend dips steeply to the east. Drawn on this cross-section is the north trending nodal plane of the 9 March event. Notice that the dips are nearly the same. The seismic width of the aftershock zone, about 10 km, is likely to be thinner but beyond the resolution possible with the network configuration. In the longitudinal section (Fig. 9c), the aftershock zone is roughly 20 km long. It appears in plots of aftershocks of the 14 February event prior to the installation of BEH (Fig. 8a).

With the exception of the Dall Mountain fault about 10 km to the east, there is no structural feature in the epicentral area with topographic expression subparallel to the N28°E trend of the aftershocks. The N43°E trend is parallel to an escarpment extending from the Ray Mountains in the west, to the east along the northern boundary of the Yukon Flats. Also on this trend are several hot springs in the Ray Mountains, which may indicate that the lineament extends through the granite of

the mountains. On a geologic map of the Beaver quadrangle (1:250000: Brosgé *et al.*, 1973), there is no mapped fault parallel to, or geologic discontinuity across, the escarpment. However recent mapping just to the west of the epicentral region indicates that a northeast trending fault parallels the escarpment (Dover and Miyaoka, 1985). This fault (with an associated 1-3 m wide zone of fault gouge) was observed in a quarry off the Dalton Highway by one of the authors (Estabrook).

Discussion

Focal mechanisms of the two largest events show either left-lateral faulting on NNE oriented planes or right-lateral faulting on ESE oriented planes. The major trend of the aftershocks is parallel to the NNE trending nodal plane. On this basis, and in consideration of the parallelism of the NNE nodal planes with the mapped trace of the Dall Mountain fault, the NNE plane is preferred.

Figure 10 is a plot of 18 of the largest events of the sequence (see Table 4 for location parameters). These events were selected because they were all large enough to be recorded at BRW (Barrow), a low-gain station that is only able to record events with magnitudes greater than 4.0 at this distance. Notice that the events cluster near the intersection of the two aftershock trends (compare with Figure 9a). The large events

also show temporal grouping and possible westward migration. The events of 14 February and 9 March cluster in the east, those of 10 March are located 3-5 km to the southwest. Either this is a migration on a single fault plane oriented northeast or faulting on a series of parallel north-south trending faults which intersect the secondary aftershock trend. If the NNE nodal plane is the fault plane and the larger shocks actually do migrate from east to west, then we interpret that there is a parallel set of north-south trending faults in the vicinity of the Dall Mountain fault that intersect the northeast trending faults.

The location of the larger earthquakes in a relatively small area of the aftershock zone implies that stress must be concentrated in this region. The probable asperity (stress concentration) is at the intersection of the two aftershock trends. The majority of the aftershocks occurred on a trend parallel to the fault plane of the 9 March mainshock. The N43°E aftershock trend would then represent sympathetic motion on an intersecting fault.

The seismicity data compiled by Estabrook *et al.* (1985) indicates that the Dall City aftershocks plot just north of the aftershock zone of the 1968, M_S 6.5 Rampart earthquake northward to 66.5°N with slightly different trends (Fig. 11). This map clearly shows that since the two earthquake sequences do not touch or follow the same trend, they occurred on

different lineaments. The Dall City aftershocks are parallel to faults to the west (Dover and Miyaoka, 1985), while the Rampart events follow a trend that connects two segments of the Kaltag fault system (Huang and Biswas, 1983), stopping just south of the Yukon River. The two aftershock zones are separated by faults of the Kaltag fault system.

Portions of the Kaltag, Porcupine and Tintina fault systems are all found within the region. Both the Kaltag fault and the Porcupine lineament, inferred from aeromagnetic data, parallel the northeast trending escarpment. To add to the confusion, a line can be drawn which follows the trace of the Tintina fault through the Dall City epicentral region; however, this trend is not consistent with either of the two aftershock trends. Only the faults mapped by Dover and Miyaoka (1985) to the west and the northeast trending escarpment have similar trends to the aftershocks. In fact, several faults that they mapped intersect at approximately the same angle as that of the two aftershock trends (15°). On this basis we surmise that the Dall city earthquakes occurred at the intersection of two faults of the same system as those mapped by Dover and Miyaoka, with the largest earthquakes occurring near the intersection.

Acknowledgments

We would like to thank Florence Weber, Rod Combellick and Dave Hopkins for recounting their observations during a flight over the Dall City area in March, 1985. The Alaska Pipeline Service Company (ALYESKA) allowed access to several critical sites along the Pipeline. ALASCOM provided technical assistance and access to their microwave repeater sites. Robert Horner of the Canadian Seismic Network, John Lahr of the U. S. Geological Survey and Klaus Jacob of Lamont-Doherty Geological Observatory kindly provided first motion data. Discussions with John Lahr helped to solve some of the peculiar earthquake location problems. Dianne Marshall and Gilein Steensma helped with the field work. Funding for the study came from Alaska Division of Geological and Geophysical Surveys, State of Alaska funds accrued through the Geophysical Institute, USGS grant 14-08-00001-G-1109 and AFOSR grant 85-0266.

References Cited

Brogan, G. E., L. S. Cluff, M. K. Korringa and D. B. Slemmons, Active faults of Alaska, *Tectonophysics*, *29*, 73-85, 1975.

Brosgé, W. P., E. E. Brabb and E. R. King, Geologic Interpretation of Reconnaissance Aeromagnetic Survey of Northeastern Alaska, *U. S. Geol. Surv. Bull. 1271-F*, 1970.

Brosgé, W. P., H. N. Reiser and W. Yeend, Reconnaissance Geologic Map of the Beaver Quadrangle, Alaska, *U. S. Geol. Surv. Misc. Field Studies Map MF-525*, 1973.

Dover, J. H. and R. T. Miyaoka, Major rock packages of the Ray Mountains, Tanana and Bettles Quadrangles, in *The United States Geological Survey in Alaska -- Accomplishments During 1983*, S. Bartsch-Winkler and K. M. Reed, eds., *U. S. Geol. Surv. Circ. 945*, 32-36, 1985.

Estabrook, C. H., *Seismotectonics of Northern Alaska*, Master's Thesis, University of Alaska, Fairbanks, 1985.

Estabrook, C. H., J. N. Davies and D. B. Stone, Seismotectonics of Northern Alaska, submitted to

J. Geophys. Res., 1985.

Gedney, L. and E. Berg, The Fairbanks earthquakes of June 21, 1967; aftershock distribution, focal mechanisms, and crustal parameters, *Bull. Seism. Soc. Am.*, *59*, 73-100, 1969a.

Gedney, L., E. Berg, H. Pulpan, J. Davies and W. Feetham, A field report on the Rampart, Alaska, earthquake of October 29, 1968, *Bull. Seism. Soc. Am.*, *59*, 1421-1423, 1969b.

Gedney, L., L. Shapiro, D. Van Wormer and F. Weber, *Earthquake epicenters in Interior Alaska, 1968-1971, and their correlation with mapped faults*, Report UAG R-218, Geophysical Institute, Univ. of Alaska, Fairbanks, Alaska, 1972.

Gedney, L., S. A. Estes and N. N. Biswas, Earthquake migration in the Fairbanks, Alaska seismic zone, *Bull. Seism. Soc. Am.*, *70*, 223-241, 1980.

Huang, P. and N. N. Biswas, Rampart seismic zone of central Alaska, *Bull. Seism. Soc. Am.*, *73*, 813-829, 1983.

Jordan, J., G. Dunphy and S. Harding, The Fairbanks, Alaska

earthquakes of June 21, 1967, *Preliminary Seismological Report, U. S. Dept. of Commerce, ESSA, U. S. Coast and Geodetic Survey*, 60 pp., 1968.

Kirschner, C. E., M. A. Fisher, T. R. Bruns and R. G. Stanley, Interior Provinces in Alaska, *Abstracts and Programs, AAPG-SEPM-SEG Pacific Section*, p. 63, 1985.

Lahr, J. C., HYPOELLIPSE/VAX: a computer program for determining local earthquake hypocentral parameters, magnitude, and first motion pattern, *U. S. Geol. Surv. Open File Report 80-59*, 1982.

Lebedev, T. S. and V. A. Korchin, Dynamics of changes in elastic properties of rocks under varying P-T conditions of the Earth's Crust, in *Theoretical and Experimental Investigations of Physical Properties of Rocks and Minerals under Extreme P, T conditions*, H. Stiller, and M. P. Volarovich, eds., Berlin, 1979.

Lee, W. H. K. and S. W. Stewart, Principles and applications of microearthquake networks, *Adv. Geophys. Suppl. 2*, 1981.

National Earthquake Information Service, *Preliminary Determination of Epicenters*, U. S. Geol. Surv., May

1967-April 1985.

Norris, D. K. and C. J. Yorath, The North American plate from the Arctic Archipelago to the Romanzof Mountains, in *The Ocean Basins and Margins, v. 5: The Arctic Ocean*, A. Nairn, M. Churkin and F. G. Stehli, eds., New York: Plenum Press, 37-103, 1981.

Press, F. Seismic velocities, *Handbook of Physical Constants*, S. P. Clark, ed., *Geol. Soc. Am. Mem., 97*, 195-221, 1966.

Author Affiliation

Geophysical Institute

University of Alaska

Fairbanks, AK 99775-0800 (CHE, JND, LG, SAE and JPD)

Division of Geological and Geophysical Surveys

State of Alaska

Geophysical Institute

University of Alaska

Fairbanks, AK 99775-0800 (JND)

Figure Captions

Fig. 1. (a) Location map for Dall City earthquake studies. (b) Interior Alaska seismograph stations (three letter codes) used to locate the Dall City earthquakes of February to April 1985. The shaded area delineates the location of all of the seismicity plots. P5 and P6 are pump stations along the Trans-Alaska Pipeline. The Kaltag and Tintina faults (heavy lines in the west and east, respectively) and the Porcupine lineament (dotted line) are from King (1969).

Fig. 2. Histogram of Dall City earthquakes as recorded at Gilmore Dome (GLM).

Fig. 3. Map of surface effects of the March 1985 earthquakes. Hatchered area is zone of spring rejuvenation. Tick marks on streams indicate zone of stream overflow and broken ice. The asterisk shows the location of the M_L 6.0 event of 1408, 9 March. Solid dots are earthquakes with $M_L \geq 5.0$. The Dall Mountain fault is from Brosgé, *et al.* (1973).

Fig. 4. Fault plane solutions of the 14 February, 9 March 1985 and 9 March 1975 earthquakes. They are equal area lower hemisphere projections showing quadrants of compressional (dark circles) and tensional (open circles) first motion. The

letters 'P' and 'T' are the pressure and tensional axes respectively. Tick marks on the nodal planes represent the poles to the other planes.

Fig. 5. Seismogram of an event used in the Vp/Vs ratio and crustal structure study.

Fig. 6. Wadati diagram of the earthquake in figure 5. The line connecting the points is a least-squares fit giving a Vp/Vs ratio of 1.68.

Fig. 7. Location error $(ERH^2+ERZ^2)^{1/2}$, travel-time residual (RMS) and depth as a function of P-wave velocity for Vp/Vs = 1.68.

Fig. 8. Earthquakes which occurred from (a) 1 to 17 February 1985, prior to the installation of BEH; (b) 17 February to 9 March, prior to the 1408 event; (c) 9 March to the installation of FISH and RGV on 15 March; and (d) after the installation of FISH and RGV to 30 April. Depths are indicated by letter: A=0 to 5 km, B=5 to 10 km....

Fig. 9. (a) Earthquakes recorded during the period from 15 March to 30 April (as in Figure 8d) with ERH and ERZ $\leq$ 10 km, RMS $\leq$ 0.5 sec, GAP $\leq$ 135° and no. stations $\geq$ 5. (b) is the NW-

SE cross-section (A-A') of the Dall City earthquakes. (c) is the NE-SW cross-section (B-B').

Fig. 10. The largest events (M_L. $\leq$ 4.0) in the Dall City earthquake sequence. Their location indicates the location of the probable asperity.

Fig. 11. Seismicity of north-central Alaska. The earthquakes plotted here are from the catalog compiled by Estabrook *et al.* (1985) for the years 1967 to 1985. They have ERH and ERZ $\leq$ 10 km, RMS $\leq$ 0.75 s and no. stations $\geq$ 5. The earthquakes before February 1985 are plotted as pluses, the events of February-April are plotted as stop signs. Faults are from Beikman (1980), Dover and Miyaoka (1985) and King (1969). The number of events in the Rampart aftershock zone is not representative of the actual number recorded by Alaskan seismic stations; its extent, however, is consistent with that determined by Huang and Biswas (1983).

APPENDIX II

ANNUAL TECHNICAL REPORT

TO

AIR FORCE OFFICE OF SCIENTIFIC RESEARCH

CRUSTAL STRUCTURE STUDIES UTILIZING EARTHQUAKE SEQUENCES

Grant AFOSR-85-0266

Principal Investigator: Larry Gedney

Geophysical Institute
University of Alaska
Fairbanks, Alaska 99775-0800

September 1986

Summary

During the course of this investigation, two earthquake sequences, one 100 km southwest of Fairbanks and one 180 km to the northwest, were studied in depth to enhance the present knowledge of crustal structure and tectonic plate interactions in central Alaska. The former sequence consisted of intermediate-depth earthquakes at the extreme northern tip of the encroaching Pacific plate, and the latter consisted of shallow crustal earthquakes in an intra-plate regime. The deeper cluster to the south was found to be a product of down-dip tension in the subducting plate. The crustal earthquakes to the north result from left-lateral faulting which arises from nearly horizontal compressive stress from the south-southeast. An improved crustal model was obtained for the area. The best-fit parameters for the central part of the zone include an upper mantle P-wave velocity of 7.91 km/sec at a depth of 34 km. Overlying this there are two crustal layers, the uppermost of which is 24 km thick and has a P-wave velocity of 6.0 km/sec. The lower crustal layer is 10 km thick, with a velocity of 7.2 km/sec. Upper mantle (Pn) velocities were observed to vary with azimuth around the margins of the central area from as low as 7.63 km/sec to as high as 8.12 km/sec. This no doubt reflects the flexing and deepening of the Moho beneath the root of the Alaska Range.

STATEMENT OF WORK

One objective of this project was to provide additional information on the stress regime in a very complicated area of Central Alaska where the North Pacific plate is indenting the continent in the area of the great bend of the Alaska Range around Mt. Mckinley. This was enhanced by the discovery of a tightly-compacted cluster of intermediate-depth earthquakes that have apparently been going on unnoticed for an indeterminate period of time. As related in the following section, this cluster was found to define the northernmost tip of the encroaching Pacific plate.

A second objective was to obtain an improved crust and upper mantle model for Central Alaska in a region about which little was known. This was made possible by the occurrence, in February, March and April of 1985, of several moderate earthquakes and over 1,400 aftershocks in an area previously considered to be relatively aseismic. A magnitude 6.0 mainshock on March 9 is the largest

earthquake ever to have been documented this far north in Alaska.

Because the epicentral region was in close proximity to the transportation corridor paralleling the Alaska pipeline, it was possible to install three seismographic stations in the immediate vicinity, and to telemeter the signals directly back to the Geophysical Institute in Fairbanks.

One distinguishing feature of the Dall City earthquakes (which they were named after an abandoned mining camp in the area) was that they almost invariable showed very distinct Pn and Pg phases at nearly all of the permanent University of Alaska stations around the epicentral region. In addition, an intermediate crustal phase was often seen. Depth control was good because of the newly-installed temporary stations, and it was recognized that this presented a good opportunity to study the crustal structure. This was done, and the results are presented in the following section.

STATUS OF RESEARCH

The Gold King Cluster

In the search for earthquake groupings for use in this study, it was discovered that a previously unrecognized cluster could be identified near a landing strip at Gold King, about 100 km SSW of Fairbanks. These earthquakes nearly all occurred within a volume of about 20 km in diameter (Figs. 1 and 2) at a depth centered at around 100 km (Fig. 3). Although the first event which could be identified as belonging to the group was recorded in 1969, most of the analysis which followed used only data dating from the period of improved instrumental coverage from 1978 forward (these are the events depicted in Figs. 2 and 3).

As cross-sections A-A' and B-B' show (Figs. 1 and 3), the Gold

King cluster plainly represents the northernmost remnant of the subduction zone which extends southwestward from that point to the western edge of Cook Inlet and out along the Aleutian Chain.

A composite focal mechanism solution obtained from 37 of the better-recorded events reveals a tensional axis dipping steeply to the NNW in the plane of the subducting plate. This indicates that these earthquakes are due to gravitational sinking within the plate. (A more detailed presentation will appear in the October, 1987, issue of the Bulletin of the Seismological Society of America.)

The Dall City cluster

Beginning with a magnitude (ML) 5.4 earthquake on February 14, 1985, a three-month series of strong earthquakes began in Central Alaska, near the trans-Alaska pipeline about 30 km north of the Yukon River crossing of the pipeline and 180 km northwest of Fairbanks (Figs. 4 and 5). This series culminated in a magnitude 6.0 shock on March 9, which was the largest ever recorded this far north in the state. In all, at least four earthquakes of magnitude 5.0 or better (Table 1), and a total of 38 events of magnitude 4.0 or greater were recorded during the period.

Because this is an unusual area for significant earthquakes in Alaska, the series aroused the immediate interest of the Geophysical Institute seismology staff. Being relative accessible (by Alaskan standards), it was soon possible to establish three local telemetered stations around the site (FISH, RGV and BEH, Fig. 5). This was done despite the fact that it was mid-winter, the temperature was hovering at around -40, and there were 40 knot winds at times.

The development of the cluster with time can be seen by comparing the two-to-three week interval plots in Figure 6. The dispersion in

Table 1

Largest earthquakes of the 1985 north-central Alaska sequence through March 16. Coordinates given are those determined at the Geophysical Institute. The magnitudes shown are local and body-wave magnitudes from the NOAA Alaska Tsunami Warning Center. The earthquake at 1416 on 9 March was masked on Alaskan records by preceding events, and the data given are from the USGS National Earthquake Information Service.

DATE	TIME(UT)	MAGNITUDE	DEPTH(KM)	LAT(N)	LONG(W)
14 Feb 85	0504	5.4	13	66.35	149.82
9 Mar 85	1357	4.8	6	66.34	149.83
9 Mar 85	1408	6.0	7	66.35	149.85
9 Mar 85	1416	5.4	10	66.2	150.2
9 Mar 85	1546	4.5	1	66.33	149.84
9 Mar 85	1621	4.4	13	66.36	149.87
9 Mar 85	1649	4.3	8	66.38	149.87
10 Mar 85	0358	4.4	5	66.31	149.90
10 Mar 85	1210	4.3	16	66.33	149.91
10 Mar 85	1330	5.6	7	66.30	149.90
10 Mar 85	1916	4.2	8	66.32	149.90
10 Mar 85	2305	4.4	2	66.33	149.90
16 Mar 85	1333	5.0	17	66.26	149.83

Figure 6(A) compared with the relative compactness of the later plots is an indication of the refinement in location capabilities that the installation of the nearby stations permitted.

Figure 7 demonstrates that the Dall City earthquakes were significantly removed from activity further to the south, although they seem to lie near a northern extension of a lineal aftershock zone that followed a magnitude 6.5 earthquake near Rampart, Alaska, on October 9, 1968 (Gedney et al., 1969; Huang and Biswas, 1983).

The focal mechanism solution obtained is best interpreted as left-lateral faulting on a NNE-SSW trending plane. This would be in accord with that found by Huang and Biswas (1983) for the Rampart earthquake to the south. The mechanism for the March 9 event also has a remarkable parallel in an earlier event in the same area exactly 10 years earlier on March 9, 1975 (Estabrook et al., 1986; Fig. 8).

With the nearby stations installed, reasonably accurate focal depths could be obtained. To take advantage of at least two very distinctive crustal phases seen on the seismograms and clear Pn phases, an iterative program was written which operated on the following assumptions:

(1) Given an accurate focal depth and origin time, travel times to seismographic stations at near-to-intermediate (100 to 500 km) distances are determined by the layer-velocity structure between source and receiver.

(2) Realizing that it is an oversimplification, if one assumes a horizontally plane-layered, two-layer-over-halfspace model, the arrival times of the different phases at individual stations at different distances should be a function of, (a) the velocity of the basal Pn layer at the Moho, (b) the depth of this layer, (c) the

velocity of layer 1 in the crust, (d) the thickness of layer 1, (e) the velocity of layer 2 in the crust, and (f) the thickness of layer 2.

(3) Factors (a) and (c) can be reasonably well determined by observational means, so that the observer is left with solving for four unknowns. If a good estimate can be obtained for the total crustal thickness (b), solving for either (d) or (f) obviates the need for determining the thickness of the other crustal layer.

(4) The consolidation and "interfingering" of observations of Pn and crustal phases at a number of different locations at varying distances around the epicentral area should provide an indication of which crustal model best matches all sites.

To find the best-fit model, an exhaustive program was written that utilized a number of the better-recorded earthquakes showing distinct Pn and crustal phases. This program iterated Moho depths and mantle velocities with crustal layer thicknesses and crustal layer velocities in every plausible combination. It then matched the models with the observed values at the various stations, discarding the "impossible" models and retaining those which might have produced the observations. The result was an enormous volume of printout (a page of which is reproduced as Figure 9). It was then attempted to pick the combination which best matched the observed observations of Pn and the crustal phases with the theoretical calculations at as many different observing stations as possible.

In actuality, no single model turned out to be "perfect." This is understandable because the "ideal" structural model does not exist; absolutely level, plane layering in the Tanana-Yukon Uplands cannot be expected, although the study area's location between the

massifs of the Brooks and Alaska Ranges is probably as close to it as can be expected any place in the state.

It was found that iterations involving increments less than 0.1 km/sec in velocity of the crustal layers or 1.0 km in thickness were of little benefit. Accordingly, the best-fit parameters for the area between the Dall City area and Fairbanks were found to be:

Vp (km/sec)	Depth (km)
6.0	0-24
7.2	24-34
7.91 ± 0.12	below 34

With the exception of the depth to the Moho, these values agree well with those obtained by Biswas (unpublished) which have been used for the University's routine location program in the Alaskan Interior. Biswas' values, obtained largely from quarry blasts were:

Vp (km/sec)	Depth (km)
5.9	0-24.4
7.4	24.4-40.2
7.9	below 40.2

It should be noted that Biswas' values were obtained largely from sites further to the south and closer to the Alaska Range. It might well be expected that greater depths to the Moho would be measured there.

The Dall City sequence also provided the opportunity to make repeated measurements of Pn velocities at various azimuths radiating out from around the epicentral area. Referring to Figure 4, these values were:

Stations	Azimuth	Vp(km/sec)
GLM-HDA	141	8.12 ± 0.19
FBA-HDA	148	8.08 ± 0.29
RDS-WRH	154	7.91 ± 0.12
WRH-GKC	157	7.65 ± 0.14
NEA-MCK	169	7.63 ± 0.16

In this table, Azimuth refers to the direction in which the ray leaves the epicenter to arrive at the first recording station. Apparently, the variance in apparent Pn velocities reflect the downward flexure of the Moho as the ray approaches the Alaska Range, slantingly at first, and then more at right angles.

Supportive of this concept is the observation that the leg from RDS to WRH is 7.91 km/sec (which has here been taken to be representative of this portion of the Interior), but in a straight-line path beyond that, as the Alaska Range is approached from WRH to GKC, the apparent velocity drops to 7.65 km/sec.

PUBLICATIONS

Estabrook, C., J. Davies, L. Gedney and S. Estes, Strong Alaska earthquake sequence, EOS, V.66, p.685, Oct. 1, 1985.

Gedney, Larry and John Davies, Additional evidence for down-dip tension in the Pacific plate beneath Central Alaska, Bull. Seis. Soc. Am., (to appear), V.76, Oct., 1986.

Estabrook, C., J. Davies, L. Gedney, S. Estes and J. Dixon, Seismicity and focal mechanism studies of the Dall City earthquakes, north-central Alaska, currently undergoing peer review, will probably be submitted to Bull. Seis. Soc. Am.

REMARKS

Charles Estabrook received his Master of Science degree in geophysics in June of 1986. His thesis, titled "Seismic investigations in northern Alaska" was based largely on research of the Dall City earthquakes described above.

REFERENCES

Estabrook, C., J. Davies, L. Gedney, S. Estes and J. Dixon, Seismicity and focal mechanism studies of the 1985 Dall City earthquakes, north-central Alaska, currently undergoing review, will probably appear in Bull. Seism. Soc. Am., 1986.

Gedney, L., E. Berg, H. Pulpan, J. Davies and W. Feetham, A field report on the Rampart, Alaska earthquake of October 29, 1968, Bull. Seism. Soc. Am., 59, 1421-1423, 1969.

Huang, P. and N. Biswas, Rampart seismic zone of central Alaska, Bull. Seism. Soc. Am., 73, 813-829, 1983.

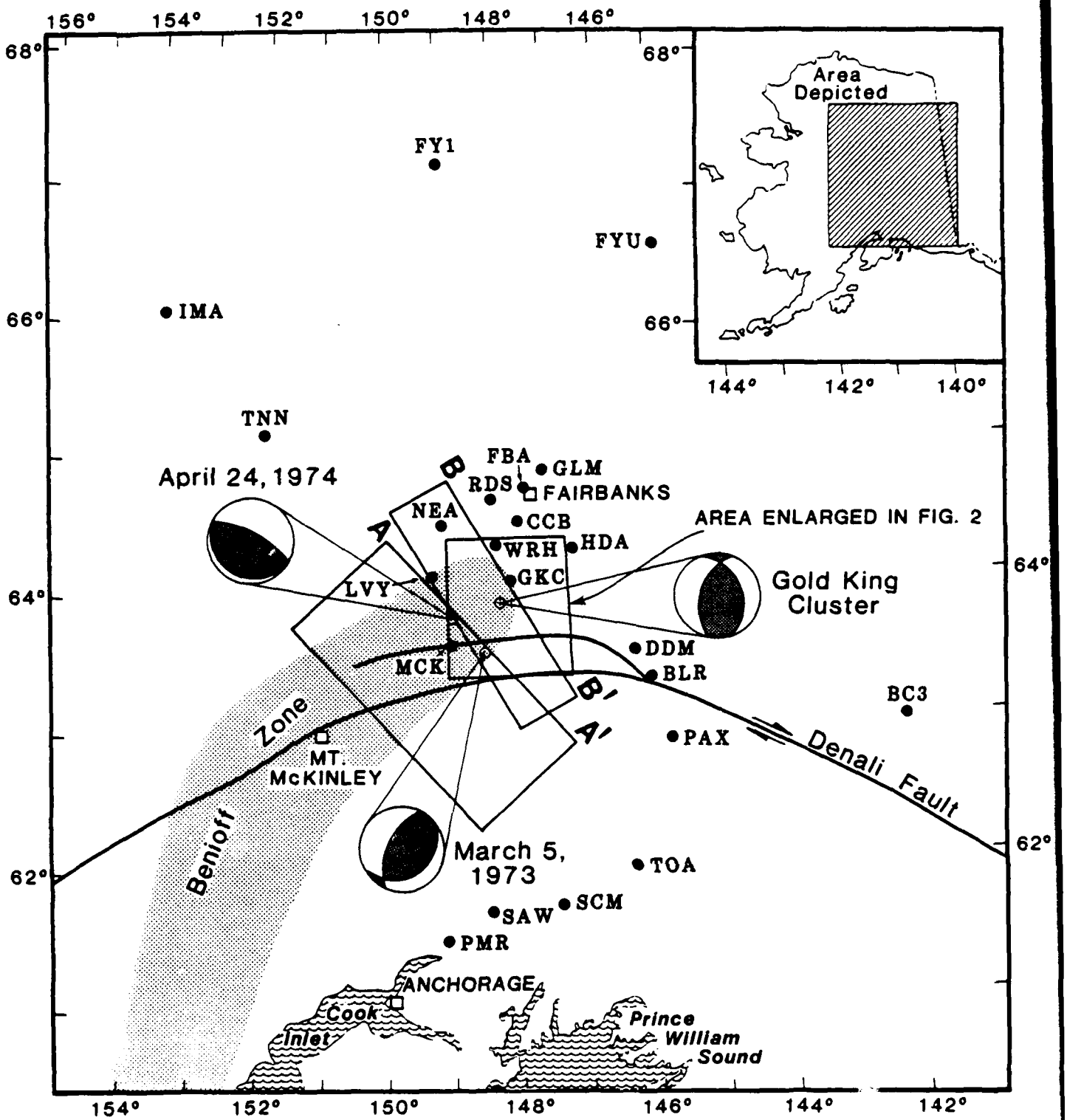

Figure 1. Three-letter station designators show the locations of the seismographic stations utilized in this study. The upper-hemisphere focal mechanisms shown all indicate steeply-dipping T-axes (stippled areas indicate compressional quadrants); the solution labeled Gold King cluster is a composite solution obtained during this study. Cross section A-A' and B-B' are shown in Figure 3 and are 100 and 50 km thick, respectively.

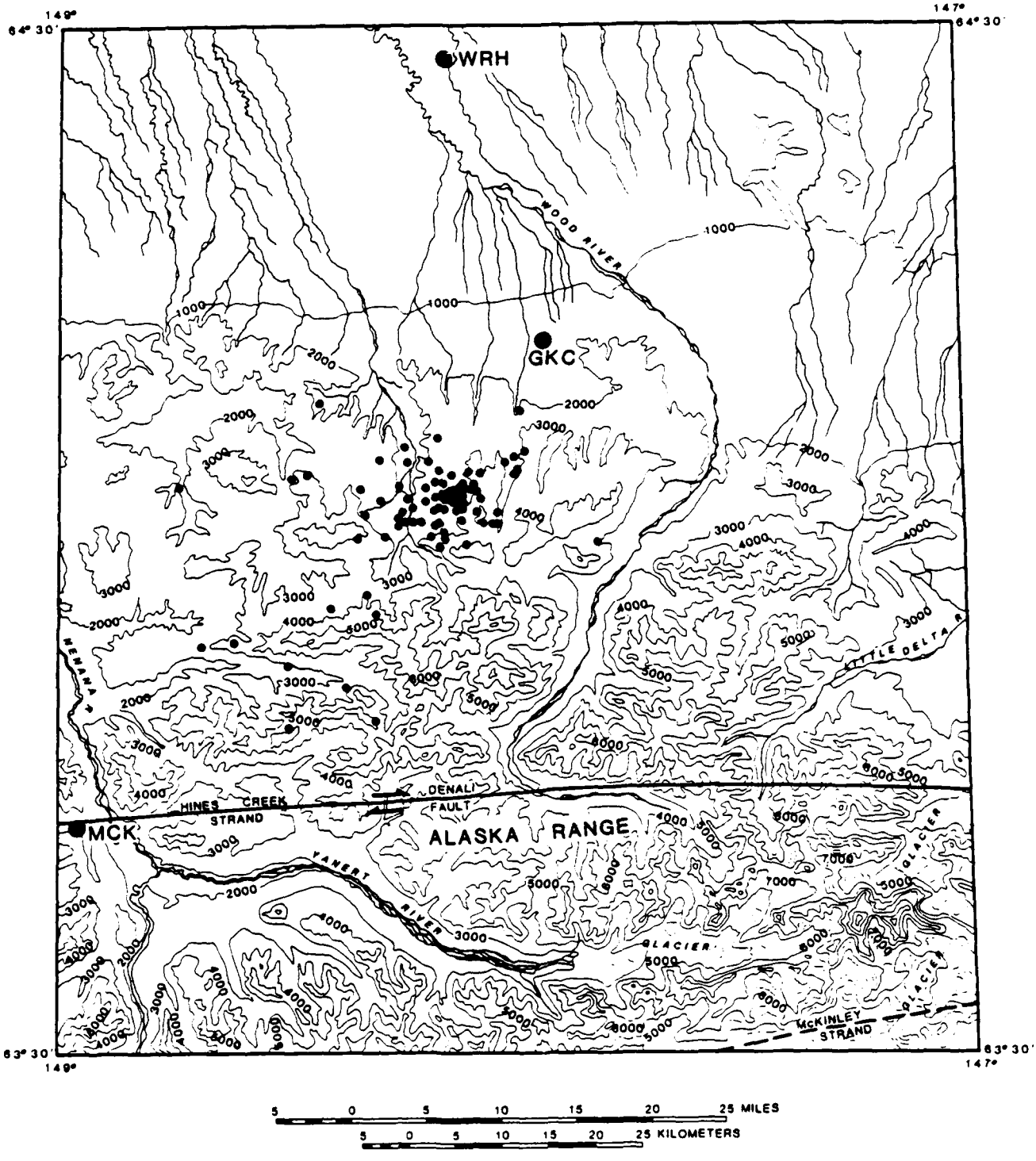

Figure 2. Epicentral plot of 86 earthquakes of the Gold King cluster located between 1978 and 1984. WRH, GKC and MCK are local seismographic stations.

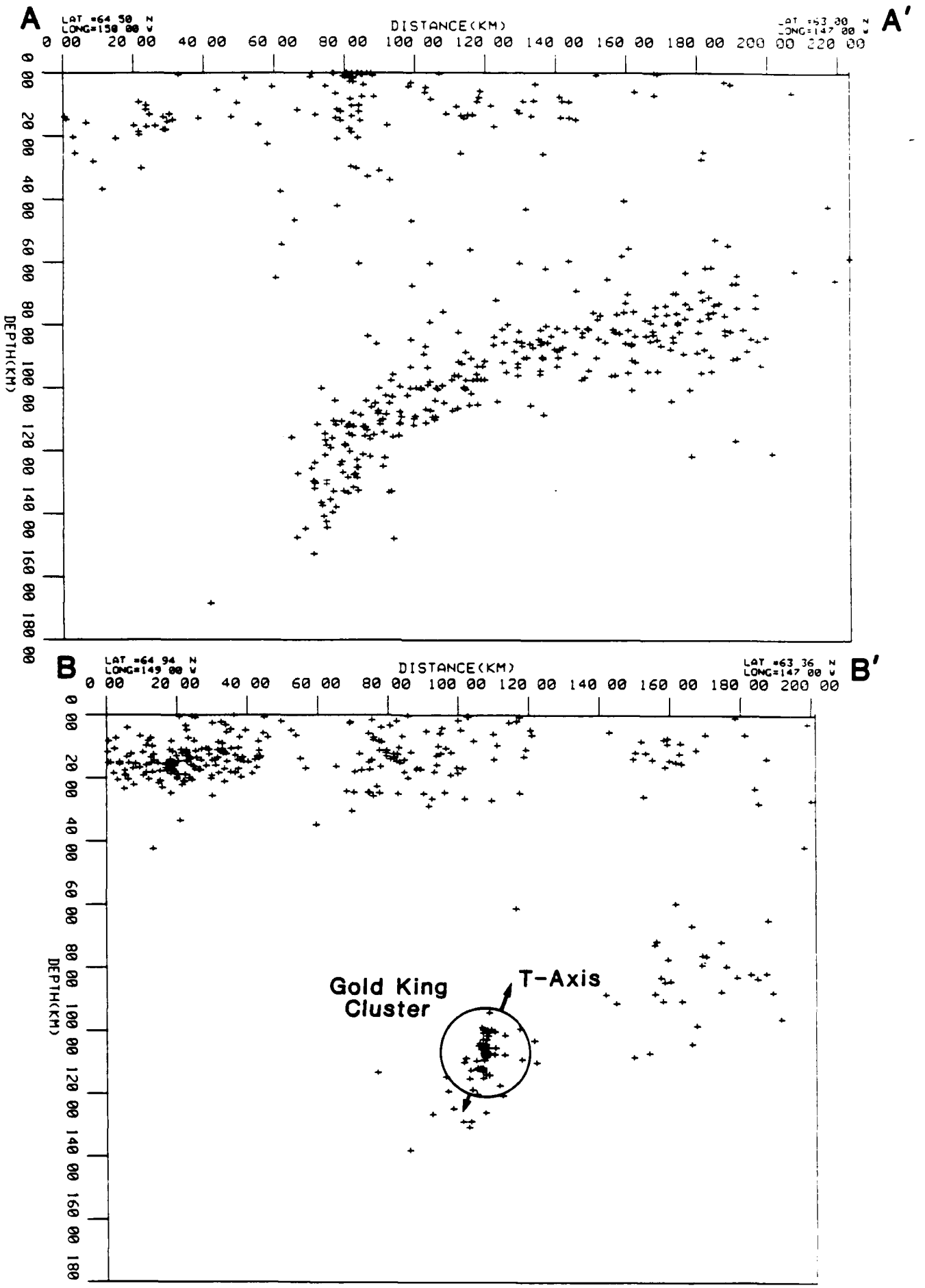

Figure 3. Cross-sections looking to the northeast along the Benioff zone (see Figure for locations). Solutions indicated were determined from five or more stations betwee 1978 and 1984. Section A-A' is 100 km thick and section B-B' at the tip of the zone is 50 km thick.

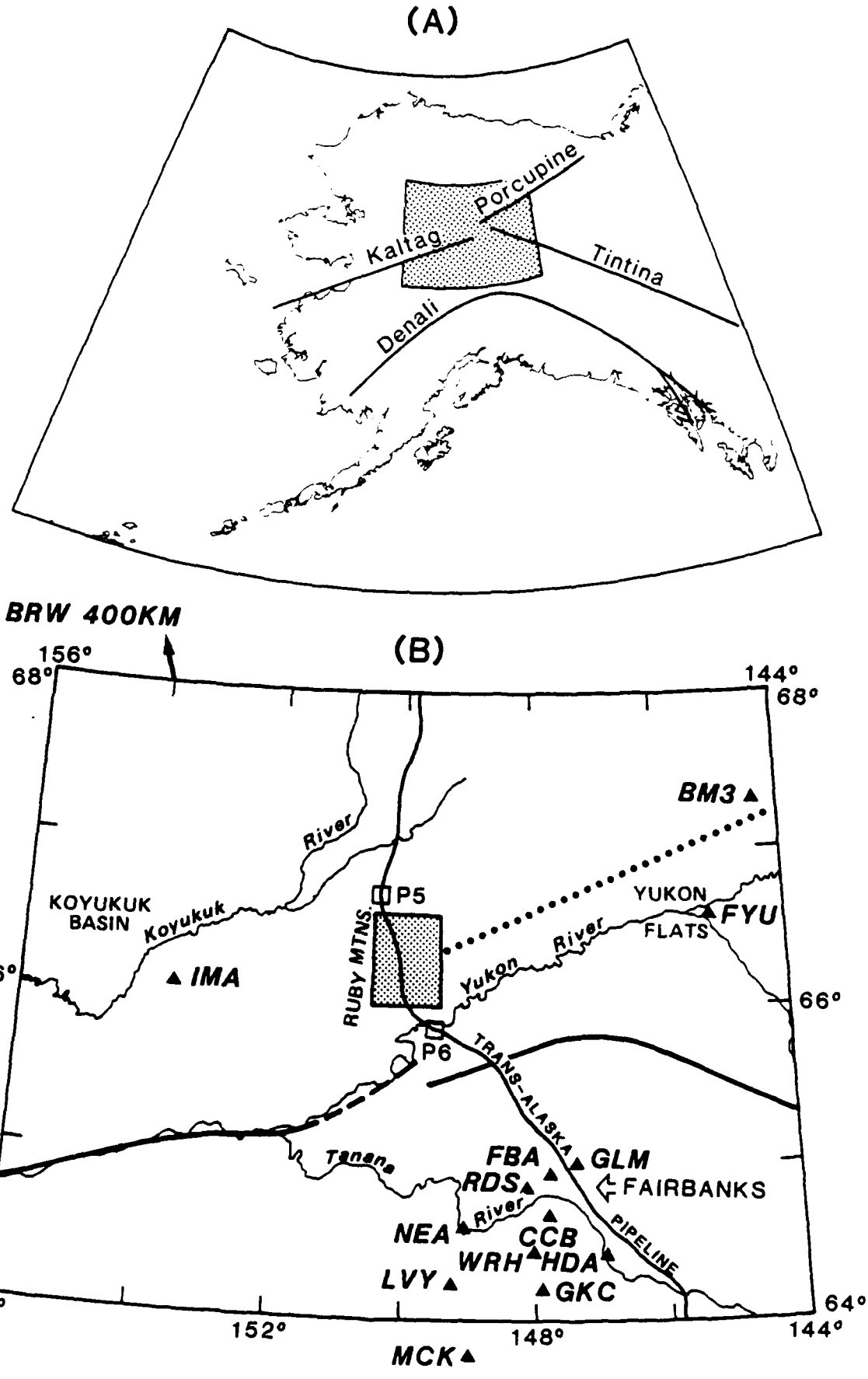

Figure 4. (A) Location map for lower part of figure. Major faults and lineaments are indicated. (B) The Dall City area enlarged in Figure 5 is shown as the stippled area. P5 and P6 are pump stations on the Trans-Alaska pipeline.

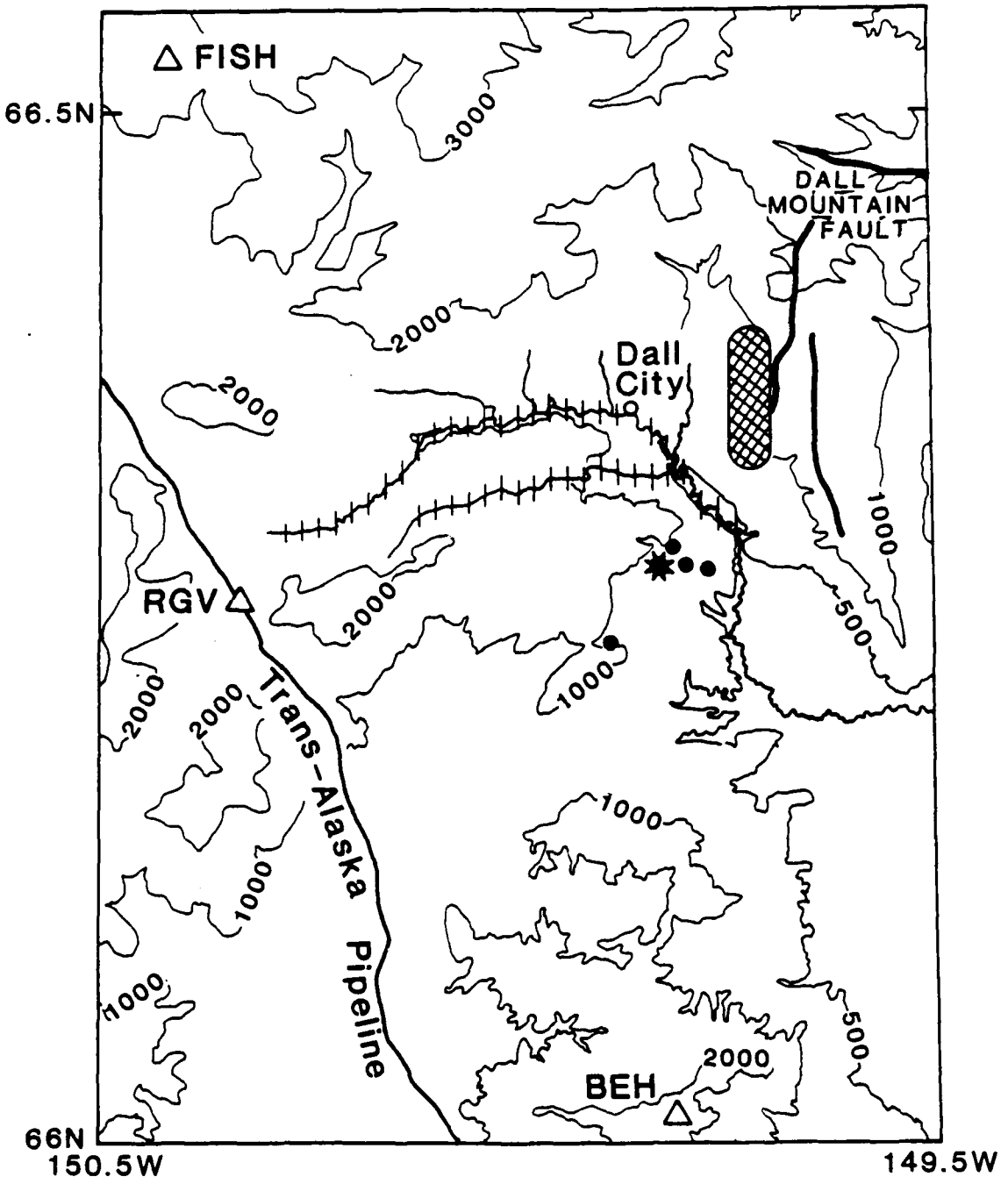

Figure 5. The Dall City epicentral area. FISH, RGV and BEH are three temporary seismographic stations which were emplaced shortly after the earthquake sequence beg The location of the main shock (star) and four other larger shocks are indicated. T tick marks on the streams indicate areas of broken ice and stream overflow. The cro hatched area indicates a hillside along which several springs were rejuvenated.

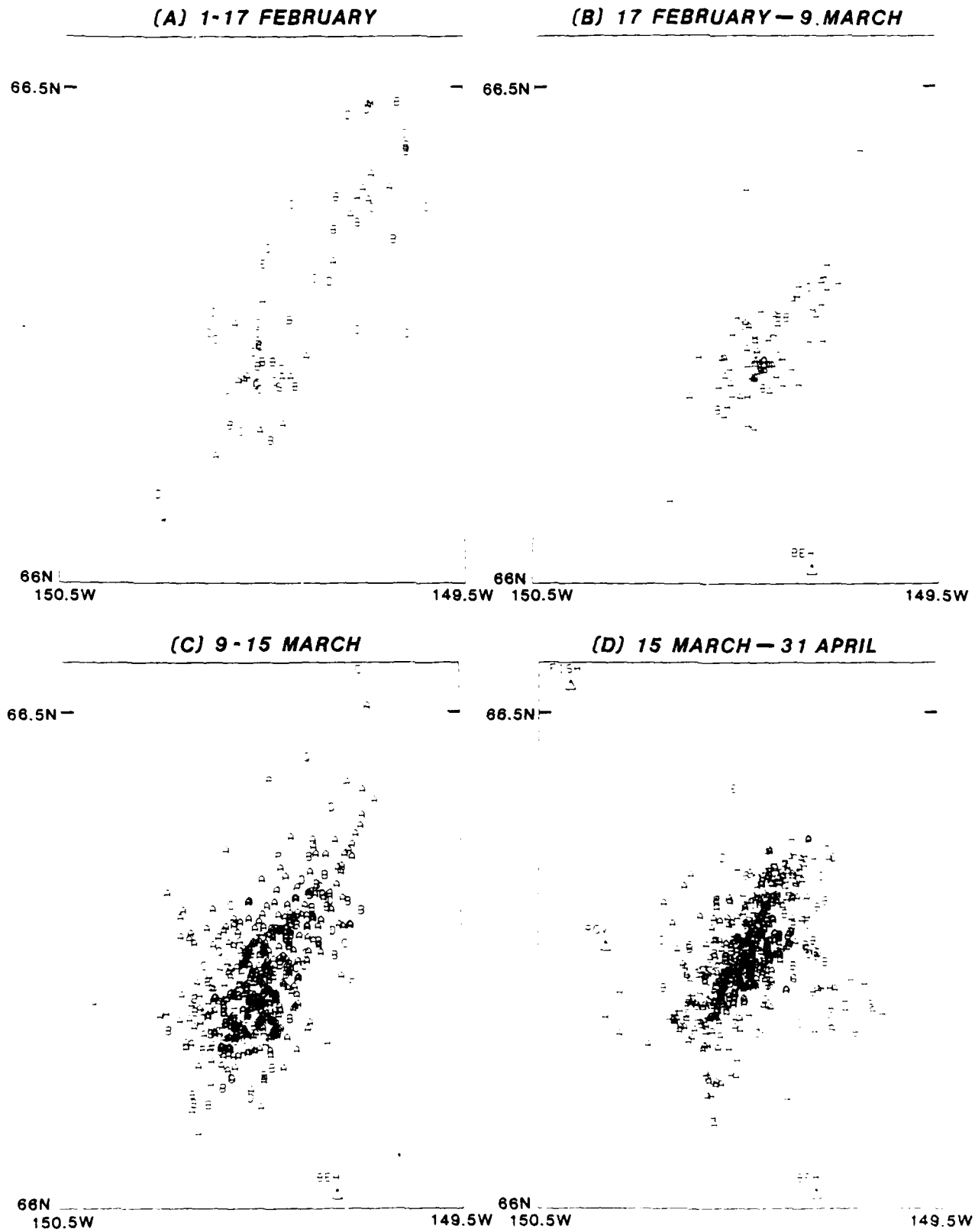

Figure 6. Progression of epicentral zone development from February, 1985, through April. The letters indicate focal depths in 10 km increments, i.e., A=0-10 km, B=10-20 km, C=20-30 km, etc.

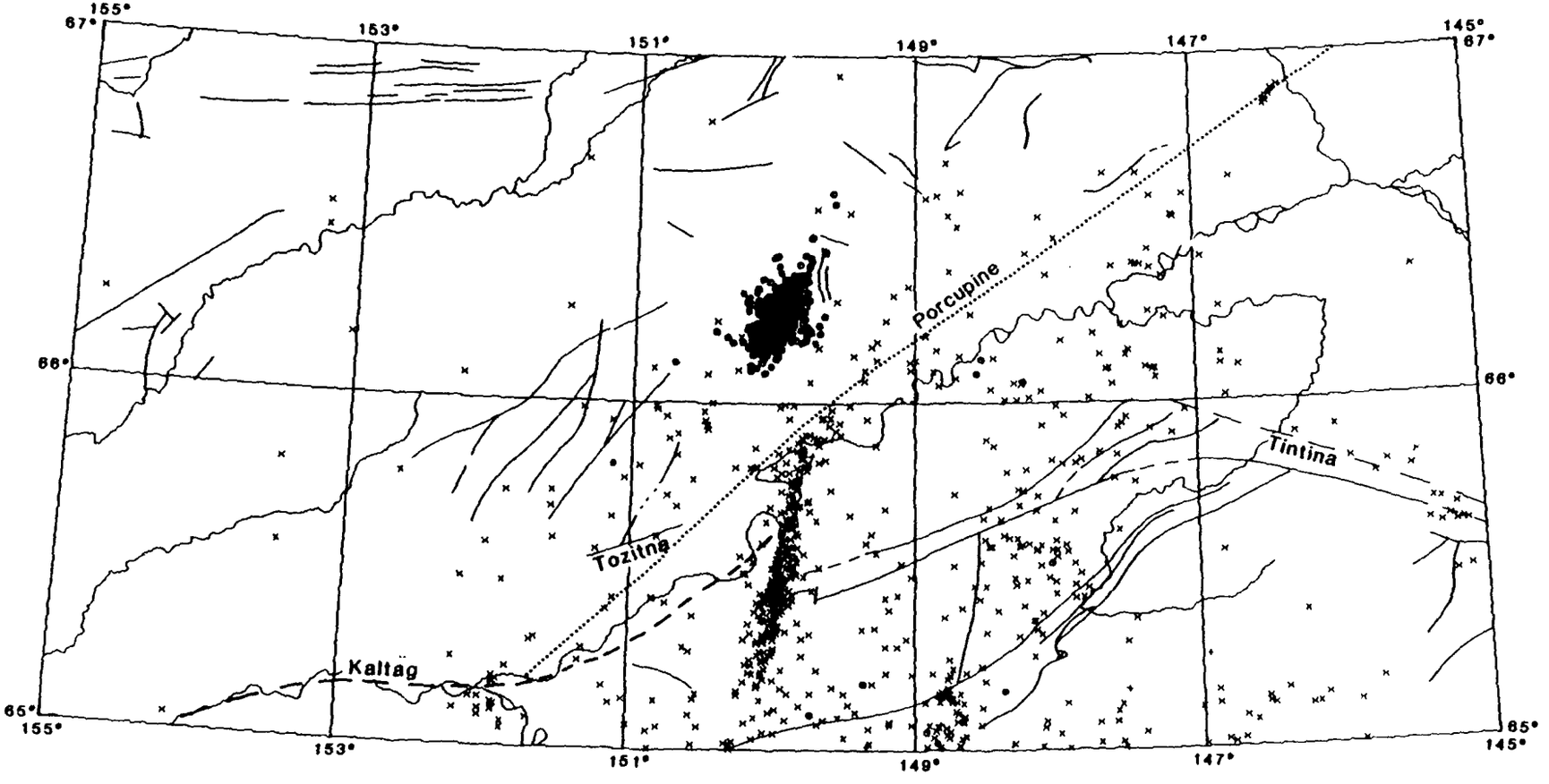

Figure 7. Location of the Dall City epicentral area (upper center) in relationship to local faults and the Rampart aftershock zone to the south.

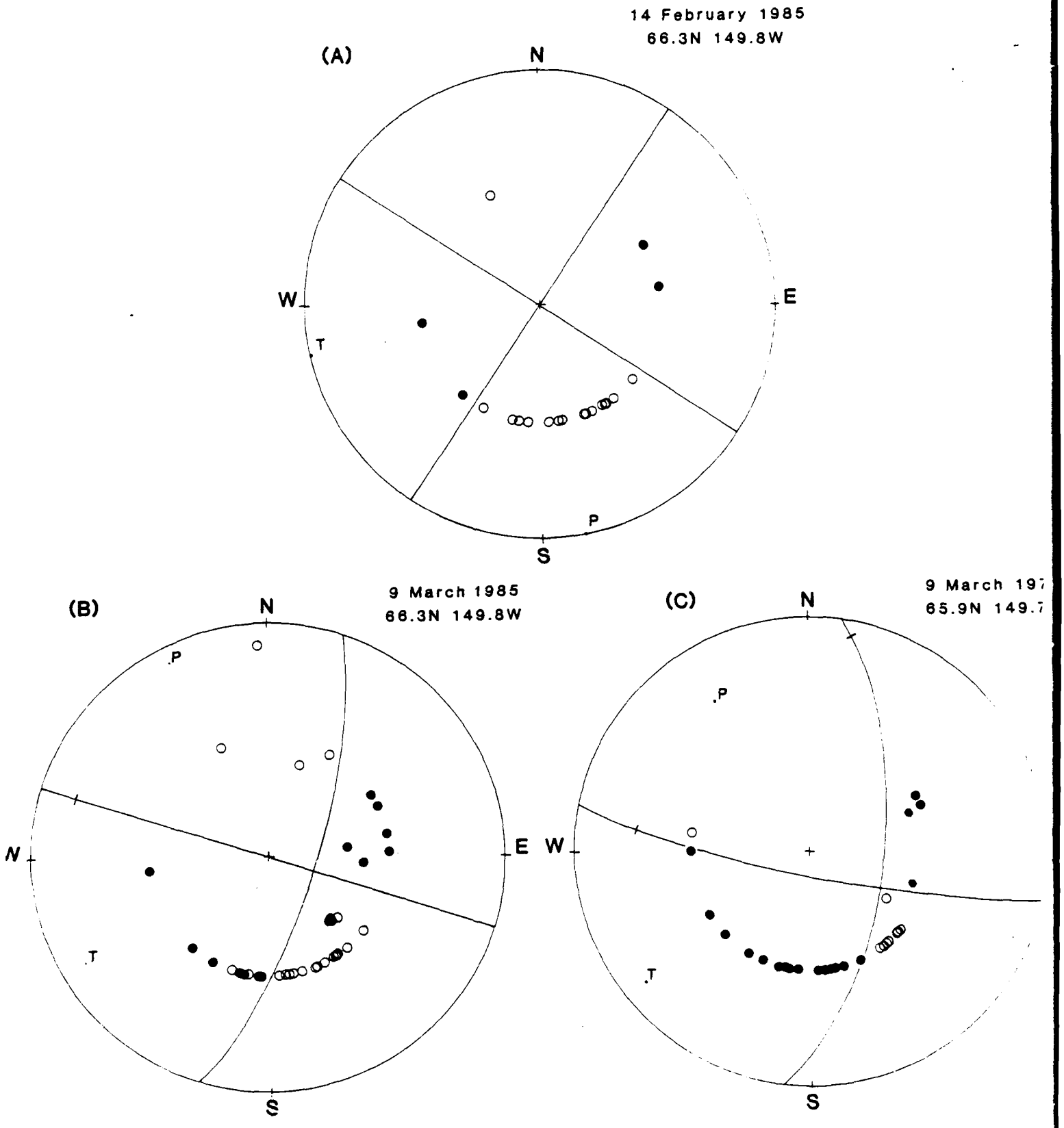

Figure 8. Focal mechanisms of three earthquakes in the Dall City area. Black circles represent compressions and open circles, dilatations. The most probable solution is left-lateral offset along the NNE-SSW trending plane. Note that (C) occurred 10 years before the present sequence. It's location is probably not as well established.

DATE-TIME: 1333 15 MAR 85 STATION: FYU COMPUTED DEPTH: 14.
MOHO VELOCITY: 8.00 TOTAL CRUSTAL THICKNESS: 39.0 EPICENTRAL DISTANCE: 199
P-PN TIME : 3.30 ITERATIONS : 20 VARIANCE : 0.1
V1 INCREMENT: 0.10 V2 INCREMENT: 0.10 Z1 INCREMENT: 2.0
STARTING V1 : 5.50 STARTING V2 : 6.00 STARTING Z1 : 0.0

V1=5.50	V2=6.00	Z1=26.0	Z2=13.0	ER=0.1	TPG=36.01	TPN=32.77	P*-PN=3.24
V1=5.50	V2=6.00	Z1=32.0	Z2= 7.0	ER=-.1	TPG=36.43	TPN=33.03	PG-PN=3.40
V1=5.50	V2=6.00	Z1=34.0	Z2= 5.0	ER=0.0	TPG=36.43	TPN=33.11	PG-PN=3.31
V1=5.50	V2=6.00	Z1=36.0	Z2= 3.0	ER=0.1	TPG=36.43	TPN=33.20	PG-PN=3.22
V1=5.50	V2=6.10	Z1=28.0	Z2=11.0	ER=0.1	TPG=36.00	TPN=32.76	P*-PN=3.24
V1=5.50	V2=6.10	Z1=34.0	Z2= 5.0	ER=-.1	TPG=36.43	TPN=33.07	PG-PN=3.35
V1=5.50	V2=6.10	Z1=36.0	Z2= 3.0	ER=0.1	TPG=36.43	TPN=33.18	PG-PN=3.25
V1=5.50	V2=6.20	Z1=30.0	Z2= 9.0	ER=0.1	TPG=36.03	TPN=32.79	P*-PN=3.24
V1=5.50	V2=6.20	Z1=34.0	Z2= 5.0	ER=-.1	TPG=36.43	TPN=33.03	PG-PN=3.39
V1=5.50	V2=6.20	Z1=36.0	Z2= 3.0	ER=0.0	TPG=36.43	TPN=33.15	PG-PN=3.27
V1=5.50	V2=6.30	Z1=32.0	Z2= 7.0	ER=0.1	TPG=36.09	TPN=32.85	P*-PN=3.23
V1=5.50	V2=6.30	Z1=36.0	Z2= 3.0	ER=0.0	TPG=36.43	TPN=33.13	PG-PN=3.30
V1=5.50	V2=6.40	Z1=34.0	Z2= 5.0	ER=0.1	TPG=36.17	TPN=32.95	P*-PN=3.22
V1=5.50	V2=6.40	Z1=36.0	Z2= 3.0	ER=0.0	TPG=36.43	TPN=33.10	PG-PN=3.32
V1=5.50	V2=6.50	Z1=36.0	Z2= 3.0	ER=0.1	TPG=36.29	TPN=33.08	P*-PN=3.21
V1=5.50	V2=6.50	Z1=36.0	Z2= 3.0	ER=0.0	TPG=36.43	TPN=33.08	PG-PN=3.35
V1=5.50	V2=6.60	Z1=36.0	Z2= 3.0	ER=-.1	TPG=36.43	TPN=33.05	PG-PN=3.37
V1=5.50	V2=6.70	Z1=36.0	Z2= 3.0	ER=-.1	TPG=36.43	TPN=33.03	PG-PN=3.40
V1=5.50	V2=6.80	Z1=38.0	Z2= 1.0	ER=0.1	TPG=36.43	TPN=33.22	PG-PN=3.20
V1=5.50	V2=6.90	Z1=38.0	Z2= 1.0	ER=0.1	TPG=36.43	TPN=33.22	PG-PN=3.21
V1=5.50	V2=7.00	Z1=38.0	Z2= 1.0	ER=0.1	TPG=36.43	TPN=33.21	PG-PN=3.22
V1=5.50	V2=7.10	Z1=38.0	Z2= 1.0	ER=0.1	TPG=36.43	TPN=33.20	PG-PN=3.23
V1=5.50	V2=7.20	Z1=38.0	Z2= 1.0	ER=0.1	TPG=36.43	TPN=33.19	PG-PN=3.24
V1=5.50	V2=7.30	Z1=38.0	Z2= 1.0	ER=0.1	TPG=36.43	TPN=33.18	PG-PN=3.24
V1=5.50	V2=7.40	Z1=38.0	Z2= 1.0	ER=0.0	TPG=36.43	TPN=33.17	PG-PN=3.25
V1=5.50	V2=7.50	Z1=38.0	Z2= 1.0	ER=0.0	TPG=36.43	TPN=33.16	PG-PN=3.26
V1=5.50	V2=7.60	Z1=38.0	Z2= 1.0	ER=0.0	TPG=36.43	TPN=33.15	PG-PN=3.27
V1=5.50	V2=7.70	Z1=38.0	Z2= 1.0	ER=0.0	TPG=36.43	TPN=33.14	PG-PN=3.29

Figure 9. Sample page of printout from iteration program which matched observed Pn and crustal phases with various possible crustal configurations. "Impossible" combinations were not printed

APPENDIX III

SEISMOTECTONICS OF NORTHERN ALASKA

Presented to the Faculty of the University of Alaska

in Partial Fulfillment of the Requirements

for the Degree of

MASTER OF SCIENCE

Charles Hershey Estabrook, B.S. December 1985

ABSTRACT

Earthquake data collected by the Geophysical Institute of the University of Alaska-Fairbanks have been reprocessed to study the seismicity and tectonics of northern Alaska. A seismic velocity structure developed in the Dall City area of central Alaska suggests granite as the main component of the upper crust. A refraction study in the eastern Brooks Range constrains the Moho dip. Microearthquakes trend east-west roughly parallel to, but south of, the northern foothills of the Brooks Range. In northern Alaska and NW Canada the Kobuk, central Kaltag, Porcupine, Dall Mt.-Rampart, NW Tintina and Richardson faults are seismically active. Eight new focal mechanisms were determined for the northern Alaska. In the south they show strike-slip faulting consistent with the historical movement on these faults. The orientation of the pressure axes is consistent with Pacific-North American plate convergence. A tectonic model developed accounts for the pervasive strike-slip faulting.

JOURNAL OF GEOPHYSICAL RESEARCH, VOL. 93, NO. B10, PAGES 12,026-12,040, OCTOBER 10, 1988

SEISMOTECTONICS OF NORTHERN ALASKA

APPENDIX IV

Charles H. Estabrook

Lamont-Doherty Geological Observatory of Columbia University, Palisades, New York

David B. Stone and John N. Davies

Geophysical Institute, University of Alaska, Fairbanks

Abstract. Data from earthquakes occurring in northern Alaska collected by the Geophysical Institute of the University of Alaska, Fairbanks, have been reprocessed using a seismic velocity model developed for the Dall City and Fort Yukon areas of north central Alaska. A study of the relocated events shows that microearthquakes occur in a zone roughly parallel to, but south of, the crest of the Brooks Range. The events also show that the Kobuk, central Kaltag, Porcupine, Dall; Rampart, northwest Tintina, and Eskimo Lakes faults in northern Alaska and northwest Canada are seismically active, with the Eskimo Lakes fault being most active. Eight new focal mechanisms were determined for northern Alaska which show strike-slip faulting south of the Brooks Range. This movement is consistent with the known movement on the associated faults. The orientation of the pressure axes derived from these and other fault plane solutions is consistent with Pacific-North American plate convergence. Large-scale shearing appears to extend northward from the Pacific-North America transform boundary into arctic Alaska and allows the interpretation that the Seward Peninsula extensional zone is a large-scale pull-apart feature.

Introduction

Northern Alaska (Figure 1) exhibits a higher level of seismicity than might be expected considering the distance from any recognizable, modern plate boundary. Several moderate to large earthquakes have occurred in northern Alaska: a magnitude 7.3 PAS (PAS = M_S determined by the California Institute of Technology) event in the Koyukuk basin in 1958, a 6.9 PAS in the Chukchi Sea in 1928, a 6.5 M_S (M_S, M_L, and m_b a- determined by the National Earthquake Information Service (NEIS), or its predecessors) at Rampart in 1968, a 5.2 M_L (4.4 m_b) at Barter Island on the Arctic coast in 1968, and a 6.0 M_S at Dall City in the Ray Mountains in March 1985. To help understand the distribution of seismicity and the occurrence of moderate to large earthquakes, a crustal velocity model has been determined. Using this model, a large set of earthquakes were relocated, and their distribution was analyzed. The data were also used to derive earthquake fault plane solutions and to formulate a tectonic model to explain the intraplate deformation of northern Alaska.

The Brooks Range is the most prominent physiographic feature in northern Alaska (Figure 1). The range trends east-west across western and central Alaska and curves toward the northeast at its eastern end. Low-angle north verging thrust faults with upward of 500 km of lateral shortening characterize the western end [Mayfield et al., 1983], but these thrust sheets are not recognized in the northeast Brooks Range but may be present farther south [Oldow et al., 1987]. Farther to the east, the mountains trend south along the west side of the Mackenzie River, eventually becoming the Richardson Mountains, which are separated from the geologically different Brooks Range by the Porcupine fault [Norris and Yorath, 1981].

The area south of the Brooks Range is dominated by several large basins and a bisecting mountain range. The Yukon-Koyukuk basin contains Cretaceous sediments, remnants of Mesozoic island arcs, and is intruded by Cretaceous plutons [Patton, 1973]. The basin is possibly underlain by oceanic crust equivalent to that exposed along the southern edge of the Brooks Range and along the western flank of the Ruby mountains. To the east of the Yukon-Koyukuk basin is a large, low-lying area of Quaternary sediments known as the Yukon Flats. The Yukon Flats is known to be a basin of considerable depth, but the nature of its basement is not known. Kirschner et al. [1985] suggest that the Yukon Flats developed as an extensional graben from strike-slip motion along the Tintina fault, though most accretion models imply that it may be underlain by oceanic crust (see, for instance, Churkin et al. [1982]).

A number of major faults have been mapped in north central Alaska (Figure 1), but the relationships between them are often obscure. For instance, the Kaltag fault, which trends across the southern portion of the study area, can be traced northeast through the Yukon-Koyukuk basin and Ruby geanticline before disappearing beneath the Yukon Flats. Norris and Yorath [1981] believe that the Kaltag fault continues northeast beneath the Yukon Flats to emerge as the Porcupine lineament. Another possibility is that it may wrap around the southern edge of the Yukon Flats to meld with the Tintina fault. Similarly, the relationship between the mapped portions of the Porcupine fault and the Eskimo Lakes fault system is obscure, as is the connection between the Porcupine fault and its apparent extension as the Porcupine lineament.

Crustal Structure

Previous Studies

There are no published crustal models that apply specifically to northern Alaska. However, several studies have been made in adjacent areas (Table 1). Jin and Herrin [1980] studied the phase and group velocities of surface waves to determine an average velocity structure for south central Alaska. Hanson et al. [1968] derived a crustal structure model from an unreversed refraction line across the Tanana

Copyright 1988 by the American Geophysical Union.

Paper number 6B6263.
0148-0227/88/006B-6263$05.00

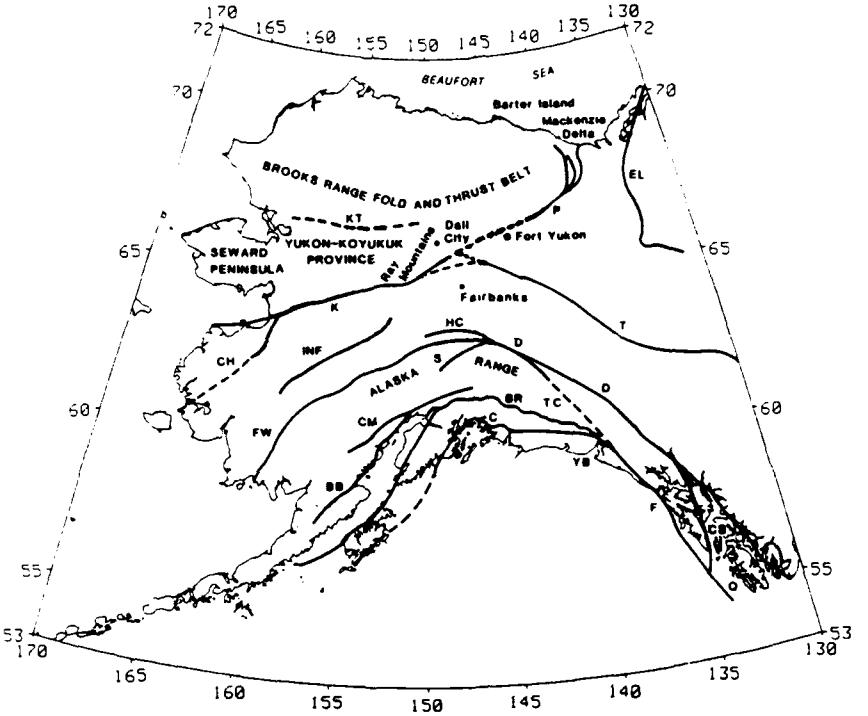

Fig. 1. Map of major faults in Alaska. BB, Bruin Bay; BR, Border Ranges; C, Contact; CH, Chiroskey; CM, Castle Mountain-Lake Clarke; CS, Chatham Strait; D, Denali; EL, Eskimo Lakes; F, Fairweather; FW, Farewell; HC, Hines Creek; INF, Innoko-Nixon Fork; K, Kaltag; KT, Kobuk Trench; P, Porcupine; Q, Queen Charlotte; S, Susitna; T, Tintina; TC, Totschunda. Also shown are the Yakutat block (YB) and other key locations mentioned in the text. The shaded areas are the Yukon-Koyukuk Province and the Yukon Flats. Note that Dall City no longer exists but is used for the general location of the Dall City earthquakes.

Basin, southwest of Fairbanks. It agrees rather well with that of Jin and Herrin [1980] for the upper 15 km. Hanson et al. [1968] give a 33-km crustal thickness for the Fairbanks area, based on the gravity models of Woollard et al. [1960]. This latter thickness is considerably shallower than the 43-km Moho depth of Jin and Herrin [1980], which is an average of the thick crust under the Alaska Range and the thinner surrounding crust. N. Biswas (University of Alaska Fairbanks, unpublished data, 1977) determined a crustal velocity structure for south central Alaska using a Monte Carlo inversion of earthquake and quarry blast travel times. The upper crustal velocity of 5.9 km/s for the top 24 km is slightly faster than that of Jin and Herrin [1980] and Hanson et al. [1968]. The crustal thickness of Biswas's model is comparable to Jin and Herrin's (40 and 43 km, respectively), but thicker than Hanson et al.'s [1968] for the Fairbanks area (33 km).

Northern Alaskan Upper Mantle Velocity, Fort Yukon Study

Refracted phases from earthquakes recorded at stations in the Barter Island, Fort Yukon, and Fairbanks networks of the University of Alaska (Figure 2) were used to construct a reversed seismic refraction profile. This was used to derive an upper mantle or P_n velocity under the Fort Yukon network [Estabrook, 1985].

A well-located earthquake in the Fairbanks area (781217; Figures 2, 3a) (all events are labeled as year, month, day, e.g., 781217 is December 17, 1978) was chosen as a southern source. It gives a P_n velocity of 7.94 ± 0.18 km/s (95% confidence limit based on work by Hanson [1968]). Earthquake 780621, located in the northeast Brooks Range (Figures 2, 3b), was chosen as a northern source. This event yields a P_n velocity of 7.88 ± 0.22 km/s. On the basis of this reversed pair of values (7.88 and 7.94 km/s) across the Fort Yukon network, we take the P_n velocity in northern Alaska to be 7.9 km/s.

Northern Alaska Crustal Velocities, Dall City and Fort Yukon Data

The close proximity of seismic stations to the 1985 Dall City earthquakes, events 7 and 8 in Figure 8 [Estabrook et al., 1985], provided the opportunity to determine a local P and S wave velocity structure. To do this, the average crustal thickness between Dall City and Fairbanks was fixed at 35 km, a thickness derived by L. Gedney (personal communication, 1986) using the arrival times of P_n and P_g waves. Wadati diagrams were used to determine the V_p/V_s ratios of 1.68 ± 0.03 for the Dall City area. This is essentially the same as the value of 1.69 ± 0.04 determined by Gedney and Berg [1969] for aftershocks of the 1967 Fairbanks earthquake. By systematically varying the crustal velocity used to relocate a set of 10 earthquakes, it was possible to determine the velocity for which hypocentral and travel time errors were a minimum. These errors were large for velocities less than 6.0 km/s and asymptotically approached a small lower limit for faster velocities. Thus 6.0 km/s is a minimum value for the

TABLE 1. Velocity Models for the Crust and Upper Mantle of Interior and Northern Alaska

Number	Model	V_p	Depth	V_p/V_s
1	Dall City area (this study)	6.1	0.0	1.68
		7.9	35.0	1.68
2	above model with mid-crustal layer	6.1	0.0	1.68
		6.6	20.0	1.68
		7.9	35.0	1.68
	Fairbanks Area			
3	upper crust from Hanson [1988];	4.5	0.0	1.68
	lower crust and Moho from	5.4	2.0	1.68
	refraction in Fort Yukon area	5.8	4.5	1.68
	(this study)	6.1	11.0	1.68
		8.0	33.0	1.68
	Brooks Range			
		5.4	0.0	1.68
		5.8	4.5	1.68
		6.1	11.0	1.68
		8.0	40.0	1.68
4	standard interior Alaska model (N.	5.9	0.0	1.78
	N. Biswas, unpublished data,	7.4	24.4	1.78
	1977)	7.9	40.2	1.78
5	above model with V_p/V_s ratio from	5.9	0.0	1.68
	this study	7.4	24.4	1.68
		7.9	40.2	1.68

V_p, velocity of p wave in km/s. Depth, depth of the top of the layer in km. V_p/V_s, ratio of the velocity of the p wave to that of the s wave; used in the hypocenter location program to convert s wave arrival times to equivalent p wave times.

average velocity of the upper 10 km of the crust in this area.

Crustal velocities were also determined using events located within and recorded by the Fort Yukon network (Figure 2). Figure 3c shows a good fit to a straight-line relationship between arrival time and distance, even though the stations surround the epicenter. This is interpreted as representing a velocity of 6.04 ± 0.12 km/s beneath the network. On the basis of the Dall City and Fort Yukon data, a P wave velocity of 6.1 km/s is taken for the upper crust of northern Alaska.

Velocity Model Tests

The combined results of the Fort Yukon and Dall City studies yield a P wave velocity model consisting of a 6.1 km/s crust, 35 km thick, overlying a 7.9 km/s upper mantle. Location errors and travel time residuals for this model are compared in Table 2 to the models of Hanson et al. [1968] and N. Biswas (University of Alaska Fairbanks, unpublished data, 1977).

When the entire northern Alaska data set is considered and only a sparse regional network is used, the similarities in the estimates of error from one model to the other indicate that there is no obvious preferred model. However, when local stations are involved, as shown for Dall city in Table 2, the errors increase for models with lower velocities in the crust (models 3, 4, and 5). Therefore velocity model 1, Table 1, has been used for this study since it has comparable errors to other models on a regional scale (at stations farther than the P_n crossover distance) and has the advantage of simplicity.

Seismicity

The present study incorporates all of the data collected by networks operated by the Geophysical Institute of the University of Alaska for the years 1967-1984.

The set of earthquake phase data for these years was compiled into a single file (5427 events), and the earthquakes were relocated using HYPOELLIPSE [Lahr, 1982] with a single-layer crustal model (model 1, Table 1).

Using the selection criteria that the horizontal location errors (ERH) be less than 10 km, the depth errors (ERZ) less than 20 km, and the root mean square of the travel time residuals less than 1 s, a subset was created which sharpened many clusters and trends of earthquakes (Figure 4). Note that the detection threshold is not homogeneous in time nor space for the earthquakes whose epicenters are shown in Figure 4. A more homogeneous representation of the seismicity of northern Alaska is given in Figure 5 which shows an epicenter map of all earthquakes greater than magnitude 3 during the years 1976-1979. During this period the Seward Peninsula, Fort

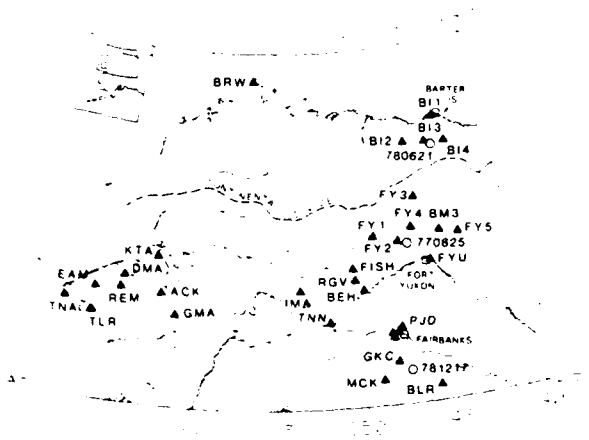

Fig. 2. Location map and station codes for seismograph stations in interior and northern Alaska. The Seward, Barter Island (BI), and Fort Yukon (FY) nets were operating together from 1976 to 1979. The refraction study used earthquakes (circles) designated by year, month, day, and all the stations east of 155°W with the exception of BM3.

Yukon, and Barter Island networks were operating simultaneously, and with the exception of a small region near Point Barrow, the detection threshold of the combined network is estimated to be about magnitude 3.0 [Estabrook, 1985]. This estimate is based largely on magnitude-distance plots for each station. Figure 5 shows a rather uniform distribution of events along the length of the Brooks Range south of the continental divide. The lack of magnitude 3 and larger events north of the Brooks Range on the Arctic Slope during the 1976-1979 time window may not be representative of the long-term level of seismicity since the time period is so short.

However, the same absence of events on the Arctic Slope is seen in Figure 6, which shows epicenters for earthquakes of magnitude 4 and larger. This map, based on data from the National Earthquake Information Service [1967-1985], is probably complete since 1970 for magnitude 4 and since 1960 for magnitude 5 and larger events. A clear, more or less north-south trend of these events near the Alaska-Canada border can be seen in Figure 6. An apparently separate distribution of larger events shows a distinct west-northwest trend from the vicinity of Fairbanks, as noted by Davies [1983].

In addition to the observation that most of the events lie to the south of the continental divide, there are several clusters and trends that can be seen on the maps of earthquakes north of 65°N. These features are numbered in Figure 4 and described in Table 3.

Focal Mechanisms

Eight new fault plane solutions were determined for earthquakes in northern Alaska (Figure 7). These solutions are composed of P wave first motions plotted on equal-area lower hemisphere projections of the focal sphere. The first motions are predominantly from Alaskan regional stations and from stations of the Canadian Seismograph Network. For the larger events (magnitude greater than 4.5), stations from the World-Wide Standard Seismograph Network were also used. The Alaskan stations were checked for polarity ambiguities using nuclear explosions and teleseisms as calibration events [Estabrook, 1985].

The depths of the earthquakes whose focal mechanisms were determined in this study were fixed at 10 km because of poor depth control. This depth was chosen because results from studies of the Dall City earthquakes [Estabrook et al., 1985] and of earthquakes in the Fairbanks area [Gedney et al., 1980] show that most interior and northern Alaska earthquakes occur within the upper 20 km of the crust. Model 1 (Table 1) was used to calculate takeoff angles and to locate the earthquakes.

Stations that are farther away than the crust-mantle crossover distance (about 150 km) are plotted at a common takeoff angle regardless of their actual epicentral distance. This condition holds until roughly 1500 km (about 15°), at which distance deep-

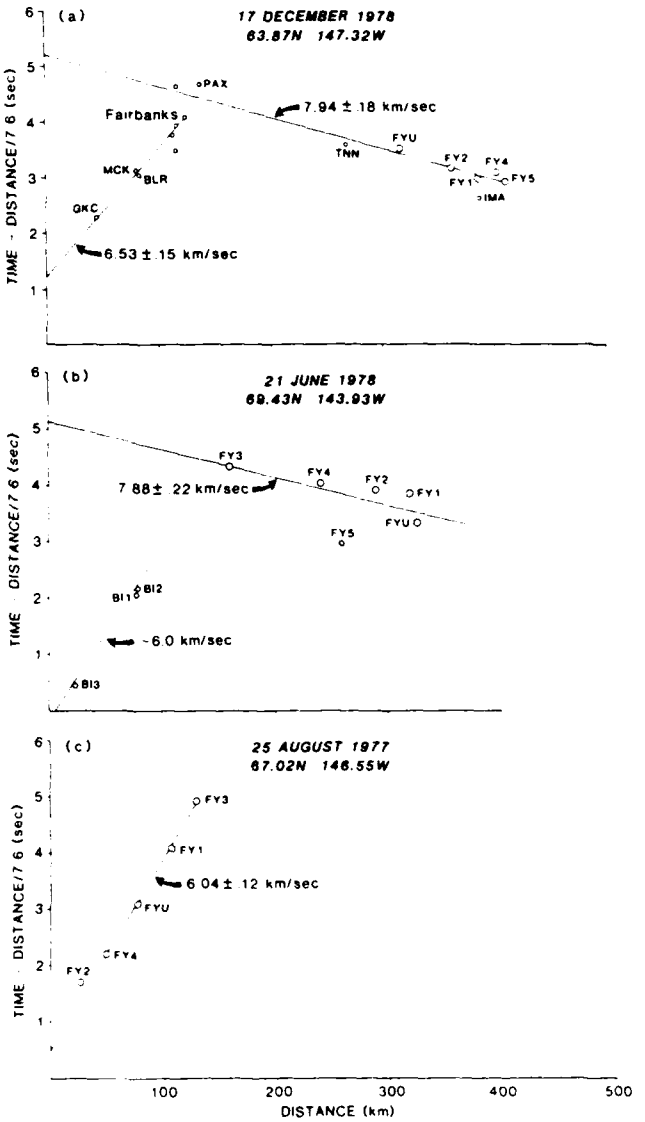

Fig. 3. Reduced travel time versus distance plot for earthquakes (a) 781217, (b) 780621, and (c) 770825. Larger circles denote station arrivals used in the velocity determination; 7.6 km/s is the reduction velocity.

TABLE 2. Velocity Model

Model	Entire Northern Alaska Data Set			Only Regional Stations at Dall City			Local and Regional Stations at Dall City		
	Number of Events	Mean	S.D.	Number of Events	Mean	S.D.	Number of Events	Mean	S.D.
1 Depth	5427	16.16	31.57	20	7.79	7.31	47	13.49	3.66
rms	5427	0.58	1.96	20	0.60	0.31	47	0.20	0.19
ERH	5427	30.37	37.35	20	9.52	21.02	47	3.33	1.78
ERZ	5427	48.66	44.06	20	40.64	43.12	47	4.28	2.49
2 Depth	5423	15.80	31.13	20	10.01	14.37	47	11.75	4.29
rms	5423	0.59	1.42	20	0.64	0.34	47	0.20	0.20
ERH	5423	31.79	37.71	20	8.67	21.12	47	3.32	1.79
ERZ	5423	48.78	44.01	20	45.61	44.33	47	4.42	2.38
3 Depth	5430	14.04	20.44	19	8.24	8.12	47	7.74	3.97
rms	5430	0.60	1.29	19	0.61	0.3[illegible]	47	0.23	0.18
ERH	5430	34.11	38.57	19	10.95	21.81	47	6.81	7.82
ERZ	5430	45.09	42.31	19	39.12	42.52	47	30.00	35.59
4 Depth	5426	16.95	25.54	20	27.28	17.32	47	5.14	4.33
rms	5426	0.58	1.28	20	0.52	0.28	47	0.25	0.14
ERH	5426	33.19	38.29	20	8.08	21.27	47	2.68	1.34
ERZ	5426	47.45	42.85	20	35.02	38.61	47	32.41	38.71
5 Depth	5427	15.83	26.39	20	12.62	15.08	47	9.31	4.59
rms	5427	0.58	1.28	20	0.64	0.34	47	0.21	0.18
ERH	5427	34.45	38.55	20	10.84	23.39	47	3.31	2.29
ERZ	5427	45.23	42.30	20	23.22	33.08	47	6.63	6.56

Statistical tests of the velocity models in Table 1. In these tests a given set of earthquakes are relocated using each of the five models, and the mean depths and standard deviations are compared. Also compared are the means and standard deviations of three measures of the quality of the hypocenter locations: (1) the root-mean-square difference between the model and observed arrival times (rms); (2) and (3) the horizontal and vertical projections, ERH and ERZ of the error ellipse calculated by HYPOELLIPSE [Lahr, 1982]. Three different data sets are used: (1) the entire northern Alaska data set, some 5430 events; (2) a set of 20 events in the Dall City area located using only regional stations (no local stations of Dall City); and (3) a set of 47 events located using both local and regional stations. Significant differences appear for (1) the mean depth calculated using model 4 for the regional-only data set; (2) and (3) the mean ERH and standard deviations for models 3 and 4, respectively, for the local and regional data set. S.D., standard deviation.

er layers of the Earth begin to be sampled. Takeoff angles for stations farther than 1500 km are taken from the Herrin tables [Herrin et al., 1968].

Earthquake fault plane solutions have been compiled for three different regions (Figure 8 and Table 4): (1) east central Interior and the Yukon Territory (events 1-9); (2) western Alaska, including parts of the Yukon-Koyukuk basin, Seward Peninsula, and the western Brooks Range (events 10-16); and (3) northeast Alaska and the Canadian margin (events 17-23).

Region 1: East Central Interior Alaska and Yukon Territories

Mechanisms for region 1 are all very similar: all are strike-slip solutions with northwesterly trending pressure axes. Event 1 (this study) is a M_S 5.0 earthquake on the Tintina fault on the south side of the Yukon Flats. Here the east-west trending nodal plane is chosen as the fault plane, indicating right-lateral strike-slip motion. This is consistent with the historical movement on this major fault [Gabrielse, 1985]. Event 2 was a strike-slip mechanism [Cook et al., 1984; Coley, 1983]. The northeast trending nodal plane is chosen as the fault plane because it parallels mapped faults as shown by Beikman [1980].

Events 3 [Gedney, 1970] and 4 [Jordan et al., 1968] reflect right-lateral movement on northwest trending fault planes which parallel the trend of the Fairbanks seismic zone [Gedney and Berg, 1969; Gedney et al., 1980]. Event 5, the M_S 6.5 Rampart earthquake [Gedney et al., 1969; Huang, 1979; Huang and Biswas, 1983; Coley, 1983], has a strike-slip mechanism similar to the Dall City (events 7 and 8) and Fairbanks area events. Huang [1979], Huang and Biswas [1983], and Coley [1983] suggested that the faulting of the Rampart event was left-lateral strike-slip on a north-south trending plane because it paralleled the aftershock zone (Figure 7).

Events 6, 7, and 8 (this study) have left-lateral strike-slip mechanisms on north to northeast trending fault planes. The north-south trending nodal planes were chosen on the basis of a detailed study of the Dall City earthquake sequence which reveals that the largest events (magnitude greater than 4.5) occurred near the middle of a north-northeast trending elongate aftershock zone [Estabrook et al., 1985]

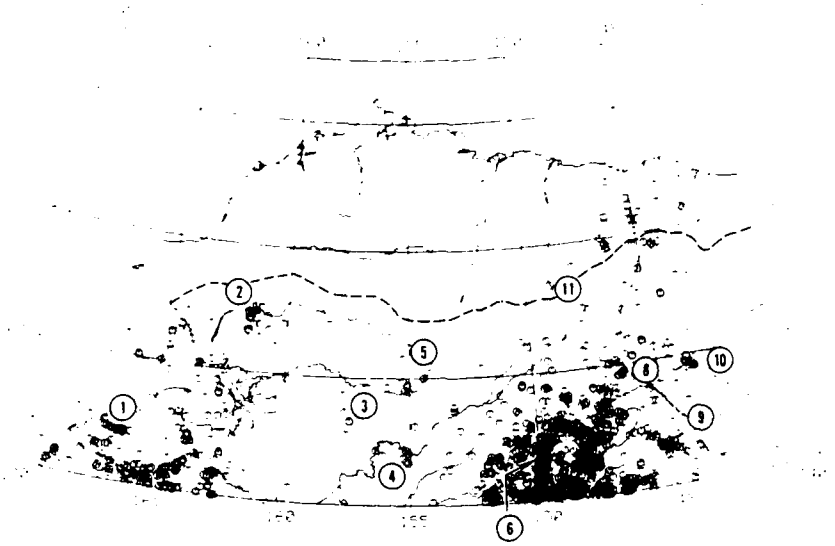

Fig. 4. Earthquake epicenters for the period 1967-1984 with horizontal location errors (ERH) <10 km, depth errors (ERZ) <20 km, root-mean-square travel time residuals (RMS) <1.00 s and number of stations >4. Dashed line represents the continental divide. Numbers refer to clusters of events described in Table 3.

and close to the active Dall Mountain fault (which trends north-south) [Brogan et al., 1975] (G. Plafker, unpublished data, 1986). Event 6, located to the south of the other two in this group, indicates a possible *southward continuation* of the Dall Mountain fault. A minor additional aftershock trend coincides with an east-northeast/south-southwest trending topographic high, which could be the surface expression of an unmapped fault subparallel to the Kaltag fault and Porcupine lineament.

Event 9 (this study), a M_b 4.6 earthquake on the Kobuk Trench, has also been studied by Gedney and Marshall [1981]. It is grouped with other events from interior Alaska because they all have similarly oriented strike-slip solutions. The solution from this study has nodal planes with slightly different orientations than those of Gedney and Marshall, as a result of incorporating data from the International Seismological Centre (ISC) [1983] bulletin. Critical to the determination of the strike of the east-west nodal plane are the regional Alaskan stations FYU and BM3 (Figure 2). These two stations have almost identical waveforms, yet opposite first motions. The station polarities were thoroughly checked and could not explain the discrepancy. The only other possibility is that of a polarity changing reflection along the ray path. The east-west trending plane is chosen as the fault plane because it is parallel to the strike of

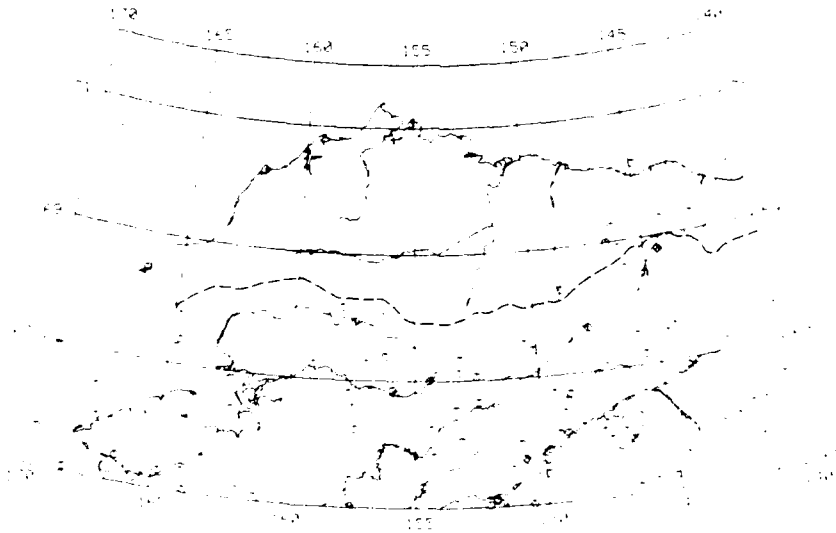

Fig. 5. Earthquakes with magnitudes greater than 3 for the years 1976-1979 when Seward Peninsula, Barter Island, and Fort Yukon nets were operational. When these networks were operating, the magnitude threshold for much of northernmost Alaska was smaller than magnitude 3. Dashed line represents the continental divide.

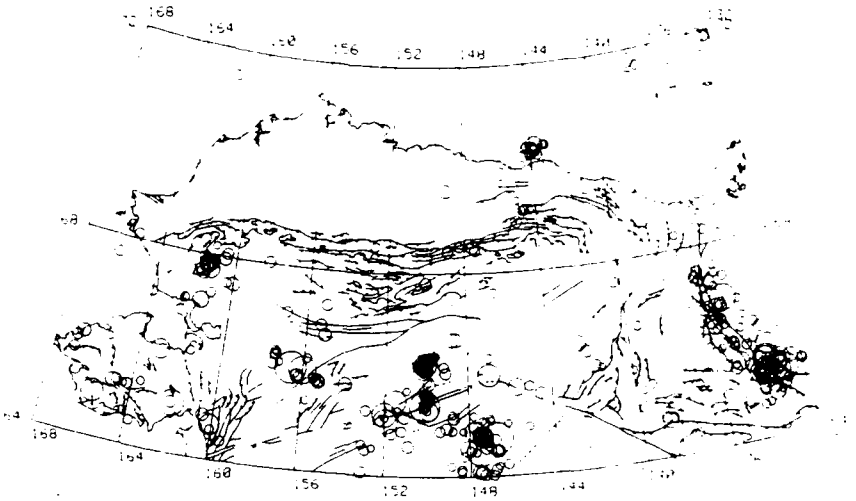

Fig. 6. Earthquakes with magnitudes greater than 4 for all years. Source NEIS. Faults are from King [1969].

the presently active Kobuk Trench [Brogan et al., 1975].

Region 2: Western Alaska

Earthquake focal mechanisms from western Alaska (events 10-16) can be divided into two groups; those north of 66°N are strike-slip, while those south of that latitude give normal faulting solutions.

Solutions by several workers [Ritsema, 1962; Fara, 1964] for event 10, the 1958 Huslia earthquake (M_S 7.3), give a normal fault mechanism on a northeast trending plane. Davis [1960] mapped ground breakage with a similar trend. A normal fault mechanism is atypical for this area. Event 11 (this study) is a composite fault plane solution determined for four events with magnitudes greater than 4.0 that occurred on the Purcell Mountain trend. If this trend is the fault plane, then event 11 represents a left-lateral strike-slip fault. It is not clear whether the Purcell Mountain trend is related to event 10, the Huslia earthquake.

Event 12, a m_b 5.2 earthquake which occurred in 1981 north of Kotzebue, has been studied by D. B. Cook (personal communication, 1985), Coley [1983], and Biswas et al. [1983]. Cook and Coley selected the east-west trending nodal plane as the probable fault plane because it is parallel to the trend of aftershocks which they relocated using the master event technique. This solution is used here because the solution to Biswas et al. [1983] is a composite with many inconsistent readings. Event 13 [Coley, 1983] is a strike-slip solution similar to event 12, possibly indicating right-lateral motion on the Kobuk Trench. These mechanisms have nodal plane orientations similar to other strike-slip events in central interior Alaska.

Earthquakes 14, 15 (D. B. Cook, personal communication, 1985), and 16 [Liu and Kanamori, 1980; Sykes and Sbar, 1974] in the southern Seward Peninsula and Norton Sound area show mainly normal faulting on east-west oriented planes. This agrees with the general trend of mapped Neogene normal faults [Hudson and Plafker, 1978]. Event 14 (D. B. Cook, personal communication, 1985) is a normal fault with a strike-slip component, with nodal plan perpendicular to events 12 and 13.

Region 3: Northeast Alaska and Beaufort Sea

A focal mechanism was determined for event (this study), an earthquake along the continent margin of the Beaufort Sea. This complements tl solutions determined by Fujita et al. [1983] for tl Barter Island M_b 4.7 earthquake (event 18) and tv from the Canadian margin (event 20 and 21) dete mined by Hasegawa et al. [1979] and Hasegav [1977], respectively. A somewhat different soluti was obtained by Biswas et al. [1986] for event 1 however, the solution of Fujita et al. [1983] was us because of the verification of the solution by surfa wave radiation patterns. All of the solutions fro along the margin (events 18, 19, 20, and 21) sh significant strike-slip components but are incons tent in nodal plane orientation. Event 20, an m_b 5 in the Mackenzie Delta area, has a P axis orient perpendicular to the spreading direction of the arc spreading center. Event 19 (this study) is similar event 20 [Hasegawa et al., 1979], possibly indicati a similar tectonic process in the region of the Ma kenzie River delta. However, the P axes of events (D. B. Cook, personal communication, 1985) and [Hasegawa et al., 1979] are rotated 90° compar with those of events 19 and 20.

The solution for event 17 (this study) is either normal faulting mechanism or a thrust mechanis but in either case the tension axis trends nort south. The normal fault solution is preferred becau the east-west trending nodal plane parallels t structural grain of the northeast Brooks Rang These regionally inconsistent solutions cannot reconciled unless one invokes slip along preexisti. fractures or local stress fields acting in place of t regional one for some of the events discussed.

Two solutions have been determined for eart quakes in the Richardson Mountains of the Yuk Territory. Event 22 is a very well constrained strik slip solution [LeBlanc and Wetmiller, 1974] whi falls on the north-south trending Eskimo Lakes fa system. If the fault plane is north-south, then t

TABLE 3. Earthquake Clusters

No.	Name	Location	Description
1	Ear Mountain cluster	65.7°N 166.0°W Figure 4	Seward Peninsula: The largest, M_L 2.7, and the other 27 events, were recorded throughout the lifetime of the Seward Peninsula network (1977-1983).
2	Baird Mt. cluster	67.8°N 161.5°W Figure 4	North of Kotzebue main shock (m_b 5.2 1982) and aftershocks. This cluster contains 12 events with m_b greater than 4.0.
3	Purcell Mountains trend	66.5°N 157.5°W Figure 4	North-south trend of 86 events, five have m_b greater than 4.0. Activity pronounced between 1971 and 1973, though earthquakes continue to the present.
4	Indian Mountain cluster	66.0°N 155.5°W Figure 4	Active since the beginning of seismic recording by the Geophysical Institute. Most activity and largest event, M_L 3.5, occurred in 1976. Many events with M_L between 2 and 3.
5	Kobuk trench	67.0°N 154.7°W Figure 4	A 1980 sequence of magnitude 4-5 earthquakes [Gedney and Marshall, 1981]. Numerous aftershocks were recorded at IMA, the closest station.
6	Rampart trend	65.5°N 150.0°W Figure 4	1968 Rampart sequence, a 1968 magnitude 6.5 event and its north-south trending aftershocks, 120 km northwest of Fairbanks. A resurgence of activity occurred in 1972 [see Huang, 1979; Huang and Biswas, 1983].
7	Dall City aftershocks	66.25°N 150.0°W Figure 6	These earthquakes, events 7 and 8 in Figure 8, were recorded between February and April 1985 (continuing to the present) and thus do not appear in Figure 4; the largest was a magnitude 6.0 (M_S) [Estabrook et al., 1985].
8	Chandalar River cluster	66.9°N 146.3°W Figure 4	M_L 3.5 event occurred in a sequence of 14 events during January-March 1979. Total of 19 events. It is noteworthy that this cluster and the Porcupine River cluster were active at nearly the same time.
9	Tintina fault	65.7°N 145.2°W Figure 4	A line of events that coincides with the Tintina fault. Much of this activity is in the Tintina Trench, northwest of central Alaska.
10	Porcupine River cluster	66.9°N 144.0°W Figure 4	M_L 3.0 is longest event in a cluster of 11 events, mostly during November 1978 to January 1979, located on the mapped trace of the Porcupine lineament.
11	Sagavanirktok River cluster	68.5°N 149.0°W Figure 4	Main shock and aftershock sequence of a m_b 4.3 earthquake, May 1980.
12	Barter Island swarm	71.3°N 143.5°W Figure 8	Barter Island swarm, January 1968, largest event M_L 5.2, occurred prior to the installation of northern Alaska stations. The Canadian Seismograph Network recorded five events with magnitudes greater than 4.0 in this swarm.
13	Eskimo Lakes fault (also known as the Richardson fault)	66.0°N 135.0°W Figures 1 and 8	Historical earthquake file of NEIS gives five events with magnitudes greater than 6.0 and 109 events with magnitudes greater than 4.0. Earthquakes associated with the Richardson Mountains and the Rocky Mt. Front. A temporary local network and determined that the seismicity was associated with a north-south trending right-lateral strike-slip fault [LeBlanc and Wetmiller, 1974].

focal mechanism is right-lateral strike slip. Event 23 [Sykes and Sbar, 1974] is an ambiguous thrust mechanism, yet the fault planes are parallel to mapped thrust faults in the Canadian Cordillera [King, 1969]. These two events have P axes oriented in a northerly direction consistent with a common tectonic stress system.

Discussion

The seismicity distribution and the focal mechanisms determined in this study and by others, together indicate that pervasive intraplate deformation is occurring in Alaska and northwest Canada, well to the north of the Alaskan subduction zone. This study

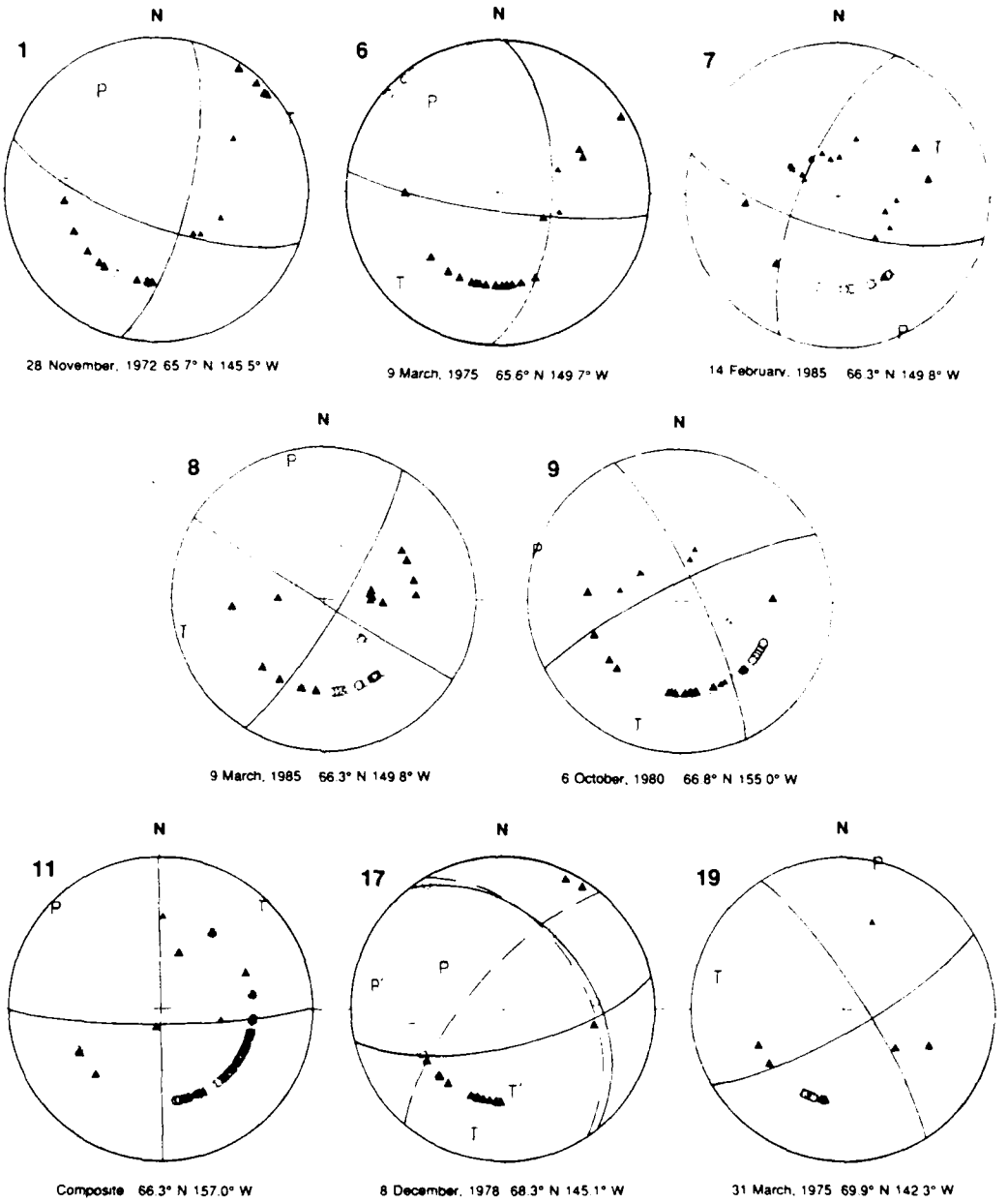

Fig. 7. Earthquake fault plane solutions determined for this study. Triangles are compressional (solid) and dilatational (open) first motions. Small triangles are station readings from the ISC catalog. The letters "P" and "T" are the pressure and tensional axes, respectively.

has also shown or confirmed that many of the major crustal faults in northern Alaska and northwest Canada are seismically active. Among these are the Tintina, Kaltag, Kobuk, Eskimo Lakes faults, and possibly the Porcupine lineament (Figure 1). Furthermore, fault plane solutions for earthquakes on the Tintina, Kobuk, and Eskimo Lakes faults reveal that the present faulting is in the same sense as their historical movement. However, as the seismicity maps reveal, most of the earthquakes smaller than magnitude 5 are not aligned along these major faults and lineaments.

A number of workers [e.g., Jones et al., 1981; Churkin et al., 1982; Moore et al., 1985] have suggested that central and northern Alaska are cor posed of tectonostratigraphic terranes, as is southe Alaska. By definition, these terranes are fau bounded, and the seismicity associated with some these deep crustal faults may indicate that these te ranes are still responding to externally appli stresses. The seismicity within the terranes is mo enigmatic, possibly occurring on reactivated min faults and other zones of weakness. The large earthquakes in northern Alaska do not always occ at terrane boundaries or along a single major fau Of the earthquakes larger than magnitude 6, eart quakes along the Eskimo Lakes fault [LeBlanc a Wetmiller, 1974] and events on the Tintina fault

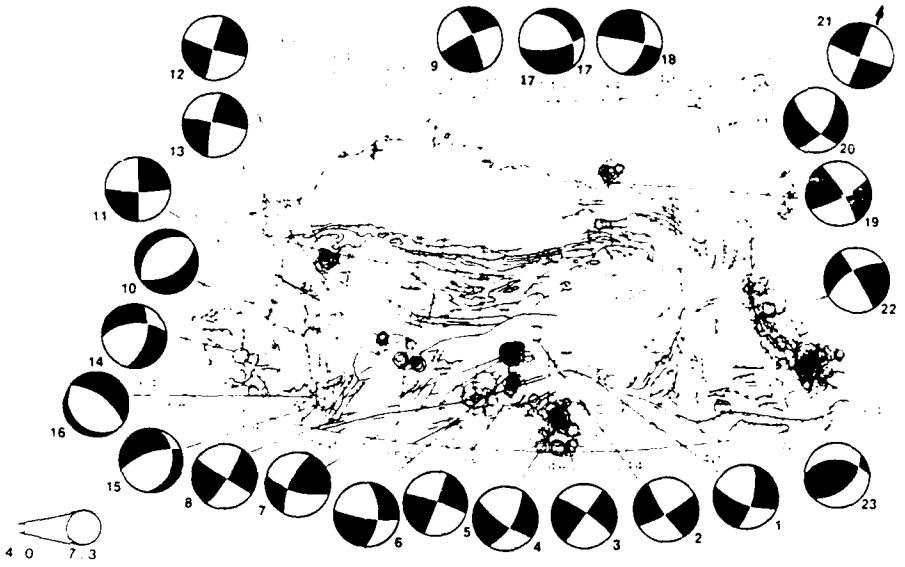

Fig. 8. Earthquake fault plane solutions, magnitude 4 and larger earthquakes (NEIS), and geologic faults [King, 1969]. Fault plane solutions are equal-area lower hemisphere projections showing quadrants of compressional (shaded) and tensional first motion. Mechanisms are oriented with north-south parallel to the edge of the paper, not parallel to map north. Mechanism parameters are found in Table 4.

associated with major tectonic boundaries. Other large earthquakes (Huslia, Fairbanks, and Dall City) were not on known terrane-bounding faults, which supports the suggestion that there must be significant deformation within crustal blocks and terranes [e.g., Davies, 1983].

Several models have been proposed for the high seismicity in northern Alaska. These can be grouped into those involving separate tectonic plates [e.g., Stone, 1983], deformation within a single plate [Nakamura et al., 1980; Davies, 1983; Biswas et al., 1983], or a combination of the two (this study). Stone [1983], among others, has hypothesized the existence of a Bering-Arctic plate, which includes much of Alaska and postulates a very slow moving transform fault along the Canadian Arctic Islands coinciding with a diffuse band of seismicity extending from interior Alaska to the Beaufort Sea [Gedney et al., 1977; Biswas and Gedney, 1979].

Focal mechanisms 19 (this study) and 20 [Hasegawa et al., 1979] have north-south oriented P axes, perpendicular to the trend of the Nansen-Gakkel spreading ridge, and nodal planes that parallel the continental margin. However, the low level of seismicity over the entire margin may preclude even a very slow (less than 1 cm/yr [Stone, 1983]) deformational margin.

Nakamura et al. [1980] show stress trajectories for Alaska based on the direction of the maximum horizontal compression, as determined from the orientation of volcanic dikes and active faults (Figure 9). Davies [1983] introduced the concept of the rigid indentor as applied to Alaska to explain the stress trajectories (see Molnar and Tapponnier [1975], for an explanation of the concept as it was first applied to Indian-Asian collision tectonics). Plasticity theory predicts a fanning of the stress trajectories from the corners of a rigid indentor being pushed into a plastic medium. For Alaska the indentor is defined as the contact area between the Pacific and North American plates, roughly the zone between the trench and the 50-km contour to the Wadati-Benioff zone. This model explains fairly well the orientations of focal mechanism pressure axes compiled in this study. However, the amount of seismicity in northern Alaska and northwest Canada is not easily explained in terms of this model (Figure 9). As expected, the most active seismicity is observed along the main stress trajectory (west-northwest from the northernmost portion of the indentor). Yet high levels of seismicity are also observed northeast of this trend in the Yukon Territory with little seismicity in between (Figure 6).

Central to any satisfactory hypothesis of the present deformation in northern Alaska and northwest Canada must be an explanation of the prominence of strike-slip faulting. Many of these faults show right-lateral offset of tens to hundreds of kilometers. Table 5 is a listing of the major right-lateral strike-slip faults with their corresponding offsets, if known, and the ages of movement. The parallel trends of the Tintina-Kaltag, Denali, and Castle Mountain–Lake Clark fault systems and the apparently younger motion from north to south, together imply that there has been a consistency of process through time [Grantz, 1966; Gedney et al., 1974; Gabrielse, 1985]. The Castle Mountain-Lake Clark [Lahr et al., 1986], Denali [Gedney and Estes, 1982], and Tintina (this study) faults are all presently showing right-lateral strike-slip motion. This suggests that the Pacific-North American plate boundary is distributed across a low-strain rate shear zone, approximately 500 km wide and extending from the continental margin to at least the Tintina fault. A similar suggestion has been made by Lahr and Plafker [1980]. When the seismicity and focal mechanisms in northern Alaska and the Yukon are seen in the light of this hypothesis, many features which were inconsistent with the other models are explained. The seismicity and focal mechanisms along the Eskimo Lakes fault are con

TABLE 4. Focal Mechanism Parameters for Earthquakes in Northern Alaska and Northwest Canada

No.	Date	Time, UT	Latitude, °N	Longitude, °W	Magnitude	Plane 1 Strike/Dip, deg	Plane 2 Strike/Dip, deg	P Axis Trend/Plunge, deg	T Axis Trend/Plunge, deg	B Axis Trend/Plunge, deg	Source
1	Nov. 28, 1972	1335	65.7	145.5	5.0 M_S	110/70	013/72	331/27	062/01	154/63	E
2	Dec. 20, 1966	0026	66.8	148.1	4.8 m_b						
	Dec. 20, 1966	0057	66.8	148.4	4.9 m_b						
	composite		66.8	148.1		058/80	146/80	014/14	283/00	193/76	C
3	June 21, 1967	1804	64.9	147.6	5.6 M_S	304/81	034/90	170/06	261/04	034/81	G
4	July 22, 1937	1709	64.5	147.1	7.2 M_S	125/76	030/68	350/26	258/05	154/63	J
5	Oct. 29, 1968	2216	65.4	150.0	6.5 M_S	019/88	287/84	151/01	243/07	038/83	HB
6	March 9, 1975	1419	65.9	149.7	4.6 M_L	002/61	098/80	324/28	227/13	115/59	E
7	Feb. 14, 1985	0504	66.3	149.8	5.0 m_b	203/70	105/71	154/01	064/28	246/62	E
8	March 9, 1985	1408	66.3	149.8	6.1 M_S	031/81	122/88	347/08	256/05	134/80	E
9	Oct. 6, 1980	1457	66.8	155.0	4.6 m_b	243/81	335/79	289/01	199/14	023/76	E
10	April 7, 1958	1530	66.0	156.6	7.3 M_S	058/55	226/36	356/79	143/09	234/06	C
11	Dec. 6, 1971	1729	67.1	157.0	4.4 m_b						
	May 12, 1972	0653	66.0	157.3	4.2 m_b						
	Oct. 3, 1972	0318	66.3	157.5	5.1 M_L						
	Oct. 5, 1973	0922	66.3	157.4	4.1 m_b						
	composite		66.3	157.0		000/90	090/82	314/06	045/06	180/82	E
12	July 12, 1981	0127	67.7	161.2	5.2 m_b	196/87	106/85	331/01	061/06	227/84	C
13	Aug. 26, 1966	1019	66.7	162.7	5.0 m_b	280/84	191/80	145/11	054/03	311/78	DC
14	Dec. 13, 1964	0033	64.9	165.6	5.3 m_b	263/57	015/60	230/47	138/02	046/43	DC
15	April 11, 1973	0512	64.6	160.0	4.2 m_b	250/70	012/35	199/54	317/19	058/29	C
16	April 16, 1965	2223	64.7	160.2	5.9 M_S	305/66	137/24	205/69	039/21	307/05	LK
17	Dec. 8, 1978	1001	68.3	145.1	4.0 M_L	078/70	323/42	305/51	194/16	093/34	E
	alternate solution					220/72	328/46	280/16	174/45	024/41	E
18	Jan. 22, 1968	2344	70.3	144.4	4.7 m_b	016/54	280/85	232/29	323/19	092/53	F
19	March 11, 1975	1253	69.9	142.3	3.8 m_b	328/80	060/78	014/01	284/16	108/74	E
20	June 14, 1975	2050	72.0	132.3	5.1 m_b	136/73	034/59	358/34	262.09	160/54	H79
21	Dec. 27, 1972	2259	76.8	106.5	5.7 M_S	110/85	200/90	065/05	335/05	206/85	H77
22	July 26, 1972	1846	66.5	136.0	4.8 m_b	236/65	328/86	196/21	099/14	337/64	LW
23	Oct. 5, 1965	0017	65.4	132.9	5.0 m_b	271/50	044/52	336/01	250/63	067/26	SS

Parameters for focal mechanisms shown in Figure 8. Dip is to the right of strike; m_b and M_S magnitudes are from the ISC and NEIS, M_L are from the University of Alaska. Locations and origin times are from the ISC. Sources: C, Coley [1983]; DC, D. B. Cook (personal communication, 1987); E, this study; F, Fujita et al. [1983]; G, Gedney [1970]; H77, Hasegawa [1977]; H79, Hasegawa et al. [1979]; HB, Huang and Biswas [1983]; J, Jordan et al. [1968]; LK, Liu and Kanamori [1980]; LW, LeBlanc and Wetmiller [1974]; and SS, Sykes and Sbar [1974].

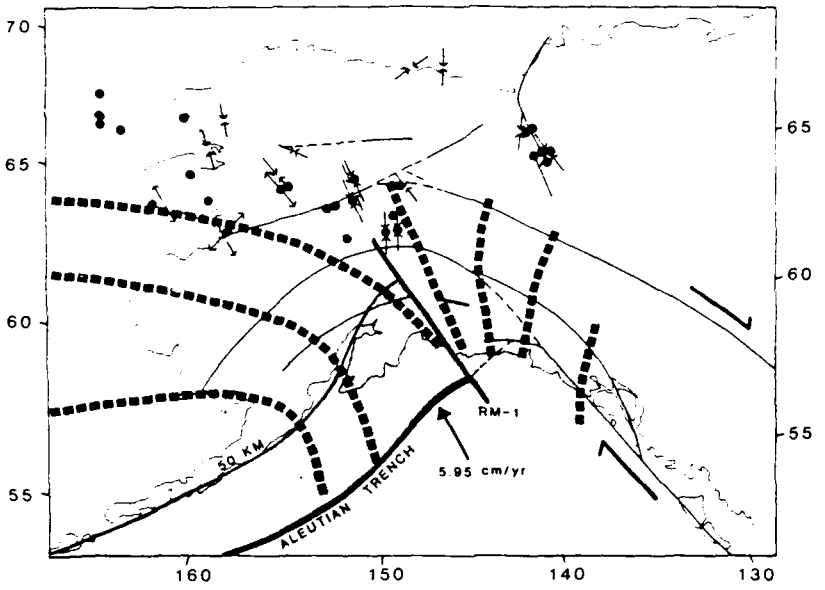

Fig. 9. Model proposed for deformation of continental Alaska and northwest Canada. The exact boundaries of the "rigid indentor" (stippled) are speculative. The 50-km Wadati-Benioff zone contour is from Stephens et al. [1984] and Stone [1983]. Pacific-North America motion (RM-1) and convergence rate are from Minster et al. [1974]. Stress trajectories (heavy dashed lines) are from Nakamura et al. [1980], selected earthquakes ($M>6$) are from NEIS. Small arrows represent the P and T axes; the large arrows represent the distributed shear zone discussed in the text.

sistent with compression from the south. The seismicity occurs at a sharp bend in the Rocky Mountain front, the bend being a possible stress concentrator. The focal mechanisms in interior Alaska, being mostly strike-slip, are consistent with a shear system extending into the area from the southeast. The northern extent of the shear system has been shown to be as far north as 68°N where east-west striking strike-slip faults cut across Brooks Range structures [Dillon, 1985].

The Huslia earthquake described earlier and the extensional tectonics on the Seward Peninsula [Turner et al., 1981; Biswas et al., 1983; Lockhart, 1984] are enigmatic features in a region dominated by strike-slip faulting. The Huslia earthquake, the largest event in northern Alaska in historic times, must fit into any reasonable tectonic model. Normal faulting can, however, be consistent within a strike-slip regime if the concept of wrench faulting and formation of pull-apart basins is invoked.

Cenozoic extension on the Seward Peninsula must be accounted for in any tectonic model of northern and western Alaska. This extension has been studied extensively using geologic and geophysical methods. The region is characterized by north-south extension on east-west striking normal faults. Extensive Cenozoic alkali and tholeiitic basalts [Turner et al., 1981] and a zone of seismically active normal faults in the southern Seward Peninsula [Biswas et al., 1983] are manifestations of the extensional deformation. Lockhart [1984] concluded that the extension is not caused by localized rifting but by regional

TABLE 5. Offsets on Major Strike-Slip Faults in Alaska and Northwestern Canada

Fault	Age of Motion	Offset	Reference
Castle Mountain – Lake Clark	Early Cretaceous – Present	tens of km	Grantz [1966]
Denali, east of Mount McKinley	Cretaceous – Present	400 km	Turner et al. [1974]
Denali, west of Mount McKinley		100-115 km	Grantz [1966]
Tintina, in Yukon and Alaska	Paleozoic and Mesozoic, most in Cretaceous	450 km	Dover [1985]
Tintina, northern British Columbia	Middle Jurassic – Early Cretaceous	+900 km	Gabrielse [1985]
Kaltag	Late Cretaceous – Present	140 km	Patton and Hoare [1968]

extension reactivating ancient faults. This is based on an extensive gravity study of the area, on comparison of the Seward Peninsula to other rifts around the world, and on the high proportion of alkali versus tholeiitic basalts, indicating a differentiated and not a primitive mantle source for the basalts.

The Seward Peninsula regional extension, if not caused by continental rifting, could have a source similar to that proposed for the Huslia area of the Koyukuk basin: wrench faulting in a compressive strike-slip tectonic regime. A problem with this model is the immense size of the extensional area compared with other pull-apart basins [Aydin and Nur, 1982]. Another possibility is a back arc tensional regime. However, the dimensions of the area and the distance to the arc are longer than are commonly associated with back arc extension.

Conclusions

A simple P wave velocity structure of a 35-km-thick, 6.1 km/s crust over a 7.9 km/s upper mantle was developed for interior and northern Alaska. The crustal velocity value, determined using different techniques in the Dall City area and eastern Brooks Range, is consistent with continental crust.

The Alaskan North Slope is apparently aseismic, and earthquakes larger than magnitude 3.0 are evenly distributed within and south of the Brooks Range and follow the curve of the range to the northeast. This seismicity occurs on major tectonic faults and also within terranes or crustal blocks. The central Kaltag, northwest Tintina, central Kobuk, Eskimo Lakes, Porcupine, Dall City, and Rampart faults are presently seismically active. The largest earthquakes (greater than magnitude 6.0) occur to the south of the Brooks Range on a west-northwest trend parallel to the main stress trajectory that would result from the convergence of the Pacific and North American plates. In the interior of Alaska they occur either on tectonic faults or within crustal blocks at the intersection of lineaments.

Focal mechanisms determined for earthquakes in central interior Alaska indicate strike-slip faulting with north-northwest oriented compressional axes. These parallel the predicted stress trajectories of the Pacific plate indenting into North America. The concept of large-scale shearing as a mechanism of deformation, in addition to the compressional interaction of the Pacific plate with southern Alaska, can account for the preponderance of strike-slip mechanisms on major crustal faults. We propose that the Pacific-North American transform boundary includes a zone of low strain rate deformation about 500 km wide which exhibits right-lateral strike-slip faulting. Most of the relative motion is on the Fairweather fault (greater than 5 cm/yr), with less on the Denali fault (about 1.0 mm/yr [Horner, 1983]), and probably much less motion on the Tintina fault.

Acknowledgments. We would like to thank L. Gedney, N. N. Biswas, and H. Pulpan for allowing us access to unpublished earthquake phase data and for many helpful comments and suggestions and K. Fujita and R. Page, who provided many constructive comments. The U.S. Geological Survey (USGS), the Canadian Seismic Network, and the Lamont-Doherty Geological Observatory provided first-motion data. Funding for this study came from the Rice University–University of Alaska Industrial Associates Program, USGS grant 14-08-00001-G-1109, and the Alaska Division of Geological and Geophysical Surveys.

References

Aydin, A., and A. Nur, Evolution of pull-apart basins and their scale independence, Tectonics, 1, 91-105, 1982.

Beikman, H. M., Geologic map of Alaska, scale 1:250,000, U S. Geol. Surv., Denver, Co., 1980.

Biswas, N. N., and L. Gedney, Seismotectonic studies of northern and western Alaska, environmental assessment of the Alaskan Continental Shelf, Vol. X , Hazards and Data Management, pp. 155-189, NOAA, U.S. Department of Commerce, Anchorage, Ak., 1979.

Biswas, N. N., J. Pujol, G. Tytgat, and K. Dean, Synthesis of seismicity studies for western Alaska, Rep. NA81-RAC00112, 69 pp., Nat. Oceanic and Atmos. Admin., Anchorage, Ak., 1983.

Biswas, N. N., K. Aki, H. Pulpan, and G. Tytgat, Characteristics of regional stresses in Alaska and neighboring area, Geophys. Res. Lett., 13, 177-180, 1986.

Brogan, G. E., L. S. Cluff, M. K. Korringa, and D. B. Slemmons, Active faults of Alaska, Tectonophysics, 29, 73-85, 1975.

Churkin, M., H. L. Foster, R. M. Chapman, and F. R. Weber, Terranes and suture zones in east central Alaska, J. Geophys. Res., 87, 3718-3730, 1982.

Coley, M. J., Intraplate seismicity in central Alaska and Chukotka, M.S. thesis, 97 pp., Mich. State Univ., East Lansing, 1983.

Cook, D. B., M. J. Coley, and K. Fujita, Intraplate seismicity of north-central and western Alaska, Geol. Soc. Am. Abstr. Programs, 16(5), 276, 1984.

Davies, J. N., Seismicity of the interior of Alaska – A direct result of Pacific-North American plate convergence?, Eos Trans. AGU, 64, 90, 1983.

Davis, T. N., A field report on the Alaskan earthquakes of April 7, 1958, Bull. Seismol. Soc. Am., 50, 489-510, 1960.

Dillon, J. T., Structure and stratigraphy of the southern Brooks Range and northern Koyukuk basin near the Dalton Highway, in Guidebook to Bedrock Geology Along the Dalton Highway, Yukon River to Prudhoe Bay, Alaska, edited by C. G. Mull, pp. 35-74, Alaska Division of Geological and Geophysical Surveys., Fairbanks, Ak., 1985.

Dover, J. H., Tectonic framework of Interior Alaska–A model of continental margin extension, collapse and dispersion, paper presented at meeting, Am. Assoc. of Pet. Geol. – Soc. of Paleontol. and Mineral. – Soc. of Explor. Geophys. Pac. Sect., Anchorage, Ak., 1985.

Estabrook, C. H., Seismotectonics of northern Alaska, M.S. thesis, 139 pp., Univ. of Alaska, Fairbanks, 1985.

Estabrook, C. H., J. N. Davies, L. Gedney, and S. A. Estes, A strong Alaskan earthquake sequence, Eos Trans. AGU, 66, 685, 1985.

Fara, H., A new catalogue of earthquake fault plane solutions, Bull. Seismol. Soc. Am., 54, 1491-1517, 1964.

Fujita, K., D. B. Cook, and M. J. Coley, Tectonics of the western Beaufort and Chukchi seas, Eos Trans. AGU, 64, 263, 1983.

Gabrielse, H., Major dextral transcurrent displacements along the Northern Rocky Mountain Trench and related lineaments in north-central

British Columbia, Geol. Soc. Am. Bull., 96, 1-14, 1985.
Gedney, L., Tectonic stresses in southern Alaska in relationship to regional seismicity and the new global tectonics, Bull. Seismol. Soc. Am., 60, 1789-1802, 1970.
Gedney, L., and E. Berg, The Fairbanks earthquakes of June 21, 1967; aftershock distribution, focal mechanisms, and crustal parameters, Bull. Seismol. Soc. Am., 59, 73-100, 1969.
Gedney, L., and S. A. Estes, A recent earthquake on the Denali fault in the southeast Alaska Range, Short Notes on Alaskan Geology - 1981, Geol., Rep. 73, Alaska Div. of Geol. and Geophys. Surv., Fairbanks, Ak., 1982.
Gedney, L., and D. L. Marshall, A rare earthquake sequence in the Kobuk Trench, northwestern Alaska, Bull. Seismol. Soc. Am., 71, 1587-1592, 1981.
Gedney, L., E. Berg, H. Pulpan, J. Davies, and W. Feetham, A field report on the Rampart, Alaska, earthquake of October 29, 1968, Bull. Seismol. Soc. Am., 59, 1421-1423, 1969.
Gedney, L., J. Van Wormer, and L. Shapiro, Tectonic lineaments and plate tectonics in south-central Alaska, in Proceedings First International Conference on New Basement Tectonics, pp. 27-34, Utah Geol. Assoc. Pub. No. 5, Salt Lake City, Utah, 1974.
Gedney, L., N. Biswas, P. Huang, S. Estes, and C. Pearson, Seismicity of northeast Alaska, Geophys. Res. Lett., 4, 175-177, 1977.
Gedney, L., S. A. Estes, and N. N. Biswas, Earthquake migration in the Fairbanks, Alaska seismic zone, Bull. Seismol. Soc. Am., 70, 223-241, 1980.
Grantz, A., Strike-slip faults in Alaska, U.S. Geol. Surv. Open File Rep., 267, 82 pp., 1966.
Hanson, K., A seismic refraction profile and crustal structure in central Interior, M.S. thesis, Geophysical Institute, 59 pp., Univ. of Alaska, Fairbanks, 1968.
Hanson K., E. Berg, and L. Gedney, A seismic refraction profile and crustal structure in central interior Alaska, Bull. Seismol. Soc. Am., 58, 1657-1665, 1968.
Hasegawa, H. S., Focal Parameters of four Sverdrup Basin earthquakes in November and December 1972, Can. J. Earth Sci., 14, 2481-2494, 1977.
Hasegawa, H. S., C. W. Chou, and P. W. Basham, Seismotectonics of the Beaufort Sea, Can. J. Earth Sci., 16, 816-830, 1979.
Herrin, E., et al., 1968 seismological tables for P phases, Bull. Seismol. Soc. Am., 58, 1193-1241, 1968.
Horner, R. B., Seismicity in the St. Elias region of northwestern Canada and Southeastern Alaska, Bull. Seismol. Soc. Am., 73, 1117-1138, 1983.
Huang, P., Aftershocks of the 1968 Rampart, Alaska, earthquake, M.S. thesis, 155 pp., Geophys. Inst., Univ. of Alaska, Fairbanks, 1979.
Huang, P., and N. N. Biswas, Rampart seismic zone of central Alaska, Bull. Seismol. Soc. Am., 73, 813-829, 1983.
Hudson, T., and G. Plafker, Kigluaik and Bendeleben faults, Seward Peninsula, The United States Geological Survey in Alaska - Accomplishments During 1977, edited by K. M. Johnson, U.S. Geol. Surv. Circ., 722B, B47-B50, 1978.
International Seismological Centre, Bulletin of the International Seismological Centre, Newbury, Berkshire, England, May 1967-Feb. 1983.
Jin, D. J., and E. Herrin, Surface wave studies of the Bering Sea and Alaska area, Bull. Seismol. Soc. Am., 70, 2117-2144, 1980.
Jones, D. L., N. J. Siberling, H. C. Berg, and G. Plafker, Preliminary terrane map of Alaska, scale 1:250,000, U.S. Geol. Surv. Open File Map, 81-792, 1981.
Jordan, J., G. Dunphy, and S. Harding, The Fairbanks, Alaska earthquakes of June 21, 1967, U.S. Dep. of Commer., ESSA Prelim. Seismol. Rep., 60 pp., U.S. Coast and Geod. Surv., Washington, D.C., 1968.
King, P. B., Tectonic map of North America, scale 1:5,000,000, U.S. Geol. Surv., Denver, Co., 1969.
Kirschner, C. E., M. A. Fisher, T. R. Bruns, and R. G. Stanley, Interior provinces in Alaska, paper presented at meeting, Am. Assoc. of Pet. Geol. - Soc. of Econ. Paleontol. and Mineral. - Soc. of Explor. Geophys. Pac. Sect., Anchorage, Ak., 1985.
Lahr, J. C., HYPOELLIPSE/VAX: A computer program for determining local earthquake hypocentral parameters, magnitude, and first motion pattern, U.S. Geol. Surv. Open File Rep., 80-59, 1982.
Lahr, J. C., and G. Plafker, Holocene Pacific-North American plate interaction in southern Alaska: Implications for the Yakataga seismic gap, Geology, 8, 483, 1980.
Lahr, J. C., R. A. Page, C. D. Stephens, and K. A. Fogleman, Sutton, Alaska, Earthquake of 1984: Evidence for activity on the Talkeetna segment of the Castle Mountain fault system, Bull. Seismol. Soc. Am., 76, 967-983, 1986.
LeBlanc, G., and R. J. Wetmiller, An evaluation of Seismological data available for the Yukon Territory and Mackenzie Valley, Can. J. Earth Sci., 11, 1435-1454, 1974.
Liu, H.-L., and H. Kanamori, Determination of source parameters of mid-plate earthquakes from the waveforms of body waves, Bull. Seismol. Soc. Am., 70, 1989-2004, 1980.
Lockhart, A. B., A gravity survey of the central Seward Peninsula. Alaska, Geol. Soc. Am. Abstr. Programs, 16(5), 319, 1984.
Mayfield, C. F., I. L. Tailleur, and I. Ellersieck, Stratigraphy, structure, and palinspastic synthesis of the western Brooks Range, northwestern Alaska, U.S. Geol. Surv. Open File Rep., 83-779, 58 pp., 1983.
Minster, J. B., T. H. Jordan, P. Molnar, and E. Haines, Numerical modelling of instantaneous plate tectonics, Geophys. J. R. Astron. Soc., 36, 541-576, 1974.
Molnar, P., and P. Tapponnier, Cenozoic tectonics of Asia: Effects of a continental collision, Science, 189, 419-426, 1975.
Moore, T. E., W. P. Brosgi, M. Churkin, and W. K. Wallace, Pre-Mississippian accreted terranes of northeastern Brooks Range, Alaska, paper presented at meeting, Am. Assoc. of Pet. Geol. - Soc. of Econ. Paleontol. and Mineral. - Soc. of Explor. Geophys. Pac. Sect., Anchorage, Ak., 1985.
Nakamura, K., G. Plafker, K. H. Jacob, and J. N. Davies, A tectonic stress trajectory map of Alaska using information from volcanoes and faults, Bull. Earthquake Res. Inst. Univ. Tokyo, 55, 89-100, 1980.
National Earthquake Information Service, Preliminary Determination of Epicenters, U.S. Geol. Surv., Reston, Va., May 1967-April 1985.
Norris, D. K., and C. J. Yorath, The North American plate from the Arctic Archipelago to the Romanzof Mountains, in The Ocean Basins and Margins,

APPENDIX V

Bulletin of the Seismological Society of America, Vol. 76, No. 5, pp. 1207-1214, October 1986

ADDITIONAL EVIDENCE FOR DOWN-DIP TENSION IN THE PACIFIC PLATE BENEATH CENTRAL ALASKA

BY LARRY GEDNEY AND JOHN N. DAVIES

ABSTRACT

Small intermediate-depth earthquakes cluster in a volume about 20 km in diameter beneath Gold King, a landing strip on the northern flanks of the Alaska Range. These events, almost 600 km from the Aleutian trench, are the northernmost which can be identified as being associated with the Benioff zone extending inland from Cook Inlet west of Anchorage. First-motion observations of the Gold King events at local stations can be combined to determine a tensional axis dipping steeply to the north at an azimuth just west of north. This composite mechanism suggests that the slab is subjected to down-dip tensional forces, probably as a result of gravitational sinking.

INTRODUCTION

Gutenberg and Richter (1941, 1954) observed that the volcanoes associated with the Aleutian Islands persisted northeastward into south-central Alaska accompanied by earthquakes 100 km or more in depth. Benioff (1954) suggested that the focal zone of the intermediate-depth events described an inclined slab dipping at 28° beneath the volcanic arc. Tobin and sykes (1966) and Tarr (1970) showed that the intermediate-depth earthquakes extended well to the north beyond the volcanoes to the vicinity of Mt. McKinley and slightly north of the Alaska Range. Tarr (unpublished data, 1971) has observed that these events were smoothly connected as an inclined plane, or Wadati-Benioff zone, to the shallow earthquakes near the Aleutian trench. Seismicity maps by Meyers (1976) illustrate this relationship.

During the past 20 yr, regional seismograph networks operated by the University of Alaska and the U.S. Geological Survey have refined the picture, showing that the inclined seismic zone is about 20 km thick, and that there are abrupt changes in trend. One of the changes in strike occurs near Cape Douglas in lower Cook Inlet, and another is found just south of Mt. McKinley (VanWormer *et al.*, 1974; Davies, 1975; Lahr, 1975; Estes, 1978; Agnew, 1980).

It is the purpose of this short paper to describe a cluster of intermediate-depth earthquakes just south of Fairbanks which may define the absolute northern tip of the subducting north Pacific plate in North America.

THE GOLD KING EARTHQUAKES

We refer to these earthquakes as the Gold King cluster, after a nearby landing strip on the northern flanks of the Alaska Range (Figures 1 and 2). Even though this grouping is quite pronounced, it escaped notice for a number of years because the earthquakes were of fairly small magnitude and well separated in time. Further, although small shallow earthquakes are fairly common in the area, it had not been noticed that events of the present group all fell within a narrowly confined intermediate-depth range.

The cluster lies near the reported epicenters of a magntiude $6\frac{1}{4}$ earthquake on 21 January 1929 and a magnitude 7.0 event on 16 October 1947. The epicenter of the first event was about 64.0°N, 148.0°W (Davis and Echols, 1960), although this location was based largely on felt reports. There is considerable scatter in the various locations given for the 1947 earthquake (St. Amand, 1948; Hodgson and

Milne, 1951; Davis and Echols, 1960; Jordan *et al.*, 1968). H. Pulpan (1986, personal communication) relocated the epicenter to 64.35°N, 148.20°W, but there is no indication given by any of these workers that the 1947 earthquake was of greater than normal depth, and it seems unlikely that the Gold King earthquakes, which are mostly 100 km or more in depth, can be associated with that event.

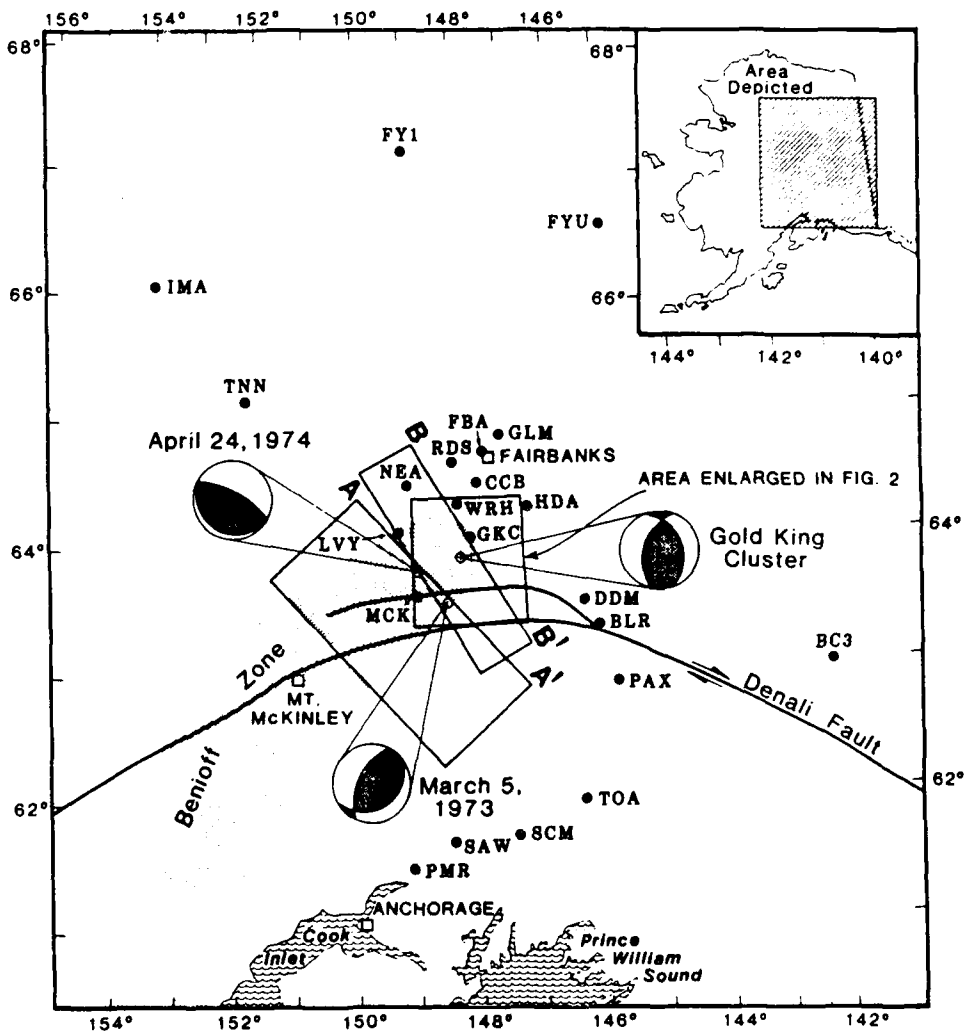

FIG. 1. Three-letter station designators show the locations of the seismographic stations utilized in this study. The two upper hemisphere focal mechanisms on the *left* were obtained by Bhattacharya and Biswas (1979), and the one on the *right* is from this report. Cross-section A-A' is 100 km thick, and B-B' is 50 km thick.

Since the first earthquakes which can be identified as belonging to the Gold King cluster were recorded in 1969, the seismographic networks in the state have had many different configurations. The stations which have operated the longest, and the ones used for most of the data presented in this report, are those shown in Figure 1.

The better solutions for the Gold King earthquakes are those available from 1978 through 1984, and 86 of these are plotted in Figures 2 and 3. (In addition, Figure 3 shows all regional events meeting the criteria given below.) In general, the solutions shown in Figure 2 fall within a depth range of 100 to 130 km, and most of them lay

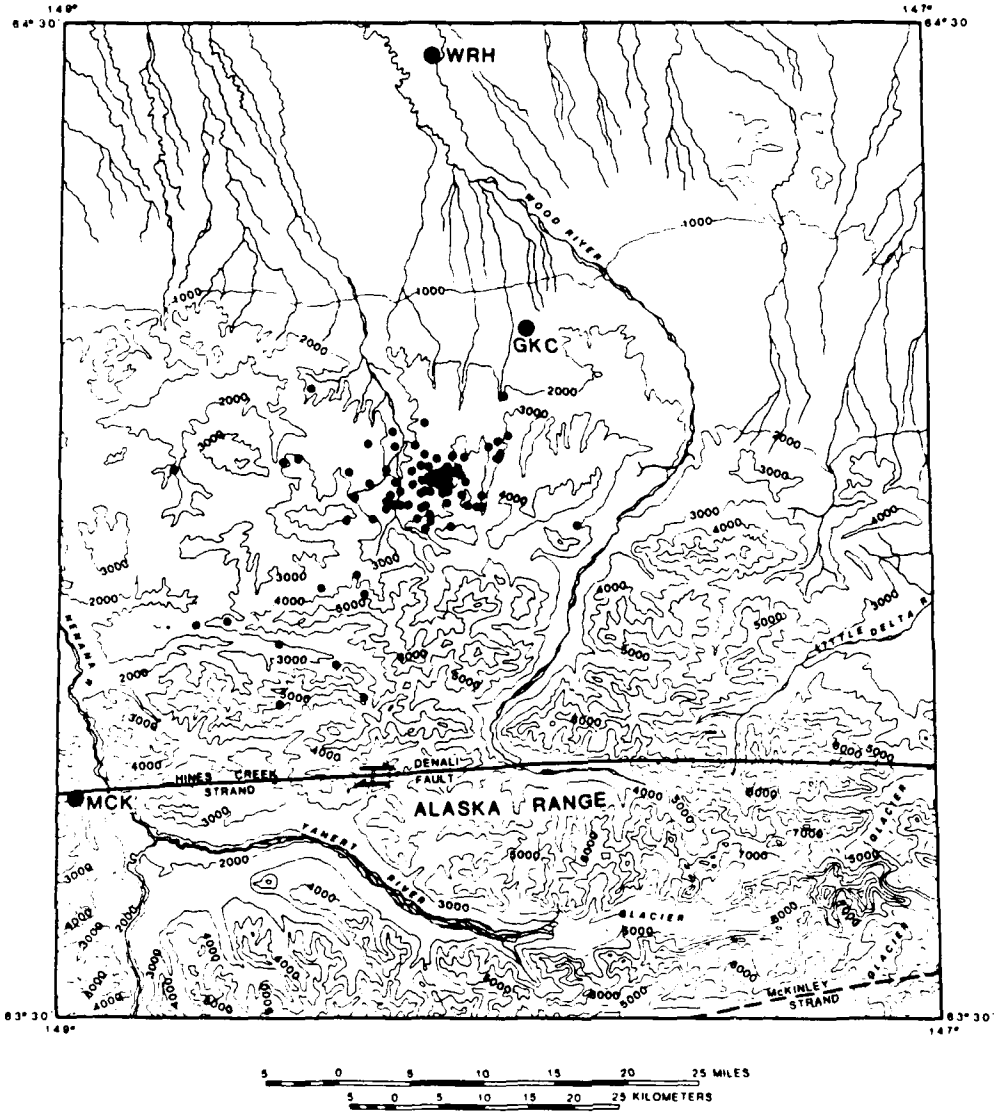

FIG. 2. Epicentral plot of 86 earthquakes of the Gold King cluster located between 1978 and 1984. WRH, GKC, and MCK are local seismographic stations.

within a radius of 10 km of 64.06°N, 148.11°W (the pronounced center of the group and the coordinates of an event described later). Although some vertical scattering is noted, 20 km is probably a good approximation for the dimensions of the cluster as a whole, because depth control is less reliable than horizontal control. Magnitudes of the earthquakes were all small; the largest was only $M_L = 3.1$.

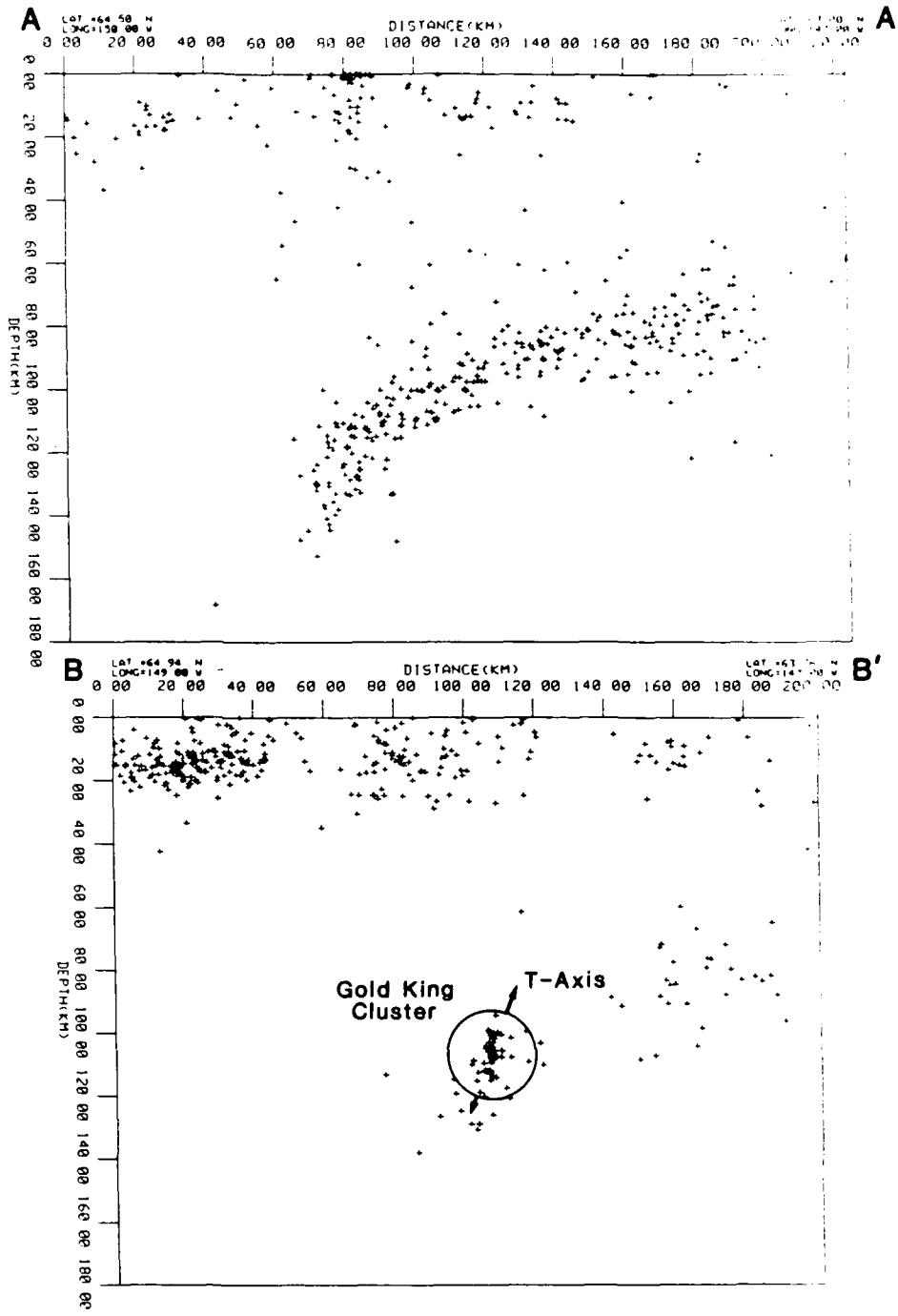

FIG. 3. Cross-sections looking to the northeast along the Benioff zone (see Figure 1 for locations). Solutions indicated were determined from five or more stations between 1978 and 1984. Section A-A' is 100 km thick, and B-B' at the very tip of the zone is 50 km thick.

Only earthquakes which were well-recorded by at least five stations have been plotted on either of these figures. *S*-wave arrivals, which were typically very distinct, were used in the solutions when available. The crust and upper mantle structure given by Huang and Biswas (1983) for central interior Alaska was used in a version of the U.S. Geological Survey's HYPOELLIPSE location program (Lahr, 1984).

The events plotted in Figures 2 and 3 were required to have rms solution errors of less than 0.5 sec. Selected events used for a composite focal mechanism solution were required to have very clear first arrivals and rms solution errors of less than 0.2 sec. The parameters of the 37 earthquakes in the latter group are given in Table 1. Nearly all fell within a few kilometers of the area of densest hypocentral concentration.

Figure 1 shows the locations of the two northeast-looking cross-sections plotted as Figure 3. Section *A-A'*, just to the northeast of Mt. McKinley, clearly shows the characteristic profile of a Benioff zone. Just beyond this to the northeast, section *B-B'* demonstrates that the subduction zone has all but died out, save for the remnant that the Gold King cluster represents.

Focal Mechanism

Table 1 presents a summary of the first motions that are plotted in the focal mechanism shown as Figure 4. The arrivals at most stations were very consistent over the years, although some reversals were noted at stations falling near a nodel plane (such as RDS and TOA).

In plotting Figure 4, the azimuths and distances given to the individual stations are those which would have resulted from an earthquake occurring at coordinates 64.06°N, 148.11°W and at 106 km focal depth. This location falls near the center of the cluster, and the coordinates are those of the earthquake on 23 May 1978 at 17:48 UTC.

The solution parameters are given in Table 2. From Figures 3 and 4, it is seen that the tensional axis lies subparallel to the surface of the Pacific lithospheric slab at an azimuth mid-way between the direction of plate motion (Minster and Jordan, 1978) and the plunge vector of the downgoing slab (Agnew, 1980). Bhattacharya and Biswas (1979) present two focal mechanism solutions of earthquakes in the adjacent area to the southwest (on 5 March 1973 and on 24 April 1974; Figure 1) in the same depth range (106 and 121 km, respectively) that also show steeply dipping *T* axes, although the orientations of the null axes vary considerably.

Discussion

To the south of the present study area, the down-dip direction for the tensional axis for intermediate-depth earthquakes has been observed within the Pacific plate on both the Alaska Peninsula (Akasche, 1968; House and Jacob, 1983) and in the Cook Inlet area (Lahr, 1975; Bhattacharya and Biswas, 1979; Engle, 1982).

However, Engle (1982) also notes that there is an alignment of the *P* axes of shallow and intermediate earthquakes in a general north-south direction around Cook Inlet. Further, Pulpan and Frohlich (1985) argue that the north-south orientation of the *P* axes in the region between 59°N and 60.5°N is stronger than the down-dip alignment of the *T* axes. They conclude, therefore, that the focal mechanism data indicate a "generally north-south horizontal compression regime" beneath Cook Inlet. They propose that the transition between a tensional stress regime south of 59° on the Alaska Peninsula to the compressional regime to the north can be attributed to segmentation of the Pacific plate.

TABLE 1

LISTING OF EARTHQUAKES FROM WHICH FIRST *P* ARRIVALS WERE USED IN COMPOSITE FOCAL MECHANISM SOLUTION*

Yr	Mo	Dy	Time	Latitude (°N)	Longitude (°W)	*H* (km)	Stations																				
							GKC	WRH	CCB	HDA	MCK	LVY	NEA	RDS	FBA	GLM	DDM	BLR	PAX	TNN	FYU	FY1	BC3	IMA	TOA	SCM	SAW	PMR
78	01	02	1041	64.02	148.17	123	C				D			C		C												
78	01	21	0522	64.03	148.16	111	C				C			D		C						D						
78	04	06	0305	64.06	148.15	103	C				C			C				D	D	D				C	C		
78	04	15	1957	64.07	148.14	104					C		D	D		C		D	D	D	D	D		D	C		C	
78	05	10	1045	64.04	148.13	109					C	D	D			C		D	D	D	D	D		D		C	C	C
78	05	23	1748	64.06	148.11	106	C				C	D	D	C		C			D	D	D	D		D	C			C
78	06	30	1234	64.01	148.34	107					C	D	D	D		C		D	D	D	D	D		D	D	C	C	C
78	07	10	0200	64.05	148.13	106	C				C	D		D		C		C							C			
78	08	31	2215	64.02	148.20	123	C							C		C					D							
78	11	03	0734	64.01	148.28	130	C						D	C		C												
79	08	23	2144	64.07	147.99	106										D		D					D					
79	09	06	1543	64.02	148.23	129	C							D		C		D					D					
79	09	26	0239	64.06	148.45	124	C				D			D		C												
79	10	25	0509	64.09	147.98	114	C							C		C			D				D					
79	11	23	0251	64.03	148.32	105	C							C		D		D	D									
80	08	21	0206	64.03	148.15	111	C				C			D			D											
80	10	04	2243	64.01	148.15	129	C			C	C			C	C						D							
80	11	04	0958	64.05	148.25	116	C			C				C			D	D										
80	11	11	0025	64.08	148.23	112	C			C	C								D									
81	01	06	0343	64.04	148.15	107	C												D						D			
81	01	15	1928	64.04	148.15	106				C	C								D									
81	02	20	0607	64.05	148.15	101				D	C			C				D										
81	02	27	1030	64.07	147.98	93	C			C	C	D			C		D		D									
81	03	07	0740	64.00	148.10	101	C			C	C						D	D	D				D		C			
81	03	12	2119	64.06	148.17	112	C			C			D						C									
83	08	23	1823	64.04	148.11	107	C		C	C			D															
83	09	20	0707	64.10	148.16	110	C		C	C			D															
83	10	16	0931	64.02	148.11	105		C			C			D														
83	11	20	2125	64.05	148.10	103						D		C					D									
83	11	27	1715	64.05	148.11	108	C	C	C	C	C	C	D	C		C			D				D			C		
83	11	29	1828	64.04	148.11	107	C		C	C	C	D	D	C	C			D					D			C		
84	01	01	1903	64.48	148.27	101			C			D		C														
84	01	06	0904	64.05	148.75	132			C	C	C			C														
84	04	17	1121	64.05	148.33	123	C		C	C	C		D	C	C	C		D	D				D			C		
84	07	27	0507	63.90	148.60	107	C	C	C	C	C			C				D										
84	11	05	1734	64.05	148.08	111	C	C			C			C		C												
84	12	01	1147	64.03	148.12	107	C	C	C	C	C	D		C	C				D				D					

* Magnitudes were mostly in the $M = 2$ to 3 range, with the largest being the magnitude 3.1 event at 10:45 on 10 May 1985. The letters C and D denote initial compressions and dilatations, respectively, at the individual recording stations.

This segmentation can be delimited by the abrupt 30° to 40° bends in the strike of the Benioff zone at 59°N and 63°N. A consistent interpretation of the Gold King data would be that, while the stress regime is predominantly compressional in the central offset section betweeen 59°N and 63°N, down-dip tension is the dominant mechanism in the slab to the north and south of this segment.

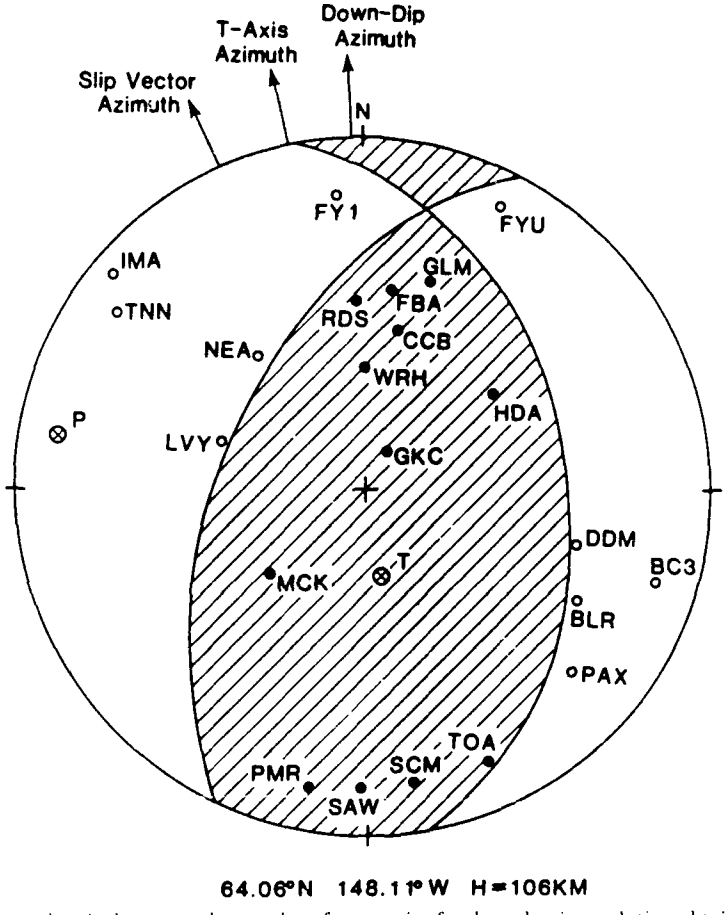

FIG. 4. Upper hemisphere, equal-area plot of composite focal mechanism solution obtained for Gold King cluster. Solid circles and open circles represent initial compressions and dilatations, respectively. First motions at individual stations are tabulated in Table 1. Down-dip vector is taken from Agnew (1980), and slip vector is from Minster and Jordan (1978).

TABLE 2

SUMMARY OF COMPOSITE FOCAL MECHANISM SOLUTION PARAMETERS

P Axis		*T* Axis		*B* Axis		Nodal Plane *A*		Nodal Plane *B*	
Azimuth	Plunge	Azimuth	Plunge	Azimuth	Plunge	Strike	Dip	Strike	Dip
100	12	349	69	193	19	N26°E	56°E	N10°W	40°W

ACKNOWLEDGMENTS

This research was supported by the Air Force Office of Scientific Research under Grant 85-0266 and by the State of Alaska funds appropriated to the Geophysical Institute, University of Alaska.

REFERENCES

Agnew, J. (1980). Seismicity of the central Alaska Range, Alaska, 1904–1978. *M.S. Thesis*, University of Alaska, Fairbanks, Alaska.

Akasche, B. (1968). Comparative investigations of the focal mechanism from short- and long-period seismograph records, *Ph.D. Thesis*, University of Frankfurt, Frankfurt, West Germany.

Benioff, H. (1954). Orogenesis and deep crustal structure—Additional evidence from seismology, *Bull. Geol. Soc. Am.* **65**, 385–400.

Bhattacharya, B. and B. N. Biswas (1979). Implications of north Pacific plate tectonics in central Alaska: focal mechanisms of earthquakes, *Tectonophysics* **53**, 99–130.

Davies, J. (1975). Seismological investigations and plate tectonics in south central Alaska, *Ph.D. Thesis*, University of Alaska, Fairbanks, Alaska.

Davis, T. N. and C. Echols (1960). A table of Alaskan earthquakes, 1788–1961, Rept. UAG R131, Geophysical Institute, University of Alaska, Fairbanks, Alaska, 45 pp.

Engle, K. Y. (1982). Earthquake focal mechanism studies of Cook Inlet area, Alaska, *M.S. Thesis*, University of Alaska, Fairbanks, Alaska.

Estes, S. (1978). Seismotectonic studies of lower Cook Inlet, Kodiak Island and the Alaska Peninsula areas of Alaska, *M.S. Thesis*, University of Alaska, Fairbanks, Alaska.

Gutenberg, B. and C. F. Richter (1941). Seismicity of the earth, *Geol. Soc. Am. Spec. Paper 34*.

Gutenberg, B. and C. F. Richter (1954). *Seismicity of the Earth and Associated Phenomena*, Princeton University Press, Princeton, New Jersey, p. 32.

Hodgson, J. H. and W. G. Milne (1951). Direction of faulting in certain earthquakes of the North Pacific, *Bull. Seism. Soc. Am.* **41**, 221–242.

House, L. S. and K. H. Jacob (1983). Earthquakes, plate subduction, and stress reversals in the eastern Aleutian arc, *J. Geophys. Res.* **88**, 9347–9373.

Huang, P. Y.-F. and N. N. Biswas (1983). Rampart seismic zone of central Alaska, *Bull. Seism. Soc. Am.* **73**, 813–830.

Jordan, J. G., G. Dunphy, and S. Harding (1968). The Fairbanks, Alaska earthquakes of June 21, 1967, Preliminary Seismological Report, U.S. Department of Commerce, ESSA, U.S. Coast and Geodetic Survey.

Lahr, J. C. (1975). Detailed seismic investigation of Pacific-North American plate interaction in southern Alaska, *Ph.D. Thesis*, Columbia University, New York.

Lahr, J. C. (1984). HYPOELLIPSE/VAX: a computer program for determining earthquake hypocentral parameters, magnitude and first motion pattern, *U.S. Geol. Surv., Open-File Rept. 80-59*.

Meyers, H. (1976). A historical summary of earthquake epicenters in and near Alaska, NOAA Technical Memorandum EDS NGSDC-1.

Minster, J. B. and T. H. Jordan (1978). Present day plate motions, *J. Geophys. Res.* **83**, 5331–5354.

Pulpan, H. and C. Frohlich (1985). Geometry of the subducted plate near Kodiak Island and lower Cook Inlet, Alaska, determined from relocated earthquake hypocenters, *Bull. Seism. Soc. Am.* **75**, 791–810.

St. Amand, P. (1948). The central Alaska earthquake swarm of October, 1947, *EOS, Trans. Am. Geophys. Union* **29**, 613–623.

Tarr, A. C. (1970). New maps of polar seismicity, *Bull. Seism. Soc. Am.* **60**, 1745–1757.

Tobin, D. G. and L. R. Sykes (1966). Relations of hypocenters of earthquakes to the geology of Alaska, *J. Geophys. Res.* **71**, 1659–1668.

VanWormer, J. D., J. Davies, and L. Gedney (1974). Seismicity and plate tectonics in south central Alaska, *Bull. Seism. Soc. Am.* **64**, 1467–1475.

GEOPHYSICAL INSTITUTE
UNIVERSITY OF ALASKA
FAIRBANKS, ALASKA 99775-0800
(L.G., J.N.D.)

ALASKA DIVISION OF GEOLOGICAL
AND GEOPHYSICAL SURVEYS
794 UNIVERSITY AVENUE
FAIRBANKS, ALASKA 99709
(J.N.D.)

Manuscript received 10 March 1986

APPENDIX VI

ANNUAL TECHNICAL REPORT

TO

AIR FORCE OFFICE OF SCIENTIFIC RESEARCH

CRUSTAL STRUCTURE STUDIES

Grant AFOSR-85-0266

Principal Investigators: David B. Stone
John N. Davies

Geophysical Institute
University of Alaska
Fairbanks
Alaska, 99775-0800

September 1987

Summary.

An array of seismometers was deployed in the area of the Yukon Flats, Alaska, to record explosions being detonated along the Trans-Alaska Pipeline corridor. The purpose of this experiment is to determine the crustal structure under the Yukon Flats area, and under interior Alaska by combining the data from the the temporary stations with data from the University of Alaska permanent seismometer network. The data are currently being analysed.

Introduction

The original proposal was designed to study the crustal structure of north-central and interior Alaska using the Dall City and Wood River sequences of earthquakes. During the course of this work it was discovered that the US Geological Survey planned to detonate a number of large (up to 6000 lb) chemical explosions as part of the Trans Alaska Lithosphere Investigation (TALI) refraction survey across Alaska. To take advantage of these "artificial earthquakes" as an aid to determining the crustal structure, the proposed work plan was modified to include the installation of a network of temporary stations in the Yukon Flats area. The Yukon Flats area was selected because it offers the possibility of tying in the existing data from the Dall City event (Estabrook et al., 1987a) with data obtained by the study of earthquakes north and south of the area (Estabrook, 1985, Estabrook et al., 1987b).

Yukon Flats Experiment

During July and August of 1987, a network of temporary seismometers were deployed along the Yukon and Porcupine rivers to the east of the Trans-Alaska pipeline bridge, along the Steese highway to Circle and at the villages of Beaver, Chalkyitsik and Birch Creek (figures 1 & 2). Seven of these stations were three component, five day recorders loaned to us by the USGS. Five of these were deployed along the Yukon river, one along the Porcupine river and one at Birch Creek. With the exception of the Birch Creek station, they were all deployed by river boat. The remainder of the stations were a mixture of smoked-drum recorders and seismometer systems designed to be connected directly to a telephone line. In the latter case the seismic signals were transmitted directly to recorders in the Geophysical Institute. Of the temporary stations two were manned, and only connected during the scheduled times of the explosions. The remaining stations were fitted with telephone answering

devices. These were set up so that after ten rings the recorder would answer, announce itself, switch the caller through to the seismometer signal, switch on a 30 minute timer then switch itself out of the circuit. This device saves the cost of long long-distance calls, and only requires visits to install and dismantle the system.

Because the Yukon flats area consists largely of geologically recent river deposits, and because it is not possible to move very far from the river bank for those stations installed by river boat, noise surveys were conducted to determine whether there were differences in background noise between different types of river bank. It was found that as long as the river was not shallow and turbulent, distance from the waters edge had very little effect on the background noise levels. However, the noise seemed to be amplified at locations were the trees were small or non-existent in comparison with recently cut banks with older larger trees. We ascribe this to the greater compaction and mechanical rigidity of the older wooded soils.

Out of the 13 temporary stations we installed we obtained recordings of at least some shots from all but 2 of them. In these two cases, equipment failures caused the loss of record. The data from the five-day recorder stations are currently being played back by the USGS at Menlo Park. The stations recorded on smoked drums or via telephone lines to the Geophysical Institute have been read, and time-distance plots are being constructed.

In addition to the temporary network, the fixed network stations run by the Geophysical Institute Seismology Laboratory (figure 1) were also used to record the shots. All of the shot signals being received at the Geophysical Institute were recorded on both film recorders and directly on the dedicated MASSCOMP computer system. Tables 1 and 2 give the locations of the explosions and the numbers of stations in the fixed network which recorded them. To date, only first arrival signals have been studied, but it is planned to use the digital recordings to construct composite record sections. The data from the USGS recorders will also be digitised from the tapes and included in the composite sections.

1987 Dall City Event

During the first sequence of USGS shots there was a magnitiude 5.5 event just to the north of the Trans-Alaska Pipeline crossing of the Yukon River. As can be seen from figure 1, it is almost on line with the stations deployed along the Yukon and Porcupine rivers. This event was recorded at four of the three component five-day recorder

sites (two other sites having fallen to either battery problems or damage by bears). Since these data can all be digitised, this should provide an excellent data set for coda and attenuation studies, and provide additional information on the crustal structure, though it is beyond the scope of this project to pursue these studies very far.

Results to date.

As mentioned above, the data from the explosions and the Dall City event recorded during the summer of 1987 are currently being processed. In addition to this data, models of posible crustal velocity structures based on the very limited data available in the literature, and a re-anlysis of explosion data from the 1985 USGS refraction line, have been assembled (Stone et al., 1987). We plan to have the preliminary analysis of the data completed by the American Geophysical Union meeting to be held in San Francisco in December 1987.

Future Explosion Studies

The USGS plan to continue their refraction experiments in 1988, with lines along the Fairbanks - Circle road (Steese highway), and the Livengood - Manley road. We are planning to deploy the five-day recorders again to obtain ray-paths that cross the Yukon Flats from the south and east to the north, to complement the dominantly south to north and east to west paths obtained during the 1987 experiment.

Starting in October 1987, the US Army intend to detonate a series of large (9000 lb) chemical explosions on the south flank of the Alaska Range near Donnelly Dome. These energy sources can be utilised to investigate the crustal structure north of the Alaska Range to Fairbanks. We plan to supplement the fixed seismometer network with about ten dial-up stations. A tentative distribution of stations is shown in figure 2. This distribution should allow constraints to be placed on the crustal structure beneath the Tanana Valley and beneath the Alaska Range.

References

Estabrook C.H., Davies J.N., Gedney L., Estes S.A., Dixon J.P., Seismicity and focal mechanism studies of the 1985 Dall City Earthquake, north central Alaska, in press, Bull. Seism. Soc. Amer., 1987a.

Estabrook C.H., Davies J.N., Stone D.B., Seismotectonics of Northern Alaska, submitted to Jour. Geophys. Res., 1987b.

Estabrook C.H., Seismotectonics of Northern Alaska, Univ. of Alaska MS thesis, pp 146, 1985.

Page R., Fuis G., Planned profiles for TALI along the Trans-Alaska Pipeline route, EOS, 1986.

Stone D.B., Davies J.N., Stihler S., Estabrook C.H., Basement (Pn) velocities in interior Alaska and the Yukon Flats, submitted to EOS, 1987.

Figure 1.
A map showing the combined temporary (circled stars) and fixed network (stars) seismometer stations used for the 1987 Yukon Flats and interior Alaska crustal studies experiment. Also shown are the shotpoints (+) for the three USGS refraction lines, and the Dall City event of 24 July 1987 (diamond).

Figure 2.
A map showing the distribution of seismometer stations, larger shot points and the major faults of Alaska. The shot points are labelled by shotpoint number followed by the size of the explosion in thousands of pounds. The large circles are of 100 and 200 km radius about the proposed winter explosions. The small open triangles are tentative locations for dial-up systems.

Table 1.
Shotpoint locations and times of detonation.

Table 2.
Sequential shot number, shotpoint, size of explosion and the number of fixed network seismometers that recorded it.

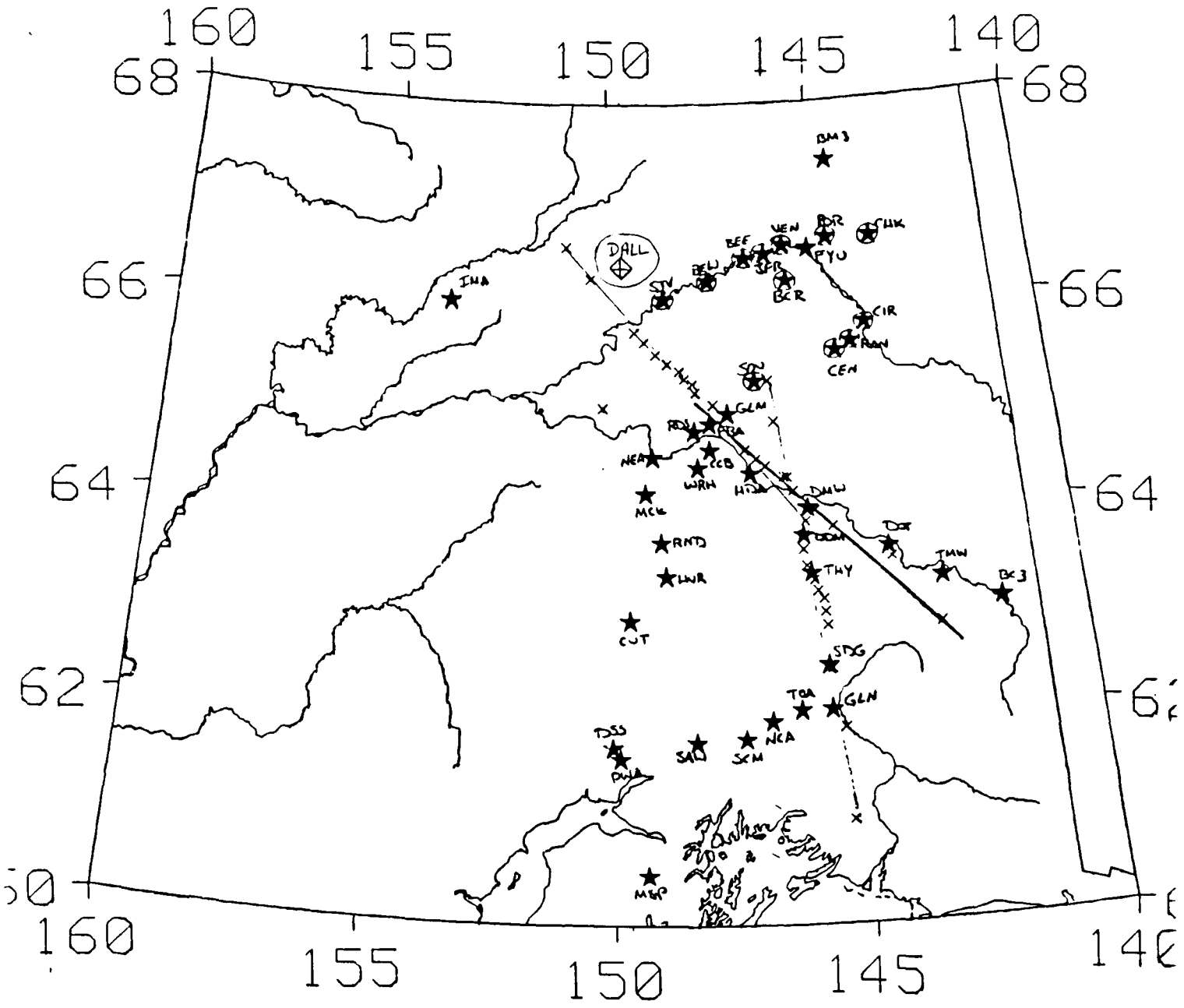

Figure 1.
A map showing the combined temporary (circled stars) and fixed network (stars) seismometer stations used for the 1987 Yukon Flats and interior Alaska crustal studies experiment. Also shown are the shotpoints (+) for the three USGS refraction lines, and the Dall City event of 24 July 1987 (diamond).

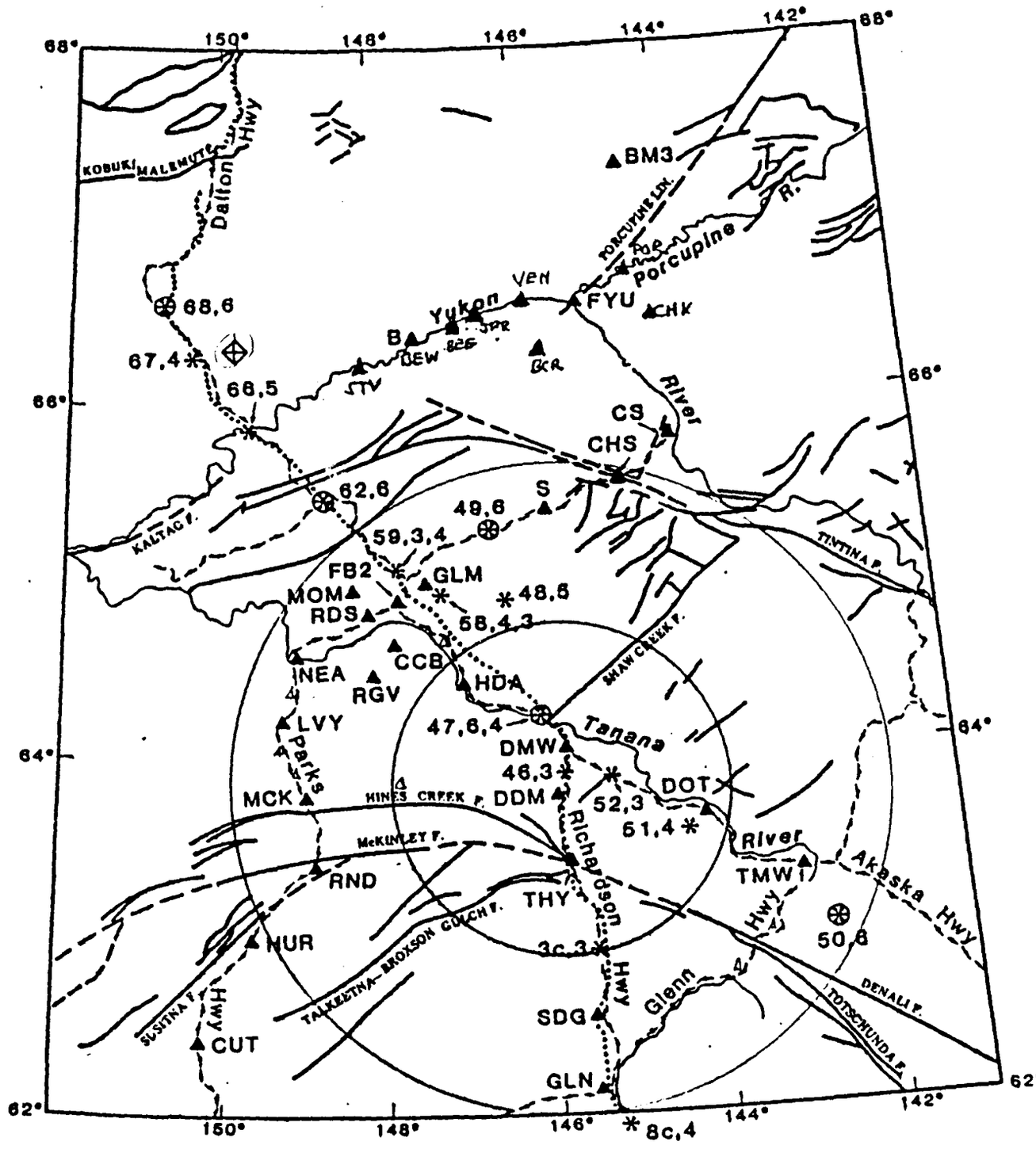

Figure 2.
A map showing the distribution of seismometer stations, larger shot points and the major faults of Alaska. The shot points are labelled by shotpoint number followed by the size of the explosion in thousands of pounds. The large circles are of 100 and 200 km radius about the proposed winter explosions. The small open triangles are tentative locations for dial-up systems.

Table 1.
Shotpoint locations and times of detonation.

SHOT NO	SHOT PT	DATE (DAY:YR)	SHOT TIME (HR:MIN:SEC)	LAT (N)	LONG (W)	SIZE (LBS)
1	19	205:87	08:00:00.016	61 01.83	145 15.68	6000
2	44	205:87	08:02:00.012	63 38.96	145 53.59	1000
3	49	205:87	08:04:00.007	65 17.81	146 25.16	6000
4	3	205:87	08:06:00.010	62 54.65	145 29.75	3000
5	8	205:87	08:08:00.008	61.56.02	145 17.54	6000
6	42	205:87	08:10:00.005	63 14.59	145 38.52	500
7	48	205:87	10:00:00.007	64 54.39	146 21.76	4000
8	1	205:87	10:02:00.005	63 20.78	145 42.13	2000
9	45	205:87	10:04:00.012	63 47.35	145 50.74	2000
10	41	205:87	10:06:00.010	63 02.28	145 30.82	1000
11	6	205:87	12:00:00.076	62 29.51	145 28.07	4000
12	2	205:87	12:02:00.010	63 09.87	145 32.00	2000
13	46	205:87	12:06:00.012	63 55.33	145 47.67	3000
14	43	205:87	12:07:30.005	63 29.38	145 50.90	1000
15	54	206:87	10:00:00.008	64 22.03	146 07.74	3000
16	46	206:87	10:02:00.010	63 55.33	145 47.67	3000
17	52	229:87	08:02:00.014	63 52.14	145 12.01	3000
18	51	229:87	08:04:00.008	63 32.32	144 00.38	4000
19	50	229:87	08:04:00.009	62 52.80	143 05.99	6000
20	56	229:87	08:06:00.012	64 32.96	146 47.95	2000
21	66	229:87	08:08:00.008	65 41.69	149 11.32	6000
22	55	229:87	08:10:00.014	64 28.84	146 35.51	500
23	53	229:87	10:00:00.012	64 01.72	145 34.92	2000
24	57	229:87	10:02:00.012	64 38.67	147 02.00	3000
25	73	229:87	10:04:00.013	64 22.02	146 12.45	700
26	59	229:87	12:00:00.009	65 04.72	147 41.77	4000
27	47	229:87	12:02:00.010	64 13.86	146 00.81	2000
28	50	232:87	08:00:00.016	62 52.80	143 05.99	6000
29	69	237:87	08:00:00.007	66 18.29	150 25.84	4000
30	62	237:87	08:02:00.006	65 19.85	148 18.44	2000
31	54	237:87	08:04:00.007	64 22.03	146 07.74	5000
32	57	237:87	08:06:00.157	64 38.67	147 02.00	4000
33	65	237:87	08:10:00.007	65 34.47	148 56.31	4000
34	67	237:87	10:00:00.012	65 47.36	149 24.89	3000
35	61	237:87	10:02:00.006	65 16.89	148 07.84	1000
36	70	237:87	10:04:00.005	66 36.12	150 59.19	4000
37	64	237:87	10:06:00.011	65 28.76	148 41.70	1000
38	66	237:87	12:00:00.015	65 41.69	149 11.32	2000
39	60	237:87	12:02:00.005	65 11.93	148 04.76	2000
40	59	237:87	12:04:00.241	65 04.71	147 41.79	3000
41	63	237:87	12:06:00.011	65 24.35	148 25.14	2000
42	74	238:87	08:00:00.005	65 03.42	150 11.26	3000
43	63	238:87	12:02:00.010	65 24.35	148 25.14	1100
44*	61	240:87	22:00:00.007	65 16.89	148 07.84	
45*	59	240:87	22:02:00.009	65 04.71	147 41.79	
46*	60	240:87	22:30:00.007	65 11.93	148 04.76	
47*	60	241:87	01:30:00.007	65 11.93	148 04.76	
48*	59	241:87	01:32:00.009	65 04.71	147 41.79	
49*	61	241:87	02:00:00.007	65 16.89	148 07.84	

* SHOT SIZE IS 100-200 LBS

Table 2.
Sequential shot number, shotpoint, size of explosion and the number of fixed network seismometers that recorded it.

SHOT NUMBER	SHOT POINT	SIZE (LBS)	STATIONS*
1	19	6000	12
2	44	1000	19
3	49	6000	12
4	3	3000	23
5	8	6000	12
6	42	500	4
7	48	4000	2
8	1	2000	--
9	45	2000	1
10	41	1000	16
11	6	4000	8
12	2	2000	17
13	46	3000	2
14	43	1000	--
15	54	3000	8
16	46	3000	--
17	52	3000	15
18	51	4000	21
19	50	6000	--
20	56	2000	10
21	66	6000	7
22	55	500	11
23	53	2000	15
24	57	3000	17
25	73	700	11
26	59	4000	10
27	47	2000	16
28	50	6000	18
29	69	4000	5
30	62	2000	7
31	54	5000	22
32	57	4000	14
33	65	4000	7
34	67	3000	8
35	61	1000	--
36	70	4000	4
37	64	1000	7
38	66	2000	--
39	60	2000	5
40	59	3000	7
41	63	2000	1
42	74	3000	9
43	63	1100	3
44**	61		5
45**	59		5
46**	60		--
47**	60		2
48**	59		3
49**	61		5

* NUMBER OF STATIONS THE BLASTS WERE OBSERVED AT
** SHOT SIZE 100-200 LBS

ACCURACY OF EARTHQUAKE LOCATION DETERMINATIONS IN THE FAIRBANKS, ALASKA AREA BASED ON ARTIFICIAL EXPLOSION EXPERIMENTS

Presented to the Faculty of the University of Alaska

in Partial Fulfillment of the Requirements

for the Degree of

MASTER OF SCIENCE

Jean M. Johnson, B.S.

May 1989

ABSTRACT

Ten explosions which occurred in the Fairbanks area are used to determine, first, how accurately seismic events can be located using the computer program HYPOELLIPSE; second, the factors which influence how well the events are located; and, third, which of the four proposed velocity models best approximates the Fairbanks area. The average hypocentral error is 4.9 km, the average epicentral error is 2.6 km, and the average depth error is 3.2 km. The most important factors influencing the location accuracy are station configuration, reading errors, distance to closest station, and the velocity model used. The HYPOELLIPSE error indicators are shown to be smaller than the actual errors. The proposed velocity models are all faster than the actual structure of the Fairbanks area; however, the actual errors show that the events are fairly accurately located. The data is too limited to propose a new velocity model.